PALEOBIOLOGY OF ICHTHYOSAURS: USING OSTEOHISTOLOGY TO TEST HYPOTHESES OF GROWTH RATES AND METABOLISM IN A CLADE OF SECONDARILY AQUATIC MARINE TETRAPODS

By

Katherine L. Anderson, B.S.

A Dissertation Submitted in Partial Fulfillment of the Requirements

For the Degree of

Doctor of Philosophy

In

Geology

University of Alaska Fairbanks

August 2019

APPROVED:

Dr. Patrick Druckenmiller, Committee Chair
Dr. Gregory Erickson, Committee Member
Dr. Sarah Fowell, Committee Member
Dr. Lara Horstmann, Committee Member
Dr. Paul McCarthy, Chair
Department of Geosciences
Dr. Leah Berman, Interim Dean
College of Natural Science and Mathematics
Dr. Michael Castellini, *Dean of the Graduate School*

Abstract

Ichthyosaurians (Ichthyosauria) are one of the most prominent groups of secondarily aquatic Mesozoic marine reptiles. Over their 160 million years of evolution, the clade evolved a streamlined body plan with paddle-like limbs, convergent with modern cetaceans. Despite the fact that ichthyosaurians have been studied by paleontologists for over a century, very little is known about aspects of their biology, including quantification of their age structure and growth rates. Multiple lines of evidence, including oxygen isotope, swimming modality, and body shape analyses suggest that ichthyosaurians experienced elevated growth rates and likely maintained an elevated body temperature relative to ambient sea water. In this dissertation, I test these hypotheses using osteohistological methods.

In the first manuscript, we describe new material of the small-bodied Upper Triassic ichthyosaurian *Toretocnemus* from the Nehenta Formation and the Hound Island Volcanics (both Norian, Upper Triassic) of Southeast Alaska. During the Upper Triassic, ichthyosaurians experienced their greatest size disparity, with large-bodied species rivaling the size of modern blue whales (*Balaenoptera musculus*; 20+ m body length) living alongside small-bodied species (1 m body length) like *Toretocnemus*. Prior to this study, *Toretocnemus* was known from Carnian deposits of California and possibly Sonora, Mexico. The referred material described here expands its geographic and temporal range. There are very few known ichthyosaurians from the Norian; thus, this material sheds light on the clade's diversity before the end Triassic extinction event.

In the second and third manuscripts, we use osteohistological methods to describe the microstructure of various skeletal elements of two species of *Stenopterygius* from the

Posidonia Shale (Lower Jurassic) of Germany. The Posidonia Shale is a Konservat-Lagerstätten that preserves over 3000 ichthyosaurian specimens, approximately 80 percent of which are referable to *Stenopterygius*. First, we sampled over 40 skeletal elements from one individual specimen referred to *Stenopterygius quadriscissus* to 1) describe the mineralized tissues across the skeleton, 2) infer relative growth rate, and 3) identify elements with growth marks. Almost all elements described demonstrate fibrolamellar primary bone, indicative of a rapid growth rate. We also identify growth marks in several elements, including the dentary and premaxilla, that will be used in future growth studies. In the third manuscript, we sample a scleral ossicle from *Stenopterygius triscissus* to describe its microstructure and investigate the use of ossicles for skeletochronology. The use of scleral ossicles for determining age structure has been documented in extant sea turtles as well as dinosaurs. We sectioned one ossicle in three planes and document conspicuous growth banding in the short axis section. Although this method requires further testing, we tentatively determine a minimum age of 7 years at the time of death for this individual.

This dissertation lays critical groundwork for future studies of the paleobiology of ichthyosaurians. We are already in the preliminary stages of using these results to 1) quantify age structure and growth rates of an ichthyosaurian (*Stenopterygius quadriscissus*) for the first time, and 2) test the use of scleral ossicles for skeletochronology of ichthyosaurians. Through addressing these basic aspects of ichthyosaurian biology, we can begin to investigate how ichthyosaurian development and physiology changed over time and space and develop a greater understanding of this clade's 160 million years of evolution.

Table of Contents

Page

List of Figures

Page

List of Tables

Page

List of Appendices

Page

Acknowledgements

This body of work would not have been possible without many people who helped me along the way in all aspects of my life during my doctorate program. I feel extremely grateful for the people I have met in Fairbanks and for the opportunities that I have been given during my time in graduate school. In addition to the research presented in this dissertation, I was able to develop skills in science communication and outreach through the NSF GK-12 CASE fellowship, as well as skills in museum collection and lab management through my work as earth sciences collection manager at the University of Alaska Museum. While this was not always an easy journey, I feel so fortunate to end my time at the University of Alaska Fairbanks with my doctorate in hand and a better understanding of my field, but also a better understanding of myself.

First and foremost, many thanks go to my advisor, Dr. Patrick Druckenmiller. Thank you for seeing my potential, for your patience, and for the innumerable opportunities that you have given me. Thank you to my committee members, Dr. Gregory Erickson, Dr. Sarah Fowell, and Dr. Lara Horstmann. I appreciate your guidance, your expertise, and your mentorship. In addition, thanks to the co-authors of the manuscripts included in this dissertation, Dr. James Baichtal and Dr. Erin Maxwell. I look forward to being your colleague in the future.

I would like to acknowledge my funding sources: the Universiy of Alaska Fairbanks Department of Geosciences, the NSF GK-12 CASE fellowship (NSF DGE-0948029; PIs R. Boone, L. Conner, and K. Winker), and the University of Alaska Museum. Additional funding was provided by the University of Alaska Museum Otto Geist Fund, the Graduate School Travel Grant, and the College of Natural Science and Mathematics Travel Grant.

To my academic siblings, Eric Metz, Danielle Serratos, Dustin Stewart, and Evan Millsap, your support and comraderie are invaluable, and I look forward to seeing you at SVP for many years to come. To Chris Pastro, Kelly Thrun, and Jennifer Preston, you amaze me. Thank you for welcoming me into your classrooms and for teaching me how to teach. For my students (big and small!), thank you for teaching me to think outside of the box, to recognize all types and talents and for the many enduring life lessons. Thanks to my longest standing students Bobby Ebelhar, Camille Heninger, Thomas Sniezak, Noah Boone, Emily Van Nortwick, and Victoria Nelson. Additional thanks to Kevin May, Julie Rousseau, Dr. Rainer Newberry, Angela Linn, Jochen Mezger, Cindy and David Schraer, the Erickson family, Ellen Craig, Carrie Green, Barbara Day, Emilie Nelson, and Barbara Ellana.

Finally, and most importantly, thank you to my family. Mom, Dad, and Jimmy, you inspire me to pursue what feels like the impossible, to work hard and to persist. I can't put into words how much I value your support and encouragement. Nilesh, thank you for believing in me when I didn't believe in myself. You are a light in my life and inspire me to be a better person everyday. These acknowledgements wouldn't be complete without mention of the furry family members who made this possible: Grace, Tait, Wally, and of course Bingley, Darcy, and Baby. Thank you for your unconditional love, listening ears, and warm and fuzzy pet therapy.

Chapter 1. Introduction

Ichthyosaurians (Ichthyosauria) are one of the most prominent groups of secondarily aquatic Mesozoic marine reptiles. Over their 160 million years of evolution, the clade evolved a streamlined body plan with paddle-like limbs convergent with modern cetaceans (Motani, 2005). For this reason, ichthyosaurs are often used as a textbook example of convergent evolution. Ichthyosaurs achieved a cosmopolitan distribution and a remarkable degree of size disparity, especially during the Late Triassic (McGowan and Motani, 2003). At this time, one clade of ichthyosaurians, the shastasaurids (Shastasauridae) reached body sizes that rivaled that of modern blue whales (*Balaenoptera musculus*; 20+ meters body length) while living alongside significantly smaller ichthyosaurian taxa, such as *Torectocnemus*, that reached only 1 meter in body length. In the wake of the Late Triassic extinction event, the ichthyosaur body plan became predominantly "thunniform", or tuna-like in shape with a pronounced vertically-oriented tail fluke, dorsal fin, and well-developed pectoral fins.

Despite the evolutionary success and diversity of ichthyosaurians, very little is known about major aspects of their biology, particularly with respect to growth rates across time and space. While differences in body size and shape of ichthyosaurian taxa have been studied for over a century (Howe et al. 1981; McGowan and Motani, 2003), an understanding of their underlying developmental and physiological mechanisms remains elusive. A growing number of studies using a variety of methods, including oxygen isotope, body shape, swimming modality, and osteohistological analyses suggest that ichthyosaurians experienced elevated growth rates relative to modern ectothermic reptiles

of similar body size and in turn likely possessed elevated body temperatures relative to ambient ocean temperature (Massare, 1988; de Buffrénil and Mazin, 1990; Motani, 2002a, b, 2010; Bernard et al., 2010; Kolb et al., 2011; Houssaye et al., 2014; Anderson et al., 2018). However, a direct quantification of growth rate based on osteohistology for any ichthyosaurian taxon is lacking. This is surprising given that this methodology has revolutionized our understanding of dinosaur paleobiology (Chinsamy and Hillenius, 2004; Erickson, 2005, 2014). This lack of quantification is due, in part, to the apparent absence of annual growth marks (e.g., lines of arrested growth) in their bones (Houssaye et al., 2014). In addition, very few elements have been histologically sampled, with most studies focusing almost solely on the humeri and ribs (see Anderson et al., 2018). Furthermore, many existing osteohistological studies are exploratory and sample isolated material with generic level taxonomic identification, limiting their conclusions (Anderson et al., 2018). We now know there are skeletal elements that preserve these growth marks and will be instrumental for future growth studies (Anderson et al., 2018).

Osteohistological methods require the creation of physical or virtual (microCT) thin sections in order to study the mineralized tissues of bones and teeth. Through comparison with bone microstructure of modern vertebrates, we can infer aspects of the biology of extinct vertebrates (see Francillon-Vieillot et al., 1990 and/or Huttenlocker et al., 2013 for a comprehensive review of aspects of bone biology discussed here). With regard to bone, the mineralized tissues preserve a record of growth and development. For example, the organization of the primary bone (bone deposited during growth) can provide information about relative growth rates. Note that body size does influence the rate of bone deposition. It is important to compare vertebrates of similar body sizes. There are three main matrix

types for primary bone that vary based on the organization of the tissue: lamellar, parallel-fibered, and woven. Lamellar and parallel-fibered bone are typical of slow deposition and found in relatively slow growing extant vertebrates, such as crocodylians. Woven bone is less organized than the other two types and typically found in extant vertebrates that grow relatively rapidly, including birds and large mammals. In addition, the organization of primary vascular canals can also be informative of relative growth rates in conjunction with the matrix types. Types of vascular organization are: simple, laminar, plexiform, reticular and radial. There are also bone tissue complexes, including fibrolamellar bone which consists of a woven bone matrix typically with simple vascular canals arranged in "lamellar" rows.

Primary bone also preserves growth marks that are used for skeletochronology, or quantifying age structure, of vertebrates (see Woodward et al., 2013). Lines of arrested growth (LAGs) are lines in the primary bone that reflect a cessation of growth before growth resumed. LAGs are known to be annual in extant vertebrates, and as such have been used to infer minimum age at death for extinct vertebrates Annuli are growth marks that reflect cyclicity in growth in the form of faster deposited zones separated by slower deposited annuli; these may or may not be annual. There are also growth layer groups in bone (not to be confused with growth layer groups in teeth) which like annuli may or may not be annual. It is important to note that growth marks are less likely to be deposited early in ontogeny when growth rates are continually high and do not necessarily experience the degree of cyclicity required to deposit growth marks, as well as late in ontogeny when growth rates are low to zero (e.g., Lonati et al., 2019).

Primary bone is replaced by secondary bone during the process of remodeling (Francillon-Vieillot et al., 1990; Huttenlocker et al., 2013). This process retains the structural integrity of the bone (i.e., remodeling is the process that heals a broken or fractured bone), but it involves resorption of the primary bone or previously deposited secondary bone. In effect, remodeling destroys the growth record that was preserved in the primary bone. Secondary bone consists of secondary osteons around which lamellar bone is deposited. This is also referred to as Haversian bone and secondary osteons as Haversian canals. Secondary osteons can be distinguished from primary osteons because the deposition of the lamellar bone creates a resorption line that forms a distinct boundary with the surrounding bone.

In this dissertation, I test existing hypotheses of elevated growth rates in ichthyosaurians using osteohistological methods, and lay a foundation for the study of ichthyosaurian age structure and growth rates. The three core chapters of this dissertation are written as standalone manuscripts that are either published in, or in advanced stages of preparation for publication in peer-reviewed scientific journals; as such, there is some overlap in the introductory content of each of these chapters. In the following paragraphs, I summarize the objectives and findings of each of these chapters as well as the contributions of my co-authors and the status of publication.

In the second chapter, we describe new material of the small-bodied ichthyosaurian *Toretocnemus* from the Nehenta Formation (Norian, Upper Triassic) of Gravina Island in Southeast Alaska. The specimen consists of a partial articulated individual, including dorsal and caudal vertebrae, ribs, some pelvic girdle elements, a nearly complete hindlimb, and the other femur. The articulated caudal vertebrae preserve a tail bend, indicating the

presence of a slight downward bend in the tail during life; this is the first documentation of this feature in this genus. During the course of the study, we identified a second isolated femur from equivalent deposits of the Hound Island Volcanics (Norian, Upper Triassic) from Hound Island, Southeast Alaska. Previously known exclusively from Carnian-aged deposits of California and possibly Sonora, Mexico (Merriam, 1903; Lucas, 2002), the new material expands both the geographic and stratigraphic ranges of the genus. Globally, very few ichthyosaurians are known from the Norian with most occurrences referred to large-bodied shastasaurids (see Table 2-1). This specimen suggests that small forms typical of the Carnian also persisted into the Norian ahead of the end-Triassic extinction event. We also discuss implications for a paleo-Pacific fauna (Nicholls et al., 2002). This paper is co-authored with my advisor Dr. Patrick Druckenmiller, and United States Forest Service geologist Dr. Jim Baichtal, who collected the articulated specimen. The project was conceptualized by KA, PD, and JB; KA performed the investigation under supervision of PD and prepared the manuscript; PD and JB revised the manuscript for publication. This paper is in preparation for publication in the peer-reviewed journal *Palaeontologia Electronica*.

In the third chapter, we describe the microstructure across the skeleton of one individual referred to *Stenopterygius quadriscissus* from the Posidonia Shale (Lower Jurassic) of Germany. We sampled over 40 skeletal elements with the aim to 1) broadly document the microstructure across a large number of elements of the skeleton, many of which had never been histologically described, 2) infer relative growth rate from mineral organization, and 3) identify growth markers that would be useful for future skeletochronological and growth studies. We found that overall this species of ichthyosaurian has rapidly-deposited fibrolamellar primary bone across the skeleton

indicative of an elevated relative growth rate. The primary bone in the paddle elements is spongious, and many of the postcranial elements are extensively remodeled which negates their use for growth studies. We identify annuli in the ribs, as well as in the premaxilla and dentary. The premaxilla and dentary are the densest bones sampled and will be used for future skeletochronological exploration (Appendix B). In addition, we discuss the evidence of modified perichondral ossification preserved in the microstructure of the limb elements. The co-authors of this study are my advisor Dr. Patrick Druckenmiller, committee member Dr. Gregory Erickson, and curator of marine reptiles at the Stuttgart State Museum of Natural History Dr. Erin Maxwell. This project was conceptualized by KA and PD; KA performed the investigation and prepared the manuscript; PD, GE, and EM revised the manuscript for publication. This manuscript was published in 2018 in the peer-reviewed journal *Palaeontology*, and supplemental figures were published online in the Dryad database (included here in Appendix A).

The fourth chapter presents a preliminary investigation of the use of scleral ossicles for skeletochronology of ichthyosaurians. This chapter builds on existing work that demonstrates scleral ossicles can be used for skeletochronology in sea turtles (Zug and Parham, 1996; Avens and Goshe, 2007; Avens et al., 2009) and ongoing work that applies this method to extinct groups of dinosaurs through comparison of growth marks in scleral ossicles and other skeletal elements (Erickson et al., unpublished data). We describe the microstructure of an ossicle from one specimen of *Stenopterygius triscissus* from the Posidonia Shale (Lower Jurassic) of Germany and discuss implications for both eyeball growth and potential use for skeletochronology. While this methodology requires further testing for ichthyosaurians through comparison with growth marks in other skeletal

elements, the preliminary results are significant because the scleral ossicle of this species is minimally remodeled and therefore preserves the entire growth record. If future testing proves the ossicle is reliable for skeletochronology, this method could provide a minimally destructive way of determining individual age at death in the future, as it may require destructive sampling of only one element if it preserves the entire growth record with minimal remodeling. This contributes to a growing body of work that suggests scleral ossicles may be useful for aging of individuals across Reptilia as a whole. This manuscript is co-authored by Dr. Gregory Erickson, Dr. Patrick Druckenmiller, and Dr. Erin Maxwell. The project was conceptualized by KA, GE, and PD; KA performed the investigation with guidance from GE and prepared the manuscript; GE, PD, and EM revised the manuscript for publication. The manuscript is in preparation to be submitted for publication in the peer-reviewed journal *Historical Biology*.

This thesis lays critical groundwork for future studies of ichthyosaurian development and physiology. It is one of only two studies to conduct a thorough osteohistological sampling of various elements of one individual ichthyosaur to understand overall development across the skeleton. It is also the first investigation to test several novel bone elements for use in future skeletochronological and growth studies, including the dentary and premaxilla, as well as the scleral ossicle. Building on this, we are in the preliminary stages of quantifying ichthyosaurian growth rates for the first time and testing the use of scleral ossicles to determine an individual's age at death (Appendix B). Quantification of both growth and age in ichthyosaurians will allow the exploration of additional aspects of their life history, including maximum growth rate and age at which maximum growth rate is experienced.

1.1 References

Anderson, K.L., Druckenmiller, P.S., Erickson, G.M. and Maxwell, E.E. 2018. Skeletal microstructure of *Stenopterygius quadriscissus* (Reptilia: Ichthyosauria) from the Posidonienschiefer (Posidonia Shale, Lower Jurassic) of Germany. *Palaeontology*, 62(3):433-449. https://doi.org/10.1111/pala.12408

Avens, L. and Goshe, L.R. 2007. Comparative skeletochronological analysis of Kemp's ridley (*Lepidochelys kempii*) and loggerhead (*Caretta caretta*) humeri and scleral ossicles. *Marine Biology,* 152(6):1309-1317.

Avens, L., Taylor, J.C., Goshe, L.R., Jones, T.T. and Hastings, M., 2009. Use of skeletochronological analysis to estimate the age of leatherback sea turtles *Dermochelys coriacea* in the western North Atlantic. *Endangered Species Research,* 8(3):165-177.

Bernard, A., Lécuyer, C., Vincent, P., Amiot, R., Bardet, N., Buffetaut, E., Cuny, G., Fourel, F., Martineau, F., Mazin, J.M. and Prieur, A. 2010. Regulation of body temperature by some Mesozoic marine reptiles. *Science*, *328*(5984):1379-1382.

Buffrénil, V. de and Mazin, J.-M. 1990. Bone histology of the ichthyosaurs: comparative data and functional interpretation. *Paleobiology,* 16:435–447.

Chinsamy, A. and Hillenius, W.J. 2004. Physiology of nonavian dinosaurs, p. 643–659. In Dodson, P., Osmolska, H. and Weishampel, D.B. (eds.), *The Dinosauria*. University of California Press.

Erickson, G.M. 2005. Assessing dinosaur growth patterns: a microscopic revolution. *Trends in Ecology & Evolution,* 20:677–684.

Erickson, G.M. 2014. On Dinosaur Growth. *Annual Review of Earth and Planetary Sciences,* 42:675–697.

Erickson, G.M., Anderson, K.L., Watabe, M. and Norrell, M.A. Unpublished data. Age and growth pattern for a specimen of non-avian dinosaur *Citipati osmolskae* determined from growth lines in scleral ossicles.

Francillon-Vieillot, H., Buffrénil, V. de, Castanet, J., Geraudie, J., Meunier, F.J., Sire, J.Y., Zylerberg, L. and Ricqlès, A. de. 1990. Microstructure and mineralization of vertebrate skeletal tissues. 471–530. In Carter, J.G. (ed). *Biomineralization: patterns and evolutionary trends*. Van Nostrand Reinhold.

Houssaye, A., Scheyer, T.M., Kolb, C., Fischer, V. and Sander, P.M. 2014. A new look at ichthyosaur long bone microanatomy and histology: implications for their adaptation to an aquatic life. *Plos One,* 9(4):e95637.

Howe, S.R., Sharpe, T. and Torrens, H.S. 1981. Ichthyosaurs: a history of fossil 'sea dragons'. National Museum Wales.

Huttenlocker, A.K., Woodward, H.N. and Hall, B.K. 2013. The biology of bone. In Padian, K. and Lamm, E.-T. (eds.) *Bone histology of fossil tetrapods: Advancing methods, analysis and interpretation*. University of California Press.

Kolb, C., Sánchez-Villagra, M.R. and Scheyer, T.M. 2011. The palaeohistology of the basal ichthyosaur *Mixosaurus* Baur, 1887 (Ichthyopterygia, Mixosauridae) from the Middle Triassic: palaeobiological implications. *Comptes Rendus Palevol,* 10:403–411.

Lonati, G.I., Howell, A.R., Hostetler, J.A., Schueller, P., Wit, M. de, Bassett, B.L., Deutsch, C.J. and Ward-Geiger, L.I. 2019. Accuracy, precision, and error in age estimation of Florida manatees using growth layer groups in earbones. *Journal of Mammalogy.* https://doi.org/10.1093/jmammal/gyz079

Lucas, S.G. 2002. *Toretocnemus*, a Late Triassic ichthyosaur from California, U.S.A and Sonora, Mexico. *New Mexico Museum Natural History and Science Bulletin,* 21:275-282.

Massare, J.A. 1988. Swimming capabilities of Mesozoic marine reptiles: implications for method of predation. *Paleobiology*, *14*(2):187-205.

McGowan, C. and Motani, R. 2003. Ichthyopterygia. In Sues, H.-D. (ed). *Handbook of Paleoherpetology*. Verlag Dr. Friedrich Pfeil, München.

Merriam, J.C. 1903. *New Ichthyosauria from the Upper Triassic of California*. University of California Press.

Motani, R. 2002. Scaling effects in caudal fin propulsion and the speed of ichthyosaurs. *Nature*, *415*(6869):309.

Motani, R. 2002. Swimming speed estimation of extinct marine reptiles: energetic approach revisited. *Paleobiology*, *28*(2):251-262.

Motani, R. 2005. Evolution of fish-shaped reptiles (Reptilia: Ichthyopterygia) in their physical environments and constraints. *Annual Review of Earth and Planetary Sciences*, *33:*395-420.

Motani, R. 2010. Warm-blooded "sea dragons"? *Science*, *328*(5984):1361-1362.

Nicholls, E.L., Wei, C. and Manabe, M. 2002. New material of *Qianichthyosaurus* Li, 1999 (Reptilia, Ichthyosauria) from the Late Triassic of southern China, and implications for the distribution of Triassic ichthyosaurs. *Journal of Vertebrate Paleontology*, 22(4):759-765.

Woodward, H.N., Padian, K. and Lee, A.H. 2013. Skeletochronology. In Padian, K. and Lamm, E.-T. (eds.) *Bone histology of fossil tetrapods: Advancing methods, analysis and interpretation*. University of California Press.

Zug, G.R. and Parham, J.F. 1996. Age and growth in leatherback turtles, *Dermochelys coriacea* (Testudines: Dermochelyidae): a skeletochronological analysis. *Chelonian Conservation and Biology, 2*:244-249.

Chapter 2. New material of *Toretocnemus* Merriam, 1903 (Reptilia, Ichthyosauria) from the Late Triassic (Norian) of Southeast Alaska[1]

2.1 Abstract

During the Late Triassic, ichthyosaurians (Ichthyosauria) exhibited the greatest size disparity known from their entire geological history; however, relatively little is known about the diversity and morphology of small-bodied (1-2 m) forms, especially when compared to larger taxa. In 2003, a small-bodied (< 1.5 m total length) ichthyosaur was collected from exposures of the Nehenta Formation (Norian, Late Triassic), a part of the Alexander terrane, on Gravina Island in Southeast Alaska. The new material consists of bone fragments and external molds of an incomplete, but largely articulated postcranial skeleton. Surface peels were used to better interpret the skeleton, which includes two dorsal and 18 articulated caudal vertebrae, a partial pelvic girdle, an articulated hind limb and a second femur. Re-examination of material collected from the Hound Island Volcanics (Norian, Late Triassic) on Hound Island, Southeast Alaska revealed a second, isolated femur of similar morphology. The distinctive hindlimb morphology, including a strongly constricted femoral shaft that is distally expanded both pre- and post-axially, permits referral of these specimens to the poorly-known, small-bodied ichthyosaurian *Toretocnemus* Merriam 1903. As currently known, *Toretocnemus* is restricted to Carnian-aged strata of California and possibly Sonora, Mexico. The new Alaskan specimens extend

[1] Anderson, K.L., Druckenmiller, P.S. and Baichtal, J.F. New material of *Toretocnemus* Merriam, 1903 (Reptilia, Ichthyosauria) from the Late Triassic (Norian) of Southeast Alaska. Planned for submission to *Palaeontologia Electronica*.

the stratigraphic range of the genus into the Norian and are the first record of the genus in northwestern North America. The articulated specimen is the first of *Toretocnemus* to preserve apical vertebrae, providing insight into the evolution of the tail bend in Late Triassic, small-bodied ichthyosaurians.

2.2 Introduction

During the Late Triassic, ichthyosaurians (Ichthyosauria) exhibited the greatest size disparity known in their 160 million-year evolutionary history. Small-bodied ichthyosaurians (1-2 m in length) thrived alongside forms whose size rivaled that of extant blue whales (*Balaenoptera musculus*; 20+ m in length; Nicholls and Manabe, 2004). However, relatively little is known about the diversity and morphology of these small-bodied forms, especially when compared to the larger and better-known Late Triassic taxa, such as *Shastasaurus* and *Shonisaurus* (Camp, 1980; Callaway and Massare, 1989; Kosch, 1990; McGowan and Motani, 1999; Nicholls and Manabe, 2004). The western margin of North America has yielded a small number of Late Triassic small-bodied ichthyosaurians, including *Toretocnemus*, although most are poorly preserved and their osteology imperfectly understood (Merriam, 1903; McGowan, 1995; McGowan, 1996; Lucas, 2002). Small-bodied taxa have also been found in Late Triassic (Carnian) deposits of China, including exceptionally preserved specimens of *Qianicthyosaurus* (Li, 1999; Nicholls et al., 2002; Maisch et al., 2008).

Our understanding of ichthyosaurian diversity in the Triassic has significantly increased in recent years due to new discoveries in Southern China (Ji et al., 2016). Late Triassic ichthyosaurians are primarily known from Carnian-aged deposits of South China

and North America. By the end of the Late Triassic, marine deposits in China and North America are lacking, resulting in a gap in the fossil record of marine reptiles in the Norian and Rhaetian. Very few ichthyosaurians are known from the Norian, and of the known specimens the vast majority are referred to the large-bodied Shastasaurids (Shastasauridae; Table 2-1). Consequently, there is little known about ichthyosaurian diversity and distribution before the end-Triassic extinction event, especially with regard to small-bodied forms.

Originally discovered in 1969, an articulated but poorly preserved small-bodied (< 1.5 m total length) ichthyosaur was collected in 2004 from rocks exposed in an intertidal zone on Gravina Island in Southeast Alaska (Figure 2-1). The specimen, UAMES 3599, was found in a calcareous shale from the lower unit of the Nehenta Formation, which is early to middle Norian in age based on biostratigraphic evidence (Berg, 1973; Caruthers and Stanley, 2008; Katvala and Stanley, 2008). Additionally, an isolated femur (UAMES 34994) with similar morphology to that of the Gravina Island specimen was described by Adams (2008) from temporally equivalent deposits in the Hound Island Volcanics, also from Southeast Alaska. The distinctive hindlimb morphology permits referral of these specimens to the poorly-known, small-bodied ichthyosaur *Toretocnemus*. UAMES 3599 is the first specimen referable to *Toretocnemus* that preserves apical vertebrae, providing insight into the evolution of the tail bend in Late Triassic, small-bodied ichthyosaurs. The new Alaskan specimens extend the stratigraphic occurrence of this taxon into the Norian, helping to fill this temporal gap in ichthyosaur evolution.

Institutional abbreviations—CMNH, Chongqing Museum of Natural History, Chongqing City, People's Republic of China; UAMES, University of Alaska Museum Earth Sciences, Fairbanks, Alaska, USA; UCMP, Museum of Paleontology, University of California, Berkeley, California, USA.

2.3 Systematic Paleontology

DIAPSIDA Osborn, 1903

ICHTHYOSAURIA De Blainville, 1835

TORETOCNEMIDAE Maisch and Matzke, 2000

Toretocnemus Merriam, 1903

Type Species—*Toretocnemus californicus* Merriam, 1903

Type Specimen—UCMP 8100

Referred Specimen—UAMES 3599

Horizon—Lower unit of the Nehenta Formation, Upper Triassic (Early-Middle Norian) (Berg, 1973; Caruthers and Stanley, 2008).

Locality—Intertidal zone south of South Vallenar Point, Gravina Island, Southeast Alaska, United States of America (Figure 2-1). Exact locality data on file with Alaska Department of Natural Resources.

Referred Specimen—UAMES 34994

Horizon—Hound Island Volcanics Formation of the Hyd Group, Upper Triassic (Middle Norian) (Adams, 2008; Katvala and Stanley, 2008).

Locality—Hound Island (USGS Locality #M1900 and M1901), Southeast Alaska, United States of America.

2.4 Geological Setting

The geology of Southeast Alaska is complex, primarily consisting of displaced terranes that were accreted onto western North America in the formation of the Cordilleran Region (Coney et al., 1980). The Alexander terrane extends the length of Southeast Alaska and north to the Yukon Territory, and it is unique in its long geological record from the Late Proterozoic to the Jurassic (Berg et al., 1972; Gehrels and Saleeby, 1987). This terrane includes the Nehenta Formation, which consists of Late Triassic marine sedimentary and subordinate volcanic rocks that crop out on Gravina Island (Berg, 1973). This formation consists of Late Triassic basaltic pillow lava, basaltic pillow breccia, andesitic volcanic breccia, and hyaloclastic tuff with subordinate tuffaceous polymict conglomerate, limestone, and volcaniclastic sandstone (Muffler, 1967). The Alexander terrane also includes the Hound Island Volcanics, which are temporally equivalent to the Nehenta Formation (Katvala and Stanley, 2008). The Hound Island Volcanics consist of basaltic pillow lava, basaltic pillow breccia, andesitic volcanic breccia as well as hyaloclastic tuff with subordinate polymict conglomerate, limestone, and volcaniclastic sandstone (Muffler, 1967). These sediments were deposited at lower latitudes along the margins of island arcs in the Panthalassan Ocean. The reconstructed Triassic paleolatitude of the Alexander terrane is approximately 20°N (Haeussler et al., 1992). Exposures of both of these units are best accessible in intertidal outcrops along the shores of islands that comprise much of Southeast Alaska (Berg, 1973).

The specimen UAMES 3599 is from the calcareous lowest unit of the Nehenta Formation, which is characterized by calcareous limestone and siltstone in its lower part and calcareous conglomerate, grit, and sandstone in its upper part (Berg, 1973). Berg (1973) assigned a Late Triassic age to the formation based on the presence of the bivalve *Halobia*. The age was revised to early to middle Norian by Caruthers and Stanley (2008) based on additional macrofossil and microfossil evidence, including corals and conodonts (specifically *Epigondolella quadrata* and *E. triangularis*). Analysis of conodonts demonstrated that equivalent deposits on the east side of Hound Island are middle Norian in age (Katvala and Stanley, 2008).

2.5 Materials

UAMES 3599 was relocated in July 2003 by one of us (JB) using Berg's original photographs and description of the locality from 1969. In the 34 years since its discovery, erosion had removed a portion of the dorsal vertebrae from the specimen; in some cases, bone was lost to weathering, but external molds remained. Excavation followed in 2004, and the specimen was removed from the outcrop using a rock saw and consolidated in a plaster jacket for transport. The specimen was prepared and curated in the Earth Sciences Collection at the University of Alaska Museum in Fairbanks, Alaska, USA. To help better visualize parts of the skeleton, including the caudal vertebrae and hindlimbs, silicone molds were made to fill in the external molds of bones lost to erosion. Plaster casts were also prepared from these molds.

UAMES 34994 was collected in the summer of 2005 as part of Adams' (2008) comprehensive study of the fossiliferous layers of the Hound Island Volcanics. The

specimen was acid prepared at Southern Methodist University, and subsequently accessioned into the Earth Sciences Collection at the University of Alaska Museum.

2.6 Description

2.6.1 UAMES 3599

The specimen is preserved in left lateral view. It consists of bone fragments and external molds of an incomplete, but partially articulated postcranial skeleton, including two dorsal and 18 articulated caudal vertebrae, a partial pelvic girdle, an articulated hind limb and a second femur (Figure 2-2A). The skull and forelimbs are not preserved. The specimen is small, approximately 47 cm long; it is estimated that the ichthyosaur would have been <1.5 m long in life.

2.6.1.1 Vertebrae

There are two articulated dorsal vertebrae present; however, the anterior vertebra is poorly preserved. The complete dorsal vertebra indicates a height:length ratio of 1.8.

There are 18 articulated caudal vertebrae preserved from the middle of the tail (Figure 2-2B-D). These vertebrae are arbitrarily assigned numbers 1-18 (from anterior to posterior) for the purpose of this study and do not refer to the actual vertebral number within the caudal series. A small fault interrupts the column between the tenth and eleventh vertebrae of the sequence.

The caudal vertebrae decrease in size posteriorly in both height and anteroposterior length. Weathering of vertebrae 1-7 resulted in exposure of their hourglass shape in sagittal section, with the anterior and posterior margins markedly concave. The weathering

has also revealed a hollow space in the middle of vertebrae 1, 2, 4-6; this is likely due to the weathering of the loose spongious bone in the region of the notochordal pit of the centra. The height:length ratio, measured from caudal vertebra 8, is 1.9; height was measured along the posterior margin and length was measured along the dorsal margin of the vertebra due to the effects of weathering. The tenth vertebra is rotated to expose the anterior surface and notochord pit; the diameter of this vertebra, calculated from the measured radius from the notochord pit to the posterior margin of the rotated vertebra, is 14.2 mm. The 16th, 17th, and possibly the 18th vertebrae in the succession are wedge-shaped (the dorsal length is longer than the ventral length), providing evidence of a tail bend in life; following McGowan (1989), we measured the most well-preserved apical vertebra (16) to calculate a tail bend of minimally 6.45 degrees.

Rib facets are visible on vertebrae 1, 3-4, 11-18; the parapophyses shift from dorsal-lateral to lateral posteriorly. External molds of the bases of neural spines are present for caudal vertebrae 1-9.

2.6.1.2 Hindlimbs

The femur is longer than it is wide at its maximum anteroposterior width, with a strongly constricted femoral shaft and a distal end that is expanded both pre- and postaxially (Figure 2-2E-G). The maximum anteroposterior width is reached at approximately 2/3 of the total length, with the width of the remaining 1/3 of the femur being equal or nearly equal to the maximum anteroposterior width. The tibial and fibular facets are concave and approximately equal in anteroposterior length. Due to the concavity of the facets, the distal-most point of the femur is pointed. The tibia and fibula are elongate and separated by a well-developed epipodial foramen. The anterior edge of the tibia is

notched. There is one disarticulated proximal tarsal preserved in external mold that is assumed to be the distal tarsal II. There are six additional distal elements of the hindlimb preserved in external molds that are assumed to be additional disarticulated proximal tarsals or phalanges, four of which appear to be notched.

2.6.2 UAMES 34994

UAMES 34994 consists of an isolated femur (Figure 2-3). Adams (2008) tentatively identified the specimen as a pubis and referred it to Hudsonelpidiidae. Like the femur of UAMES 3599, it is longer than it is wide at its maximum anteroposterior width, has a strongly constricted shaft, and a distal end that is expanded both pre- and postaxially. The distal end is broken; however, it appears to vary slightly from the femur of UAMES 3599 in the curvature of its preaxial surface, which continues to expand distally in anteroposterior width. The postaxial surface is similar to UAMES 3599 in that it reaches its maximum expansion at approximately 2/3 of the preserved length of the femur.

2.7 Discussion

Toretocnemus is a poorly known euichthyosaurian described by Merriam in 1903 from the Carnian of California. Merriam (1903) described the type species *Toretocnemus californicus* based on one partial articulated specimen consisting of dorsal vertebrae, anterior caudal vertebrae, dorsal ribs, one forelimb, the pelvic girdle, and two hindlimbs. A second species, *Toretocnemus zitelli*, also described by Merriam (1903) from a partial articulated specimen was referred to the genus by Motani (1999). The two type specimens of *T. californicus* and *T. zitelli* (UCMP 8100 and UCMP 8099, respectively) lack overlapping skeletal elements for sufficient comparison, resulting in their validity as two species being

questioned, but conservatively recognized (Motani, 1999). Additionally, both holotypes potentially represent composites of partially articulated skeletons of multiple individuals, further complicating the taxonomic validity (Motani, 1999). Recent phylogenetic analysis resolves the two species as sister taxa (Moon, 2019).

UAMES 3599 is referable to *Toretocnemus* based on the following characteristics of the hindlimb: (1) distinctive femur that is distally expanded pre- and postaxially, (2) a constricted femoral shaft, and (3) elongate epipodials separated by (4) a well-developed epipodial foramen (Merriam, 1903). The isolated femur from the Hound Island Volcanics, UAMES 34994, is also referable to *Toretocnemus* based on its similarly distinct morphology, including its distal expansion and constricted femoral shaft. Due to the lack of diagnostic characteristics to distinguish the two species, the Alaskan specimens are referred to genus- rather than species-level.

Toretocnemus and *Qianichthyosaurus* were united in the family Toretocnemidae by Maisch and Matzke (2000), and it has since been noted that they share many additional characteristics (Nicholls et al., 2002). At that time, only one species of *Qianichthyosaurus*, *Qianichthyosaurus zhoui* from the Falang Formation (Carnian, Late Triassic) of the Guizhou Province, South China, had been described (Li, 1999). A second species, *Qianichthyosaurus xingyiensis,* has since been described from the Xingyi Fauna (Ladinian, Middle Triassic) of the Guizhou Province, South China (Yang et al., 2013). In a comprehensive phylogenetic study at the generic level, Ji et al. (2016) recognized Toretocnemidae as valid; however, Moon (2019) did not resolve Toretocnemidae or *Qianichthyosaurus* as monophyletic in his species level analysis. For the purpose of this study, we acknowledge Toretocnemidae and compare the Alaskan specimens to *Q. zhoui* due to its Late Triassic (Carnian) age.

In comparison to *Q. zhoui*, both Alaskan specimens are smaller in overall size, and the femora are distinctly different in shape (Figure 2-4). The pre-axial distal end of the femur is more strongly expanded in both the new Alaskan material and the type material of *Toreteocnemus*. In addition, the femoral shaft and the elongate distal end of the femur are similar in length in *Toretocnemus*; the femoral shaft is longer than the distal end of the femur in *Q. zhoui*.

The downward tail bend and associated caudal fluke are a critical component of the thunniform body plan of post-Triassic ichthyosaurians (Motani 2005). The presence of a slight tail bend (also called a tail peak) may be a unifying character of all ichthyopteryians (Motani 1999); however, apical caudal vertebrae are poorly documented in Triassic ichthyosaurians (Massare and Callaway, 1990; Hogler and Kosch, 1993; McGowan and Motani, 1999). In many cases, fragmentary material does not include apical vertebrae (Nicholls and Manabe, 2001; Nicholls and Manabe, 2004). We document apical, or wedge-shaped caudal vertebrae for the first time in *Toretocnemus,* therefore demonstrating that this animal possessed a tail bend in life. Currently, the presence of apical vertebrae has not been confirmed in *Q. zhoui*, though specimens exhibit a tail bend in preservation (Li, 1999; Nicholls et al., 2002). Further study may permit characteristics of the apical vertebrae to either distinguish between these two genera or further support their union in the family Toretocnemidae.

The new material is the first record of *Toretocnemus* in northwestern North America, although it was deposited at lower latitudes (approximately 20° N) in the Panthalassan Ocean in the Late Triassic (Haeussler et al., 1992). Additional specimens of *Toretocnemus* from the Hosselkus Limestone, as well as the closely related *Q. zhoui* from

the South China Block, were also deposited on island arcs that existed in the paleo-Pacific of the Late Triassic (Nicholls et al., 2002). These specimens corroborate the cosmopolitan nature of Late Triassic ichthyosaurian paleobiogeography as discussed by Nicholls et al. (2002), with a trans-Pacific distribution of closely related taxa rather than distinct Tethyan and paleo-Pacific faunas. By the Late Triassic, ichthyosaurians had evolved a derived body plan, as demonstrated by the paddle-like limbs and tail bend documented here. Although this slight tail bend is subtle compared to the deflection seen in Jurassic ichthyosaurians (Massare and Callaway, 1990), its presence suggests *Toretocnemus* was a well-adapted swimmer capable of inhabiting areas around island arc systems, providing a mechanism for sustaining a trans-Pacific fauna.

Prior to this study, *Toretocnemus* was restricted to Carnian-aged strata of California and possibly Sonora, Mexico (Merriam, 1903; Lucas, 2002). Based on biostratigraphic evidence, the new Alaskan specimens extend the stratigraphic range of the genus *Toretocnemus* into the Norian (Berg, 1973). Late Triassic ichthyosaurians are well known from Carnian localities in North America (the Hosselkus Limestone in California and the Berlin-ichthyosaur State Park in Nevada) and China (the Guanling Fauna); however, there are very few documented Norian-aged ichthyosaurians (Table 1). Of the currently known Norian specimens, most have affinities to the large-bodied shastasaurids, and the few exceptions are described as more closely resembling Early Jurassic rather than Late Triassic forms (*Hudsonelpidia breviceps* and *Macgowania janiceps*). These specimens provide support that small-bodied ichthyosaurians similar to those from Carnian-aged deposits persisted into the Norian alongside these Jurassic-like taxa ahead of the end Triassic extinction event.

2.8 Acknowledgements

We thank B. Schumacher, R. Blodgett, G. Stanley, A. Caruthers, R. Troll, and J. Rousseau for aid in relocation, collection and curation of UAMES 3599. We also thank H. Foss for her contributions to the line drawings included in the figures of this publication. This research was funded by the National Science Foundation GK-12 Changing Alaska Science Education fellowship (NSF DGE-0948029; PIs R. Boone, L. Conner, and K. Winker) and the University of Alaska Museum.

2.9 References

Adams, T.L. 2008. *Deposition and taphonomy of the Hound Island vertebrate fauna from the Late Triassic (Middle Norian) of Southeast Alaska*. M.S. Thesis, Southern Methodist University- Dallas, Texas, U.S.A.

Berg, H.C. 1973. Geology of Gravina Island, Alaska. *United States. Geological Survey Bulletin,* 1373, 41 p.

Berg, H.C., Jones, D.L., and Richter, D.H. 1972. Gravina-Nutzotin belt-Tectonic significance of an Upper Mesozoic sedimentary and volcanic sequence in southern and southeastern Alaska. *United States Geological Survey Professional Paper,* 800:D1-D24.

Callaway, J.M. and Massare, J.A. 1989. *Shastasaurus altispinus* (Ichthyosauria, Shastasauridae) from the Upper Triassic of the El Antimonio district, northwestern Sonora, Mexico. *Journal of Paleontology*, 63(6):930-939.

Camp, C. L. 1980. Large ichthyosaurs from the Upper Triassic of Nevada. *Palaeontographica, Abteilung A* 170:139-200.

Caruthers, A.H. and Stanley Jr, G.D. 2008. Late Triassic silicified shallow-water corals and other marine fossils from Wrangellia and the Alexander terrane, Alaska, and Vancouver Island, British Columbia. p.151-179. In Blodgett, R.B. and Stanley, Jr., G.D. (eds.), *The Terrane Puzzle: New Perspectives on Paleontology and Stratigraphy from the North American Cordillera.* The Geological Society of America, Boulder, CO.

Coney, P.J., Jones, D.L. and Monger, J.W. 1980. Cordilleran suspect terranes. *Nature*, 288(5789):329.

Dong, Z.-M. 1972. An ichthyosaur fossil from the Qomolangma Feng region. p. 7-10. In Young, C.C. and Dong, Z.-M. (eds.) *Aquatic reptiles from the Triassic of China*. Academia Sinica Institute of Vertebrate Paleontology and Palaeoanthropology, Memoir 9, Peking, China. [in Chinese.]

Druckenmiller, P.S., Kelley, N., Whalen, M.T., Mcroberts, C. and Carter, J.G. 2014. An Upper Triassic (Norian) ichthyosaur (Reptilia, Ichthyopterygia) from northern Alaska and dietary insight based on gut contents. *Journal of Vertebrate Paleontology*, 34(6):1460-1465.

Gehrels, G.E. and Saleeby, J.B. 1987. Geologic framework, tectonic evolution, and displacement history of the Alexander terrane. *Tectonics*, 6(2):151-173.

Haeussler, P., Coe, R.S. and Onstott, T.C. 1992. Paleomagnetism of the Late Triassic Hound Island Volcanics: Revisited. *Journal of Geophysical Research: Solid Earth*, 97(B13):19617-19639.

Hogler, J.A. and Kosch, B.F. 1993. Tail-bends of Triassic ichthyosaurs: a reappraisal. *Journal of Vertebrate Paleontology,* 13:41A.

Ji, C., Jiang, D.Y., Motani, R., Rieppel, O., Hao, W.C. and Sun, Z.Y. 2016. Phylogeny of the Ichthyopterygia incorporating recent discoveries from South China. *Journal of Vertebrate Paleontology*, 36(1):e1025956.

Karl, H.-V., Arp, G., Siedersbeck, E. and Reitner, J. 2014. A large ichthyosaur vertebra from the lower Kössen Formation (Upper Norian) of the Lahnewiesgraben near Garmisch-Partenkirchen, Germany. In Wiese, F., Reich, M. and Arp, G. (eds*.), "Spongy, slimy, cosy & more...". Commemorative volume in celebration of the 60th birthday of Joachim Reitner. Göttingen Contributions to Geosciences,* 77: 191–197. http://dx.doi.org/10.3249/webdoc-3929

Katvala, E.C. and Stanley Jr, G.D. 2008. Conodont biostratigraphy and facies correlations in a Late Triassic island arc, Keku Strait, southeast Alaska. p.181-226. In Blodgett, R.B. and Stanley, Jr., G.D. (eds.), *The Terrane Puzzle: New Perspectives on Paleontology and Stratigraphy from the North American Cordillera.* The Geological Society of America, Boulder, CO.

Kosch, B.F. 1990. A revision of the skeletal reconstruction of *Shonisaurus popularis* (Reptilia: Ichthyosauria). *Journal of Vertebrate Paleontology*, 10(4):512-514.

Li, C. 1999. Ichthyosaur from Guizhou, China. *Chinese Science Bulletin*, 44(14):1329-1333.

Lucas, S.G. 2002. *Toretocnemus*, a Late Triassic ichthyosaur from California, U.S.A and Sonora, Mexico. *New Mexico Museum Natural History and Science Bulletin,* 21:275-282.

Massare, J.A. and Callaway, J.M. 1990. The affinities and ecology of Triassic ichthyosaurs. *Geological Society of America Bulletin*, 102(4):409-416.

Maisch, M. W. and Matzke, A. T. 2000. The Ichthyosauria. *Stuttgarter Beiträge zur Naturkunde, Serie B*, 298:1-159.

Maisch, M.W., Jiang, D.Y., Hao, W.C., Sun, Y.L., Sun, Z.Y. and Stöhr, H. 2008. A well-preserved skull of *Qianichthyosaurus zhoui* Li, 1999 (Reptilia: Ichthyosauria) from the Upper Triassic of China and the phylogenetic position of the Toretocnemidae. *Neues Jahrbuch für Geologie und Paläontologie-Abhandlungen*, 248(3):257-266.

McGowan, C. 1989. The ichthyosaurian tailbend: a verification problem facilitated by computed tomography. *Paleobiology*, 15(4):429-436.

McGowan, C. 1991. An ichthyosaur forefin from the Triassic of British Columbia exemplifying Jurassic features. *Canadian Journal of Earth Sciences*, 28(10):1553-1560.

McGowan, C. 1994. A new species of *Shastasaurus* (Reptilia: Ichthyosauria) from the Triassic of British Columbia: the most complete exemplar of the genus. *Journal of Vertebrate Paleontology*, 14(2):168-179.

McGowan, C. 1995. A remarkable small ichthyosaur from the Upper Triassic of British Columbia, representing a new genus and species. *Canadian Journal of Earth Sciences*, 32(3):292-303.

McGowan, C. 1996. A new and typically Jurassic ichthyosaur from the Upper Triassic of British Columbia. *Canadian Journal of Earth Sciences*, 33(1):24-32.

McGowan, C. and Motani, R. 1999. A reinterpretation of the Upper Triassic ichthyosaur *Shonisaurus*. *Journal of Vertebrate Paleontology*, 19(1):42-49.

Merriam, J.C. 1895. On some reptilian remains from the Triassic of Northern California. *American Journal of Science* (1880-1910), 50(295):55.

Merriam, J.C. 1903. *New Ichthyosauria from the Upper Triassic of California*. University of California Press.

Moon, B. C. 2019. A new phylogeny of ichthyosaurs (Reptilia: Diapsida). *Journal of Systematic Palaeontology*, 17(2), 129-155.

Motani, R. 1999. Phylogeny of the Ichthyopterygia. *Journal of Vertebrate Paleontology*, 19(3):473-496.

Motani, R. 2005. Evolution of fish-shaped reptiles (Reptilia: Ichthyopterygia) in their physical environments and constraints. *Annual Review of Earth and Planetary Sciences,* **33**, 395–420.

Motani, R., Manabe, M. and Dong, Z.-M. 1999. The status of *Himalayasaurus tibetensis* (Ichthyopterygia). *Paludicola*, *2*(2):174-181.

Muffler, L. J. 1967, Stratigraphy of the Keku Islets and neighboring parts of Kuiu and Kupreanof Islands, Southeastern Alaska. *United States Geological Survey Bulletin,* 1241– C. 52 pp.

Nicholls, E.L. and Manabe, M. 2001. A new genus of ichthyosaur from the Late Triassic Pardonet Formation of British Columbia: bridging the Triassic–Jurassic gap. *Canadian Journal of Earth Sciences*, 38(6):983-1002.

Nicholls, E.L. and Manabe, M. 2004. Giant ichthyosaurs of the Triassic—a new species of *Shonisaurus* from the Pardonet Formation (Norian: Late Triassic) of British Columbia. *Journal of Vertebrate Paleontology*, 24(4):838-849.

Nicholls, E.L., Wei, C. and Manabe, M. 2002. New material of *Qianichthyosaurus* Li, 1999 (Reptilia, Ichthyosauria) from the Late Triassic of southern China, and implications for the distribution of Triassic ichthyosaurs. *Journal of Vertebrate Paleontology*, 22(4):759-765.

Orr, W.N., Vallier, T.L. and Brooks, H.C. 1986. A Norian (Late Triassic) ichthyosaur from the Martin Bridge Limestone, Wallowa Mountains, Oregon. *United States Geological Survey, Professional Paper,* 1435:41-47.

Riehle, J.R., Fleming, M.D., Molnia, B.F., Dover, J.H., Kelley, J.S., Miller, M.L., Nokleberg, W.J., Plafker, G. and Till, A.B. 1997. Digital shaded-relief image of Alaska. *United States Geological Survey*, *92*:C4004.

Yang, P., Ji, P., Jiang, D., Motani, R., Tintori, A., Sun, Y. and Sun, Z. 2013. A new species of *Qianichthyosaurus* (Reptilia: Ichthyosauria) from the Xingyi Fauna (Ladinian, Middle Triassic) of Guizhou. *Beijing Daxue Xuebao*, *49*(6), 1002-1008.

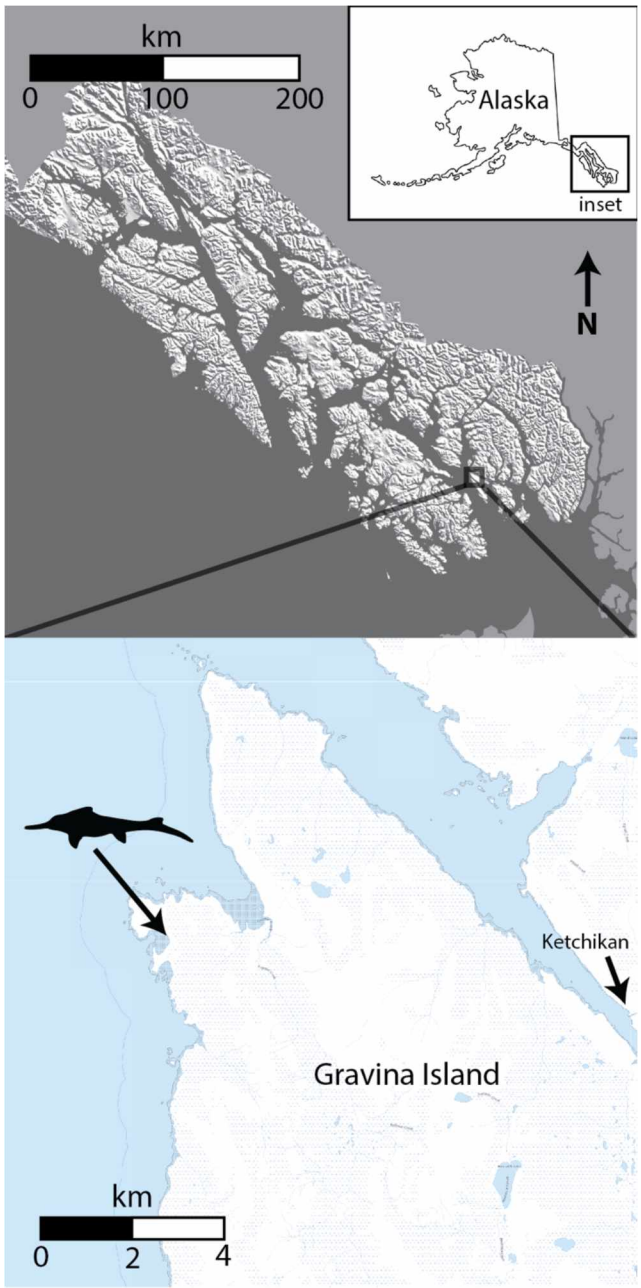

Figure 2-1. Map of locality where UAMES 3599 referred specimen of *Toretocnemus* sp. was collected on Gravina Island in Southeast Alaska, U.S.A. Digital shaded relief image modified from Riehle et al. (1997). Inset map of Gravina Island modified from USGS The National Map: National Hydrography Dataset.

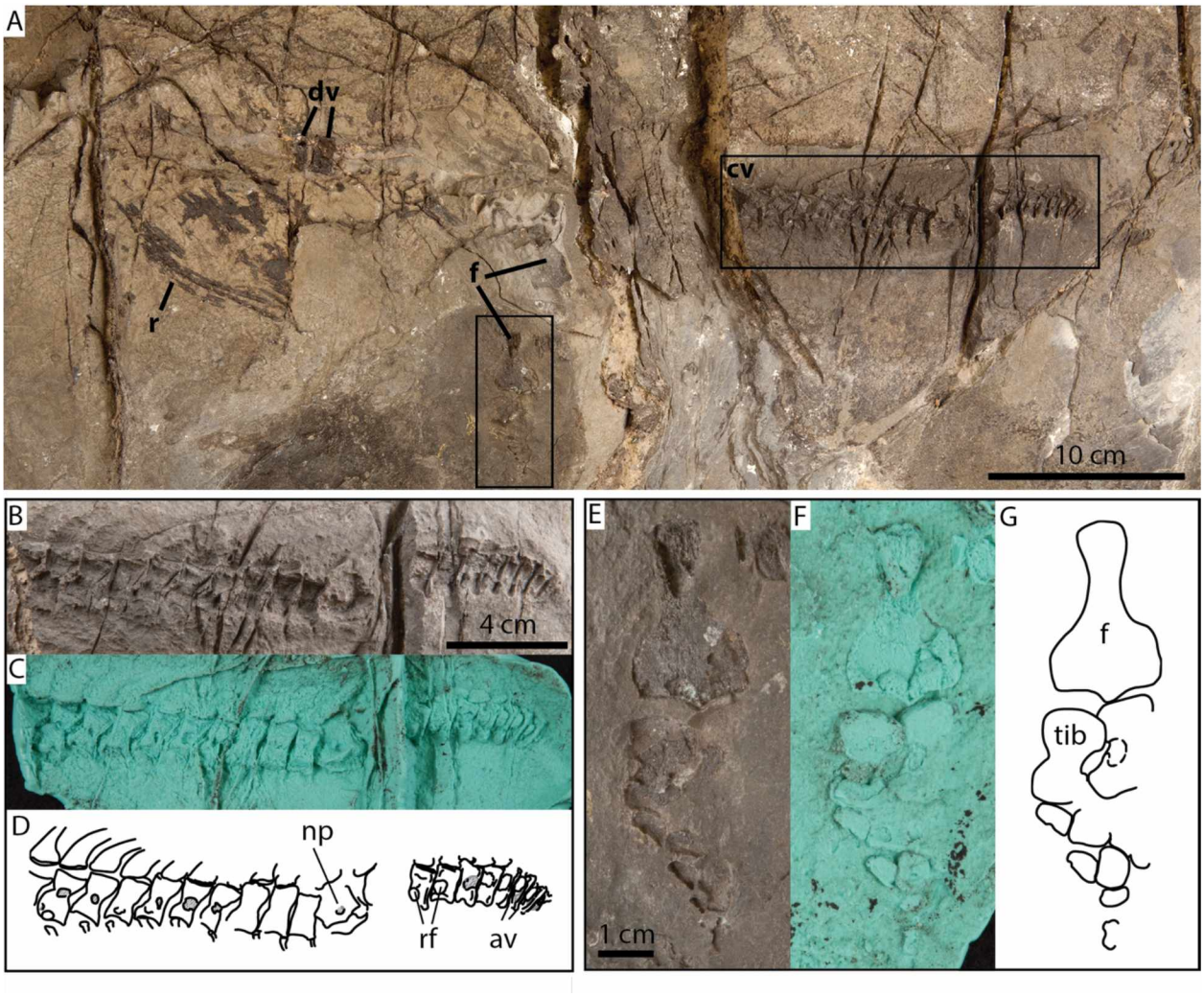

Figure 2-2. UAMES 3599 referred specimen of *Toretocnemus* sp. from Gravina Island, Southeast Alaska. A. Overview of UAMES 3599. Subsets of articulated caudal vertebrae shown in B-D, and articulated hindlimb shown in E-G. B. Articulated caudal vertebrae of UAMES 3599. C. Silputty mold of the caudal vertebrae of UAMES 3599 (image mirrored). D. Interpretation of the caudal vertebrae of UAMES 3599. E. Articulated hindlimb of UAMES 3599. F. Silputty mold of the hindlimb of UAMES 3599 (image mirrored). G. Interpretation of the hindlimb of UAMES 3599. Abbreviations: av, apical vertebrae; cv, caudal vertebrae; dv, dorsal vertebrae; f, femur; np, notochord pit; r, rib; rf, rib face; tib, tibia.

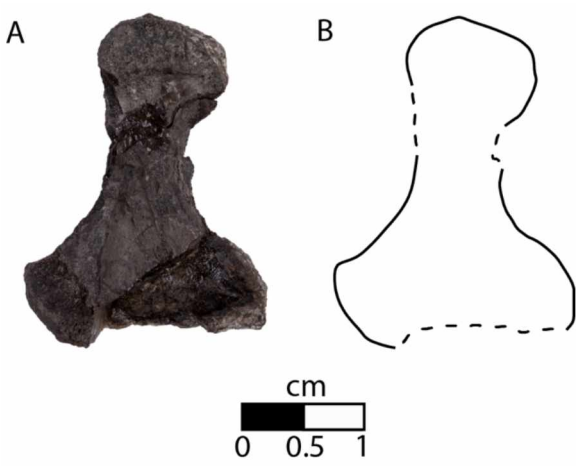

Figure 2-3. UAMES 34994 referred specimen of *Toretocnemus* sp. from Hound Island, Southeast Alaska. A. Overview of UAMES 34994. B. Interpretation of UAMES 34994.

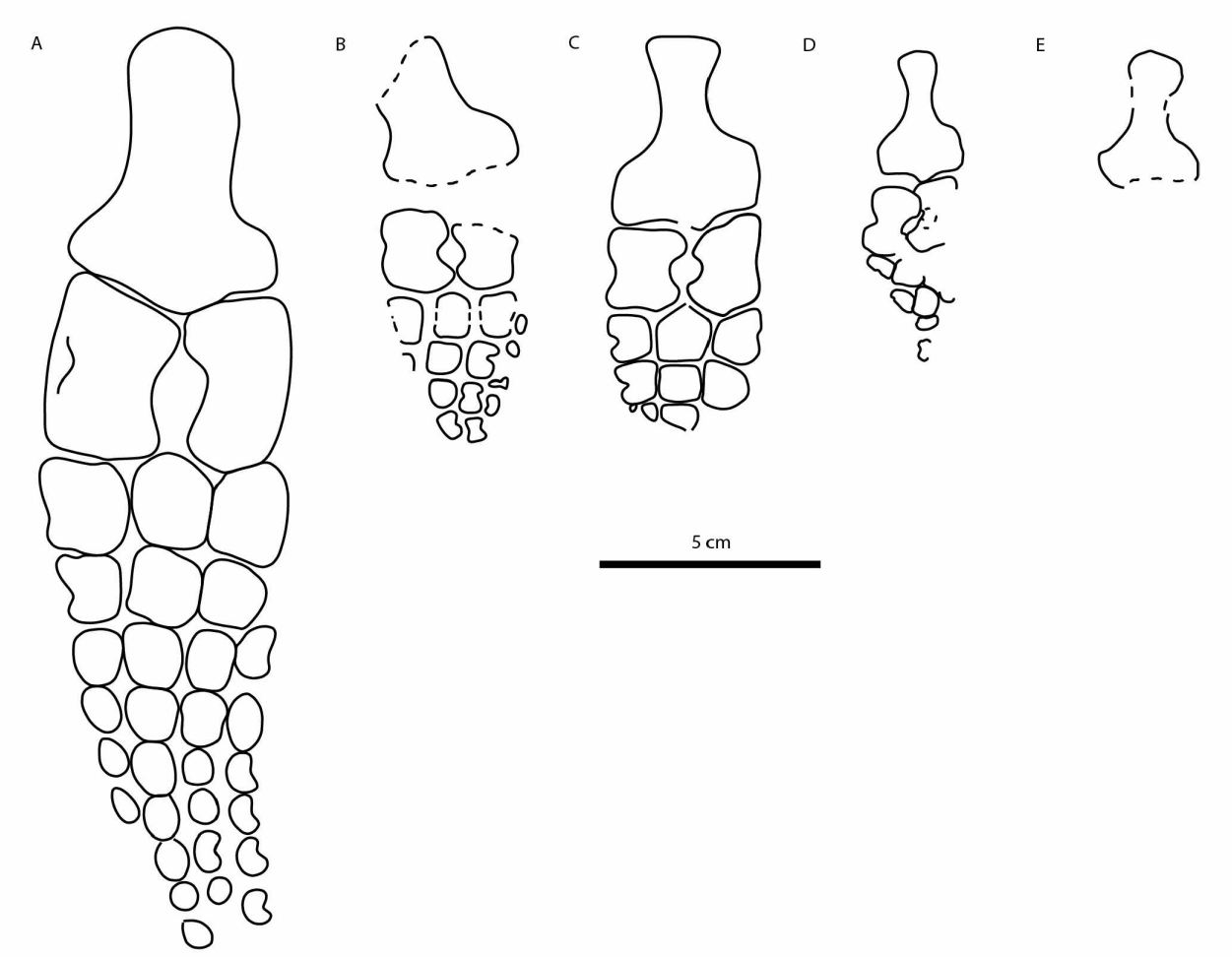

Figure 2-4. Hind paddles of small-bodied Late Triassic ichthyosaurians. A. CMNH V1412/C1120 *Qianichthyosaurus zhoui*. B. UCMP 8099 *Toretocnemus zitelli* (Merriam, 1903) type specimen. C. UCMP 8100 *Toretocnemus californicus* Merriam, 1903 type specimen. D. UAMES 3599 referred specimen of *Toretocnemus* sp. E. UAMES 34994 referred specimen of *Toretocnemus* sp.

Table 2-1. Overview of Norian ichthyosaurians by locality.

Locality	Age	Geological unit	Known taxa	References
Gravina Island, Southeast Alaska	Early-Middle Norian	Nehenta Formation	*Toretocnemus* sp.	This manuscript
Pink Mountain, British Columbia, Canada	Early-Middle Norian	Pardonet Formation	*Callawayia neoscapularis*; *Shonisaurus sikanniensis*	Nicholls and Manabe, 2001; Nicholls and Manabe, 2004
Williston Lake, British Columbia, Canada	Early-Middle Norian	Pardonet Formation	*Callawayia neoscapularis*; *Macgowania janiceps*; *Hudsonelpidia brevirostris*	McGowan, 1991; McGowan, 1994; McGowan, 1995; McGowan, 1996
Hound Island, Southeast Alaska	Middle Norian	Hound Island Volcanics	*Shonisaurus* sp.; cf. *Macgowania*; Ichthyosauria indet.; *Toretocnemus* sp.	Adams, 2008; This manuscript
Cutaway Creek, Central Brooks Range, Northern Alaska	Late Norian	Otuk Formation	Shastasauridae	Druckenmiller et al., 2014
Lahnewiesgraben near Garmisch-Partenkirchen, Germany	Late Norian	Lower Kössen Formation	*Shonisaurus* sp.	Karl et al., 2014
Eagle Creek, Wallowa Mountains, Northeastern Oregon	Norian	Martin Bridge Limestone	*Shastasaurus* sp.	Orr, 1988
Tibet	Norian	unknown	*Himalayasaurus tibetensis*	Dong, 1972; Motani et al., 1999

Chapter 3. Skeletal microstructure of *Stenopterygius quadriscissus* (Reptilia: Ichthyosauria) from the Posidonienschiefer (Posidonia Shale, Lower Jurassic) of Germany[2]

3.1 Abstract

Ichthyosaurians (Ichthyosauria) are a major clade of secondarily aquatic marine tetrapods that occupied several major predatory niches during the Mesozoic Era. Multiple lines of evidence including isotopic, body shape and swimming modality analyses suggest they exhibited elevated growth and metabolic rates, and body temperatures. However, applications of osteohistological methods to test hypotheses regarding their physiology are few. Previous studies focused on the humeri, vertebrae and ribs from a small number of taxa. Here, we use osteohistological methods to describe the bone microstructure of over 30 cranial and post-cranial elements from a nearly complete, articulated individual of *Stenopterygius quadriscissus* from the Posidonienschiefer Formation *(*Posidonia Shale, Lower Jurassic) of Germany. The specimen shows highly vascularized primary bone and spongious secondary bone in its limbs, suggesting an overall shift to a lighter spongious structured skeleton was achieved through multiple developmental mechanisms. The modified perichondral ossification in elements of the limbs distal to the stylopodium informs our understanding of functional morphology, including hydrodynamic forces on the paddles. The ribs show variation in cortical thickness and trabecular organization along

[2] ANDERSON, K.L., DRUCKENMILLER, P.S., ERICKSON, G.M. and MAXWELL, E.E. 2019. Skeletal microstructure of *Stenopterygius quadriscissus* (Reptilia, Ichthyosauria) from the Posidonienschiefer (Posidonia Shale, Lower Jurassic) of Germany. *Palaeontology* ***62***(3), 433-449.

their length. Cyclical growth is inferred from changes in vascularization and osteocyte density as well as the presence of annuli in primary fibrolamellar bone. Cranial elements, due to their relative density and better preservation of growth marks, may prove to be of particular importance in future skeletochronological studies of post-Triassic ichthyosaurians. We infer and corroborate hypotheses of elevated growth rates and metabolic rates in ichthyosaurians, and the potential for thermoregulation similar to extant homeothermic ectotherms.

3.2 Introduction

Ichthyopterygians (Ichthyopterygia) are a major clade of secondarily aquatic marine tetrapods that first appeared approximately 251 million years ago, and came to occupy most large predatory niches throughout their 160-million-year tenure during the Mesozoic Era. The most diverse and successful ichthyopterygians were the ichthyosaurians (Ichthyosauria). These animals evolved hydrodynamically-efficient thunniform body plans reminiscent of modern endothermic marine vertebrates such as tunas, lamniform sharks and cetaceans (Motani 2005), as well as enormous eyeballs that facilitated vision in low light aquatic conditions (Motani et al. 1999). Furthermore, swimming modality, body shape, and isotopic analyses suggest they exhibited metabolic rates and body temperatures akin to endothermic rather than ectothermic vertebrates (Massare 1988; Motani 2002a, b; Bernard et al. 2010; Motani 2010).

A paleobiological revolution using osteohistological methods has enhanced the ability to address questions about the development and physiology of extinct vertebrate taxa (Chinsamy and Hillenius 2004; Erickson 2005, 2014). Analyses of bone and tooth

microstructure through the use of physical or virtual (microCT) thin sections can provide direct evidence of an animal's age at death, growth, tooth replacement rates, incubation periods, and population biology, from which inferences about metabolic rates and thermoregulation can be gleaned (Francillon-Vieillot et al. 1990; Castanet et al. 1993; Erickson 1996; Erickson and Tumanova 2000; Erickson et al. 2001, 2004, 2017; Horner et al. 2000; Horner and Padian 2004; Botha and Chinsamy 2004; Sanchez et al. 2012). While these methods have extensively expanded our understanding of the paleobiology of select vertebrate groups, dinosaurs and therapsids in particular, their application to Mesozoic marine reptiles is still in its infancy.

With regard to ichthyosaurs, the focus of the present study, bone microstructure has been examined in a minimum of twelve of the known genera (Table 1). In addition, tooth microstructure has been examined in several genera (Kiprijanoff 1881-1883; Fraas 1891; Bauer 1898; Gross 1934; Besmer 1947; Edmund 1960; Maxwell et al. 2011; Scheyer and Moser 2011; Maxwell et al. 2012). While there have been an increasing number of osteohistological studies in recent years, they have primarily focused on the examination of the humeri, ribs and vertebrae, often with taxonomic identification limited to the generic level. Collectively these studies suggest ichthyopterygians: 1) occupied a diverse set of ecological niches across time and space with the majority of post-Triassic ichthyosaurians exhibiting spongious bone typical of extant cetaceans and some marine turtles, and 2) showed more rapid growth rates and possessed elevated metabolic rates relative to modern ectothermic reptiles of similar body sizes.

In secondarily aquatic tetrapods, vertebrae, ribs and stylopodial elements and their microstructure become highly modified during the evolutionary shift to an aquatic

environment (Houssaye et al. 2016). Additional elements may preserve microstructural signals such as growth marks that would be useful for skeletochronology, but have yet to be examined. With regard to ichthyosaurians, only a single study sampled a variety of elements (humerus, femur, fibula, ischium, ulna, phalanges) across an individual specimen of *Mixosaurus* sp. (additional elements [humeri, ribs, gastralia] from two other specimens were also included in the analysis; Kolb et al. 2011). In particular, the gastralia of *Mixosaurus* sp. preserved novel paleobiological data in the form of more numerous growth marks than the highly remodeled podial elements. Additionally, ichthyosaurian paddles have also been the focus of several morphological studies related to their development and ossification, but very few osteohistological studies have sampled distal to the stylopodium in order to corroborate hypotheses of modified perichondral ossification (Caldwell 1997a,b; Maxwell 2012b; Maxwell et al. 2014).

Although cyclical growth has been suggested for ichthyosaurians based on the presence of vascular cycles in their bones, definitive growth marks such as annuli or lines of arrested growth (LAGs) are only known in the ichthyosaurian taxon *Mixosaurus* (Kolb et al. 2011). Currently, elevated growth rates in ichthyosaurians are suggested qualitatively in relation to extant reptiles of similar body mass based on the organization of the bone matrix. The absence of these growth marks in well-studied stylopodial elements has precluded ichthyosaurians from skeletochronological analysis, thus preventing the study of quantitative age and growth despite the prevalence of this clade in the fossil record (Houssaye et al. 2014). The study of bone microstructure across the skeleton, as demonstrated by Kolb and colleagues (2011) allows the identification of elements that may be useful for skeletochronological studies, as well as increases the understanding of overall

skeletal development. Ultimately, the integration of growth and development, as well as inferences of metabolic rate and thermoregulation, into a phylogenetic context would allow a greater understanding of the evolution of this successful clade. It is pertinent to begin this process with a well-studied taxon known from abundant material.

In this study, we describe and interpret the skeletal microstructure for a diversity of cranial and post-cranial elements from an individual specimen of *Stenopterygius quadriscissus*. Previously only the humerus and femur of this species have been histologically described (de Buffrénil and Mazin 1990), however, the species level identification of this material is equivocal because both were recovered as isolated elements. We use the bone microstructure to infer aspects of physiology in this species, such as growth rate and potential for elevated metabolic rate and thermoregulation. Furthermore, we examine the paleobiological implications for both *Stenopterygius* and post-Triassic ichthyosaurians through comparison with existing data across Ichthyopterygia as a whole, as well as other secondarily aquatic marine tetrapods.

3.3 Materials and Methods

Stenopterygius quadriscissus (Quenstedt, 1856) is a medium-sized ichthyosaurian (up to 3.5 m in length) best known from the Posidonienschiefer Formation (Posidonia Shale, lower Toarcian; also known as Late Liassic or Lias ε) deposits of the Southwest German Basin surrounding the town of Holzmaden, Germany where over 3000 complete or nearly complete articulated ichthyosaur specimens have been recovered, 80 percent of which are referable to *Stenopterygius* (Hauff 1921; Sander 2000; McGowan and Motani 2003; Maisch 2008; Maxwell 2012a). The formation is divided into three subcategories (I,

II, III) and further divided into beds denoted with subscripts. It is comprised of shale interbedded with limestone deposited in an epicontinental basin that experienced periodic fluctuations in benthic oxygen levels (Röhl et al. 2001, 2002; Röhl and Schmid-Röhl 2005). Periodic anoxic conditions contributed to the exceptional preservation of both invertebrate and vertebrate fauna, making it one of the best-known examples of a Konservat-Lagerstätten (Martill 1993).

Specimen SMNS 4789 (Staatliches Museum für Naturkunde Stuttgart, Germany) (Fig. 3-1), from Lias ε II_5 (*serpentinum* Zone, *exaratum* Subzone) was discovered in 1866 near Holzmaden, Germany. It is unambiguously referred to *Stenopterygius quadriscissus* based on Maxwell's (2012a) comprehensive classification scheme. The specimen is a nearly complete articulated individual measuring 207.25 cm total length (168.25 cm pre-apical vertebrae length) — approximately 59% of the estimated maximum body length for this species. However, with a lower jaw length of greater than 42.5 cm (anterior and posterior ends of the lower jaw missing), it is larger than the smallest known gravid female of the species (McGowan 1979). Skeletal and sexual maturity are dissociated in *Stenopterygius* (Johnson 1977), and based on these measurements, this specimen is somatically a late stage sub-adult or adult. SMNS 4789 is laterally compressed and was prepared with the right side exposed (stratigraphically upwards). Its midsection, including the majority of the ribs, gastralia and forelimbs, envelope a large pyrite concretion. The pyritic formation only locally affects the surface of some elements. Historical preparation techniques resulted in the loss of some material on the exposed surfaces of bones. Nevertheless, the unprepared surfaces are well preserved and complete making it an excellent candidate for osteohistological sampling.

Elements were selected in order to provide a thorough sampling across the skeleton. Sample elements include the premaxilla, dentary, teeth, caudal vertebra, ribs, gastralia, humerus, radiale, metacarpal II, forelimb phalanges, ischiopubis, femur, fibula, calcaneum, and hindlimb phalanges. Selected sections were removed from the skeleton using a rock saw (Hitachi BSL1430 with diamond-tipped blade). The samples were embedded in epoxy (Allied High Tech Products, Inc.), sectioned using a diamond blade on a slow speed saw (Isomet 1000, Buehler), mounted on petrographic slides, and sanded and polished to thicknesses whereby the microstructure could be viewed using petrographic polarized microscopy. Specifically, the sections were analyzed using a transmitted light microscope (Zeiss 47 30 28) under both normal and cross-polarized light (Zeiss 47 30 59). Transmitted light (normal and cross-polarized) photographs were taken using a Nikon DS-Fi1 camera mounted on Leitz Ortholux IIPOL-BK microscope. The sections were also digitally documented using an Epson Artisan 837 scanner (Epson America, Inc.).

Bone and tooth microstructure are described (Orban and Sicher 1966; Francillon-Vieillot et al. 1990; Dean 2000), and used to infer development across the skeleton, growth rates and aspects of physiology such as metabolic rate and potential for thermoregulation. Results are compared and synthesized with existing studies that have inferred growth and physiology of ichthyopterygians.

3.4 Results

Many of the large elements that were sectioned are compressed and show fragmented spongiosa in the medullary region of the bone. Smaller elements tend to show less crushing of the spongiosa, presumably due to their relatively thicker cortices as well as

more compact spongiosa. Loss of material due to historical preparation of the specimen affected the amount of compact bone present, resulting in inconsistencies between the thickness of compact bone on the prepared versus unprepared surfaces. All elements are permineralized by recrystallized calcite, and the matrix shows fine microlaminations typical of the formation. Although pyrite covered some bone surfaces, it did not penetrate or otherwise affect the preservation of biogenic structures within the bone.

3.4.1 Skull and teeth.

The dentary and premaxilla are the most compact bones sampled in this study. These were sectioned in the frontal plane, 50.2 mm from the most anterior point of the fractured rostrum. They show fibrolamellar primary bone with longitudinal vascularization organized in cyclical, circumferential rows interspersed with radial and to a lesser extent plexiform vascularization (Fig. 3-2). Both the dentary and premaxilla show growth rings in the form of annuli in the primary bone (four in the dentary, and four in the premaxilla) (Fig. 3-2A-C). In the inner cortex, the annuli are associated with an increase in the number of osteocyte lacunae in the subsequent zone of fibrolamellar bone. They appear darker in color in normal light and are thus visible at low magnification. In cross-polarized light, the annuli are obscured in some cases by radially oriented fibers and, in this specimen particularly, mineral inclusions; where they are visible, they appear as distinct lines demarcating zones of different mineral orientations. The zones between annuli decrease in width toward the periphery. Secondary bone is lamellar and surrounds longitudinal Haversian vascular canals. In the premaxilla, the bone tissue wraps around an internal foramina and external grooves.

One tooth positioned next to the dentary was sectioned transversely (Fig. 3-3A). The presence of a foramen (pulp cavity) as well as a layer of cementum surrounding the dentine suggests the tooth was sectioned basal to the crown, but the exact position is indeterminable. Prevalent dentinal tubules, non-undulating and oriented radially, are visible in the orthodentine. Daily forming incremental lines of von Ebner, albeit poorly expressed are locally present, as are weekly lines in the form of light and dark banding (Fig. 3-3B). These features are also visible in additional fragmentary tooth material that was sectioned in association with the rostrum (Fig. 3-3C).

3.4.2 Axial skeleton.

3.4.2.1 Vertebral centrum and caudal rib. The caudal centrum was sectioned sagittally, and shows a thin layer of calcified cartilage in the endochondral territory on the anterior and posterior surfaces except where material was removed during preparation (Fig. 3-4). The endochondral bone is parallel-fibered and spongious with vascularization oriented perpendicular to the surface of the bone interspersed with simple circular canals (Fig. 3-4B). The two cones of periosteal bone extend dorsally and ventrally from the constricted center of the vertebra and are also spongious. The primary periosteal bone, visible at the dorsal and ventral surfaces, is parallel-fibered and highly vascularized with vascular canals oriented predominantly parallel to the dorsal and ventral surfaces with few simple round canals (Fig. 6A-1). The endochondral and periosteal territories are clearly identifiable, and their organization corresponds to microanatomical type 2 (Houssaye et al. 2018). Remodeling has led to the formation of erosion bays and very loose spongiosa in the ventral and dorsal regions, with trabeculae showing secondary lamellar bone and

remnants of primary bone (Fig. 6A-1). In the most constricted area of the centrum, there are large round erosion bays in otherwise relatively dense bone.

Dorsal and caudal neural spines were also sampled, but are too poorly preserved due to compression and crushing to describe the microstructure. Another element that is likely a partial caudal rib was cross-sectioned in association with the caudal centrum. It shows loose spongiosa consisting of secondary lamellar bone and a layer of calcified cartilage on some surfaces (Fig. 3-4C).

3.4.2.2 Ribs. Because of the preservation of the dorsal ribs of the specimen (including superimposition and taphonomic compression), it was not possible to section one single dorsal rib longitudinally or transversely at different points along its length. Hence, multiple dorsal ribs (ten total) were sectioned transversely to study microstructural changes along rib length. These sections are described based on where along the rib length they were taken: proximal (four sectioned), mid-shaft (three sectioned) and distal (three sectioned) (Fig. 3-5; Anderson et al. 2018, Fig. 6A-2). The mid-shaft sections of the ribs show pyrite adhering to the periosteal surfaces but these mineral deposits did not affect the osseous microstructure. All ribs show fibrolamellar primary bone tissue with longitudinal primary osteons. Osteocyte lacunae are organized in cyclical, circumferential rows that vary by the density of lacunae, resulting in the appearance of light and dark cycles around the circumference of the primary compact bone in normal light (Fig. 3-5C). The light cycles correspond to three annuli consisting of low numbers of osteocyte lacunae in parallel-fibered bone that are anisotropic in cross-polarized light, while the dark cycles correspond to zones consisting of high numbers of osteocyte lacunae in fibrolamellar bone. They do not possess a medullary cavity, but instead medullary regions with round intertrabecular

spaces separated by thick trabeculae. The intertrabecular spaces decrease in size toward the cortex and are surrounded by secondary lamellar bone.

Variation in structure along the rib length is evident. The compact bone of the cortex is thicker at mid-shaft relative to proximal and distal sections. The transition between the compact bone and spongy bone is gradual in the proximal rib section and abrupt in the mid-shaft. This difference results in smaller, more numerous longitudinal vascular canals present in the periosteal bone of the proximal rib than the mid-shaft. The distal rib sections are crushed, but appear to be more similar to the mid-shaft with regard to vascularization and a more abrupt transition between compact and spongy bone.

3.4.3 Other skeletal elements

3.4.3.1 Gastralia. Three gastralia were sectioned transversely (Fig. 3-5E; Fig. 6A-3). There is a thick layer of primary compact bone that is parallel-fibered. The medullary region is comprised of secondary lamellar trabecular bone.

3.4.4 Appendicular skeleton

3.4.4.1 Humerus. The humerus was sectioned transversely at its most constricted point along the shaft (Fig. 3-6A). The primary bone is fibrolamellar (Fig. 3-6B; Fig. 6A-4). The primary vascular canals are oriented in circumferential rows in the cortex at the anterior-ventral and posterior-dorsal surfaces. At the posterior-dorsal surface, the rows are coupled with annuli, resulting in four rows of vascularization separated by three annuli (Fig. 3-6B). The annuli are distinct, thin lines that are associated with an increase in osteocyte lacunae density in the subsequent zone toward the periphery. The inner area of the cortex shows dense secondary lamellar bone surrounding longitudinal Haversian

vascular canals (Fig. 3-6C). The interior of the bone, including the medullary region, is largely crushed but shows extensive remodeling.

3.4.4.2 Radiale. The radiale was sectioned at mid-diaphysis where a notch (see Caldwell 1997a,b) occurs on the anterior surface (Fig. 3-6D; Fig. 6A-5). The fibrolamellar compact bone is the thickest at the anterior surface and tapers posteriorly (Fig. 3-6E). The vascularization runs parallel and perpendicular to the external surface of the bone at the anterior, and transitions to a more oblique angle toward the posterior (Fig. 3-6F). At the anterior, four vascular cycles are evident. The posterior surface of the bone lacks perichondral bone, and instead shows articular calcified cartilage. There is formation of secondary osteons with Haversian canals in the cortex and formation of erosion bays toward the medullary region. Although the medullary region is partially crushed, the remaining material shows lamellar trabecular bone.

3.4.4.3 Metacarpal II and forelimb phalanges. Metacarpal II was sectioned transversely at mid-length, and nine phalanges of the forelimb were sectioned (five transversely at mid-length and four longitudinally at mid-width). All surfaces, with the exception of the ventral and dorsal, lack perichondral bone (Fig. 3-6G-I). Articular surfaces are concave with a layer of calcified cartilage. Proximal phalanges at the leading edge of the paddle (digit 2) taper dorsoventrally toward the anterior margin, and the anterior surface is convex and shows calcified cartilage thereby demonstrating that perichondral bone was lost on non-articular surfaces, not just articular surfaces. The dorsal and ventral edges have a thin layer of woven compact bone that tapers off at the anterior and posterior in transverse sections, and proximal and distal in longitudinal sections; the relative thickness of the compact bone decreases from larger proximal elements to smaller distal elements.

The longitudinal vascular canals in the primary bone increase in size toward the medullary region.

The metacarpal and phalanges primarily show thin layers of primary woven bone transitioning to secondary lamellar trabecular bone dominated by large erosion bays in the medullary region (Fig. 3-6J). They do not have a medullary cavity. The more distal phalanges show thicker trabeculae in the center of the section. The most distal phalanges have more compact cores than proximal phalanges and are composed of dense secondary lamellar bone with no remnant of primary woven bone. Proximal phalanges show larger, branching erosion bays, mid-phalanges show a mix of branching and round erosion bays, and the most distal phalanges show round intertrabecular spaces in their core surrounded by larger branching erosion bays (Fig. 3-6K). This reflects a transition proximo-distally in both compactness and trabecular organization.

3.4.4.4 Ischiopubis. The ischiopubis was sectioned both at the ventral and acetabular ends, but shows a consistent microstructure (Fig. 3-7A-C). There was no differentiation between the fused elements. A thin layer of woven compact primary bone with longitudinal vascularization is present. The ventral section had slightly thinner compact bone than the acetabular section. The spongiosa is largely crushed, but shows secondary lamellar trabeculae with erosion bays ranging in shape from round to oblong.

3.4.4.5 Femur. The femur was sectioned transversely at mid-diaphysis as indicated by the most constricted point of the shaft (Fig. 3-7D). The fibrolamellar primary bone has vascular canals that are both longitudinal and radial (Fig. 6A-6). The longitudinal vascularization is cyclical in the periphery and is associated with cyclical changes in the density of osteocyte lacunae (Fig. 3-7E). There is one annulus in the primary bone near the

periphery. There are Haversian canals and round to oblong erosion bays surrounded by secondary lamellar bone in the innermost periosteal bone (Fig. 3-7F). There is no distinct medullary cavity, but the medullary region consists of secondary lamellar trabecular bone. The spongiosa is looser at the posterior than the anterior, resulting in the appearance of a shift in the medullary region to the posterior.

3.4.4.6 Fibula. The fibula was sectioned transversely at mid-length (Fig. 3-8A). There is a thin layer of fibrolamellar compact primary bone with sparse longitudinal vascularization at the central region of the dorsal and ventral surfaces (Fig. 3-8B; Fig. 6A-7). The dorsal and ventral surfaces show a transition from the longitudinal vascularization to oblique angles toward the anterior and posterior. Sharpey's fibers show comparable oblique angulations in this area. They are more predominant at the anterior articular surface than the posterior (the lagging edge of the paddle). The bone is predominantly spongious, composed of loose secondary lamellar trabeculae, and erosion bays with shapes ranging from round to branching. There is no distinct medullary cavity, but a medullary region dominated by loose secondary lamellar trabecular bone with the loosest spongiosa at the posterior (Fig. 3-8C-D). Both the anterior and posterior show calcified cartilage, with the anterior being convex and the posterior being concave (Fig. 3-8E; Fig. 6A-7). The presence of calcified cartilage at both the anterior and posterior again suggests a loss of perichondral bone at both articular and non-articular surfaces of podial elements distal to the stylopodium.

3.4.4.7 Calcaneum. The calcaneum was sectioned transversely at mid-length and has similar structure to the fibula, with the exception being that the anterior and posterior show the same degree of oblique vascularization, and the thin layers of compact primary

bone are less vascularized. In addition, because part of the posterior edge is missing, it is not possible to state if it is concave or convex.

3.4.4.8 Hindlimb phalanges. Three phalanges (first phalanges of digit II-IV) of the hindlimb were sectioned transversely at mid-length. They show a very thin layer of fibrolamellar compact primary bone at dorsal and ventral surfaces (Fig. 6A-8). Like the fibula and calcaneum, the vascularization at the anterior- and posterior-ventral and dorsal surfaces radiates at an oblique angle toward the anterior and posterior, respectively. The medullary region consists of loose secondary lamellar trabecular bone with erosion bays varying in shape from round to branching. In the anterior and posterior areas relative to the medullary region, the erosion bays are looser and branching. The anterior and posterior surfaces are slightly concave and have a layer of calcified cartilage, suggesting a loss of perichondral bone at the articular surfaces (Fig. 6A-8).

3.5 Discussion

Overall, our results are consistent with existing work on the bone microstructure of *Stenopterygius* of Germany (de Buffrénil and Mazin 1990; Houssaye et al. 2014; Maxwell et al. 2014; Houssaye et al. 2018) as well as general trends seen across ichthyopterygian taxa. Of the elements sampled here, primary endochondral bone is only present in the vertebral centrum. Predominantly, the primary periosteal bone is fibrolamellar with the exception of the vertebral centrum and gastralia which show parallel-fibered periosteal bone. The primary periosteal bone of the ribs and gastralia is compact with low vascularization. In contrast, the primary periosteal bone of the humerus and femur are highly vascularized, as was also reported by Houssaye and colleagues (2014). The differences in primary

periosteal bone organization and degree of vascularization are likely a reflection of differences in growth rates among skeletal elements, with larger podial elements experiencing relatively rapid growth rates as supported by the presence of fibrolamellar bone and a higher degree of vascularity in comparison to smaller elements such as ribs and gastralia (Amprino 1947).

The primary bone tissues examined in this study are also seen in extant animals with elevated growth rates. Using Amprino's rule (see Amprino 1947; de Ricqlès et al. 1991) *Stenopterygius quadriscissus* likely experienced rapid growth relative to extant ectothermic reptiles of similar body size, such as crocodilians and varanids whose primary bone is typically lamellar with modest longitudinal vascularization (Houssaye 2013). This contributes to a growing body of evidence that supports the hypothesis that ichthyopterygians as a clade were capable of elevated growth rates (Nakajima et al. 2014). The presence of woven to fibrolamellar primary bone typical of elevated growth, like that seen here, is consistent throughout the evolution of Ichthyopterygia in time and space. Fibrolamellar bone appears early in ichthyopterygian evolution, and is seen in the Lower Triassic ichthyoptergian *Utatsusaurus hataii*, suggesting that the clade was capable of rapid bone deposition early in their evolution possibly as a precursor to the evolution of thermoregulation (Nakajima et al. 2014).

The dorsal ribs show variation in structure with length along the shaft as is also seen in mosasaurs, cetaceans, and the ichthyopterygian *Utatsusaurus hataii* and ichthyosaurian *Ophthalmosaurus natans* (Houssaye and Bardet 2012; Massare et al. 2014; Nakajima et al. 2014; D'Emic et al. 2015; Houssaye et al. 2015). This variation highlights the importance of sampling at homologous locations along rib length in comparative analyses.

The ribs studied here show fibrolamellar primary bone in zones with annuli composed of parallel-fibered bone, demonstrating elevated growth rates throughout development with cyclical slowing. This is in contrast to the ribs of the Early Triassic ichthyopterygian *Utatsusaurus hataii* that show a slowing of growth in the form of a shift from fibrous to lamellar bone toward the periphery (Nakajima et al. 2014). The vascularization in the primary periosteal bone of the ribs and gastralia is relatively low in contrast to the high vascularization in the primary periosteal bone of the stylopodium. This relatively thick periosteal bone could also have acted to counterbalance the buoyancy of the lungs, although it is very likely post-Triassic ichthyosaurians like *Stenopterygius* had oxygen stores outside of the lungs (i.e., in their blood or tissues) similar to extant secondarily aquatic tetrapods (Schmidt-Nielsen 1997).

The presence of extensive remodeling supports this individual being classed as skeletally sub-adult or adult, consistent with size-based inferences (Johnson 1977). All postcranial elements show the formation of erosion bays through remodeling. With the exception of the dentary and premaxilla, remodeling of primary endochondral and periosteal bone created spongious bone comprised of secondary lamellar trabeculae. Because the elements of the limbs are no longer constrained by weight bearing, they are predominantly composed of this secondary spongy bone, with either highly vascularized primary bone in the humerus and femur, or very little compact bone present in elements distal to the stylopodium. The density of the spongy bone varies within the elements distal to the stylopodium, with relatively dense sponge in more distal, smaller elements (phalanges) compared to the epipodial and mesopodial elements. Because distal elements of the limb ossify later in ontogeny than proximal elements, they may not have experienced

as extensive remodeling as proximal elements. More extensive remodeling can lead to the formation of the looser sponge seen in the medullary region of the proximal elements.

Historically, ichthyosaurian limb bones have been classed as "osteoporotic" or "osteoporotic-like," (or osteopenic *sensu stricto* Francillon-Vieillot et al. (1990), as it is non-pathologic decrease in bone mass) and closely resembling the bone microstructure of cetaceans and leatherback turtles (*Dermochelys coriacea*; de Buffrénil and Mazin 1990). Recent work suggests that ichthyosaur long bones are not solely "osteoporotic", but can also be characterized by the presence of dense spongiose bone in the medullary region, with both "osteoporotic" and osteosclerotic (increase in bone mass) bone in different regions of the same element (Houssaye et al. 2014). We did not observe osteosclerosis in any of the *Stenopterygius quadriscissus* sections, although that may be an artifact of where they were taken (mid-diaphysis or mid-length for transverse sections, and mid-width for longitudinal sections). Although the paddle elements demonstrate an overall spongious organization with very little compact bone and no medullary cavity, they are not classed as osteopenic.

3.5.1 Cyclical growth and growth marks

The dentary and premaxilla are the densest elements sampled in this study, and show well-defined circumferential annuli (Fig. 3-2). The ribs are also relatively dense compared to other skeletal elements, and show well-defined annuli. The humerus and femur also show annuli, but they cannot be traced circumferentially due to the presence of a high level of vascularization in the primary bone (Fig. 3-6B). While cyclical growth has been suggested for ichthyosaurians based on vascularization (Houssaye et al. 2014), the

only ichthyosaurian known to display LAGs is *Mixosaurus* (Kolb et al. 2011). In particular, the gastralia of *Mixosaurus* demonstrated numerous well-defined LAGs, which was not observed in the gastralia sampled here. *Mixosaurus* demonstrates thicker compact bone in its postcranium than *Stenopterygius*, allowing for the preservation of growth marks across the skeleton. Zones and annuli (also called zonal bone or laminar bone) have been identified in the ribs of other ichthyosaurians including *Opthalmosaurus icenicus* (Gross et al. 1934) and *Temnodontosaurus trigonodon* (Seitz 1907; Enlow and Brown 1957).

Skeletochronological studies in post-Triassic ichthyosaurians with highly cancellous bone are limited to skeletal elements that preserve primary compact bone in somatically mature adults. While ribs have relatively thick primary bone and showed annuli, their microstructure is variable with length, complicating homologous sampling in specimens where ribs overlap or are fragmentary. Furthermore, rib microstructure of ichthyosaurians is known to be variable and in some cases preserve a strong ecological signal through changes in bone mass (Kolb et al. 2011, Talevi and Fernández 2012, Fernández and Talevi 2014, Massare et al. 2014). Cranial elements like the dentary and premaxilla of *Stenopterygius quadriscissus* that do not carry a significant ecological signal may better preserve growth marks than long bones and ribs in secondarily aquatic tetrapods like ichthyosaurians. Future work will demonstrate if these elements are suitable for skeletochronological and quantitative growth studies.

Other evidence for cyclical primary growth in *Stenopterygius quadriscissus* is circumferential rows of longitudinal primary vascular canals in the primary bone of the humerus and femur (Fig. 3-6B, Fig. 3-7E). In addition, cyclical patterns in secondary bone are also evident as shown in the formation of erosion bays in circumferential rows of the

ribs (Fig. 3-5). These cycles are also seen in both primary bone (notably *Pessopteryx nisseri*) and secondary bone of ichthyosaurs (Houssaye et al. 2014), as well as extant leatherback turtles (Rhodin 1985), and other extinct marine reptiles including plesiosaurians (Liebe and Hurum 2012). Whether or not these circumferential patterns are primary or secondary structures in these taxa is not always clear based on published studies. While the secondary formation of these circumferential rows is not useful for skeletochronological studies, it does reflect cyclicity in remodeling and growth.

Daily incremental lines of von Ebner (short periods) and weekly increments (also referred to as Andresen's lines, or long periods; Dean 2000) in the dentine are reported for the first time in *Stenopterygius*. Daily lines are poorly expressed locally, but weekly groupings are clearly visible as light and dark bands with both normal and cross-polarized light (Fig. 3-3). Uneven light and dark banding has also been observed in ichthyosaurians *Platypterygius australis*, *Maiaspondylus lindoei* and *Temnodontosaurus* sp., although these were not attributed to long periods (Maxwell et al. 2012). Both short (daily) and long period incremental lines have been reported in Ichthyosauria indet. aff. *Nannopterygius* (Scheyer and Moser 2011); Scheyer and Moser also emphasize the importance of variation and scaling in increment widths among vertebrate taxa in order to understand if observed increments correspond to short or long periods, as discussed by Dean (1998, 2000). Further study of these incremental lines and banding in taxa that express them can reveal aspects of ichthyosaur biology such as tooth replacement rates (Erickson 1996) and gestation period (incubation period in dinosaurs; Erickson et al. 2017).

3.5.2 Modified perichondral ossification in *Stenopterygius*

Ichthyosaurians have highly modified limbs, or paddles, that are adapted to their obligate aquatic lifestyle. The podial elements sampled here lack a distinct open medullary cavity; instead the medullary region is composed of cancellous trabecular bone, as is seen in the podial elements of all studied ichthyosaurians with the exception of *Pessopteryx nisseri* (de Buffrénil and Mazin 1990; Houssaye et al. 2014). The loss of a distinct medullary cavity in the secondarily non-weight bearing limbs of obligate aquatic animals increases resistance and distributes forces more evenly through the limb as it is used for steering (Benke 1993). While the microstructure of the stylopodial elements has been relatively well studied in ichthyosaurians (see Houssaye et al. 2014 for an overview), the microstructure of the podial elements distal to the stylopodium is mostly unknown despite being the focus of morphological studies with regard to their development and ossification (Caldwell 1997a,b; Maxwell 2012b; but see Maxwell at al. 2014, Lopuchowycz and Massare 2002).

The notches seen in podial elements of ichthyosaurians are homologous to the shaft of dumb-bell shaped bones (Caldwell 1997a,b; Maxwell et al. 2014). While notching is known to be variable in *Stenopterygius*, the notched elements sampled here (radiale) and elsewhere (tibia; see Maxwell et al. 2014) show a thick layer of periosteal bone at the anterior that tapers posteriorly, and show calcified cartilage on their posterior, articular surface (Fig. 3-7D). The loss of the traditional dumb-bell shape and therefore loss of notches in bones of the limb is caused by the loss of perichondral bone on the diaphyses, resulting in an overall reorganization of the bone tissues. This loss of regionalization in the limbs is referred to as mesopodialization (Maxwell et al. 2014), as other podial elements

become similar to the mesopodials in their lack of perichondral bone. Instead, their anterior and posterior surfaces are endochondral, similar to the proximal and distal surfaces with caps of calcified cartilage, thereby increasing articular surface area and stability (Caldwell 1997b).

The unnotched epipodial (fibula), mesopodial (calcaneum) and metapodial (metacarpal II) elements, and phalanges sampled here showed similar microstructure (highly cancellous bone with very little periosteal bone on the dorsal and ventral surfaces, and calcified cartilage caps at the anterior and posterior surfaces) demonstrating the mesopodialization in the limb distal to the stylopodium at both the morphological and microstructural level. A layer of endochondral calcified cartilage covers all articular surfaces (anterior, posterior, proximal, distal) of the studied elements distal to the stylopodium (Fig. 3-7G-I, Fig. 3-8A). Calcified cartilage also covers non-articular surfaces of the most anterior (leading edge) and posterior (lagging edge) of elements that are not notched. Maxwell and colleagues (2014) suggest the presence of notching and compact periosteal bone indicates that the leading edge of the hindlimb of *Stenopterygius* experienced hydrodynamic forces associated with forward motion. Similarly, the loss of compact periosteal bone in unnotched elements at the anterior of the forelimb like that seen here (metacarpal II) could indicate areas that were not experiencing this stress due to the presence of soft tissue. Future work on bone microstructure of ichthyosaurian paddles could further inform our understanding of their functional morphology.

3.5.3 Implications for metabolism and thermoregulation

The relationship between growth rate and metabolic rate, and in turn the ability to infer metabolic rate from growth rate has been used to support hypotheses of thermoregulation in extinct taxa (Erickson et al. 2001). This principle would suggest *Stenopterygius quadriscissus* experienced an increased metabolic rate relative to extant ectothermic reptiles, and was therefore able to generate metabolic heat and thermoregulate to some extent. However, this simplification based on Kleiber's Law should be approached with caution (Kolokotrones et al. 2010). The bone microstructure examined in this study qualitatively suggests an elevated growth rate in *Stenopteyrgius quadriscissus*, but that alone cannot support the hypothesis that this species had an elevated basal metabolic rate and was capable of thermoregulation.

Isotopic analyses suggest post-Triassic ichthyosaurians had body temperatures higher than ambient seawater (35° C ± 2°C), similar to that seen in modern cetaceans (Morrison 1962; Bernard et al. 2010; Motani 2010). In addition, energetics modeling based on estimated swimming speeds of 1 m/s, similar to optimal cruising speeds of modern yellowfin tuna, have also supported a raised ectothermic metabolic rate in post-Triassic ichthyosaurians (Massare 1988; Block et al. 1997; Marsac and Cayre 1998; Motani 2002a, 2002b). Sustained swimming and maintenance of muscle-generated body heat is one mechanism for thermoregulation that has evolved in homeothermic ectotherms, or ectotherms that are able to maintain a constant body temperature, as seen in modern tuna and leatherback turtles (Graham and Dickson 2004; Wallace and Jones 2008). Gigantothermy has also been suggested for leatherback turtles, referring to the ability to retain heat through insulating body mass despite low metabolic rates (Palladino et al.

1990). Although this may be true of somatically mature individuals, it would not explain thermoregulation in juveniles with smaller body sizes.

Multiple lines of evidence including isotopic analysis, energetics modeling and osteohistological study support the potential for a raised metabolic rate and thermoregulation in *Stenopterygius*. The mechanism of thermoregulation likely involves retention of heat produced in the muscles during sustained swimming, resulting in a raised ectotherm or homeostatic ectotherm state. Assuming a sigmoidal mass-age growth curve, juveniles were experiencing the highest growth rates while requiring a physiological mechanism to retain body heat in order to survive. Gigantothermy, which would imply low metabolic rates inconsistent with the elevated growth rates inferred from bone microstructure, may have contributed to thermoregulation in adults if growth slowed, but not in juveniles; this suggests that juvenile *Stenopterygius* could not solely rely on body mass to thermoregulate and other mechanisms must have contributed to maintain an elevated body temperature.

3.6 Conclusions

1. The bone microstructure of *Stenopterygius quadriscissus* suggests elevated, cyclical growth relative to extant reptiles of similar body sizes. Cyclical patterns of vascularization associated with annuli in the primary bone of the stylopodium warrant further investigation.
2. Primary vascularization and extensive remodeling of the primary bone in the paddle elements has led to an overall spongious structure with very little compact bone. All

elements except the dentary and premaxilla show erosion bays and spongious bone in the medullary region.

3. Growth marks in the form of annuli were identified in the dentary, premaxilla, ribs, humerus, and femur. In addition, poorly expressed daily-forming lines of von Ebner and weekly light and dark banding are documented in the teeth.
4. The relatively dense cranial elements such as the dentary and premaxilla may prove useful in future skeletochronological studies of taxa like post-Triassic ichthyosaurians that exhibit thin and/or highly vascularized primary bone in adults.
5. The study of bone microstructure of ichthyosaurian paddles further informs our understanding of modified perichondral ossification. Elements distal to the stylopodium of both the fore- and hindlimbs that are not notched show a loss of regionalization in the form of mesopodialization. Periosteal bone is lost on the anterior and posterior surfaces of both articular and non-articular surfaces of bones that are not notched, demonstrating a major reorganization of osseous tissue.
6. We infer and corroborate the hypothesis that *Stenopterygius* experienced elevated metabolic rates and were potentially able to thermoregulate like extant homeothermic ectotherms through maintenance of muscle-derived heat.

3.7 Acknowledgements

We thank A. Houssaye and an anonymous reviewer for constructive comments on this manuscript; S.J. Fowell, L. Horstmann, and E.T. Metz for discussions about this research; and R. Newberry and A. Linn for access to equipment. We acknowledge the Palaeontological Association. This research was funded by the Otto Geist Fund Grant

through the University of Alaska Museum, the University of Alaska Fairbanks Graduate School Travel Grant, and the National Science Foundation GK-12 Changing Alaska Science Education fellowship (NSF DGE-0948029; PIs R. Boone, L. Conner and K. Winker).

3.8 References

AMPRINO, R. 1947. La structure du tissue osseux envisagée comme l'expression de differences dans la vitesse de l'accroissement. *Archives de Biologie,* **58**, 315–330.

ANDERSON, K. L., DRUCKENMILLER, P. S., ERICKSON, G. M. and MAXWELL, E. E. 2018. Data from: Skeletal microstructure of *Stenoptergius quadriscissus* (Reptilia, Ichthyosauria) from the Posidonienschiefer (Posidonia Shale, Lower Jurassic) of Germany. *Dryad Digital Repository*. https://doi.org/10.5061/dryad.032cq64

BAUER, F. 1898. Die Ichthyosaurier des oberen weissen Jura. *Palaeontographica,* **44**, 283–328.

BENKE, H. 1993. Investigations on the osteology and functional morphology of the flipper of whales and dolphins. *Investigations on Cetacea,* **24**, 9–252.

BERNARD, A., LÉCUYER, C., VINCENT, P., AMIOT, R., BARDET, N., BUFFETAUT, E., CUNY, G., FOUREL, F., MARTINEAU, F., MAZIN, J.-M. and PRIEUR, A. 2010. Regulation of body temperature by some Mesozoic marine reptiles. *Science,* **328**, 1379–1382.

BESMER, F. 1947. Die Triasfauna der Tessiner Kalkapen SVI. Beiträge zur Kenntnis des Ichthyosauriergebisses. *Schweizerische Palaeontologische Abhandlungen,* **65**, 1–21

BLOCK, B.A., KEEN, J.E., CASTILLO, B., DEWAR, H., FREUND, E.V., MARCINEK, D.J., BRILL, R.W. and FARWELL, C. 1997. Environmental preferences of yellowfin tuna (*Thunnus albacares*) at the northern extent of its range. *Marine Biology,* **130**, 119–132.

BOTHA, J. and CHINSAMY, A. 2004. Growth and life habits of the Triassic cynodont *Trirachodon*, inferred from bone histology. *Acta Palaeontologica Polonica,* **49** (4), 619–627.

BUFFRÉNIL, V. DE and MAZIN, J.-M. 1990. Bone histology of the ichthyosaurs: comparative data and functional interpretation. *Paleobiology,* **16**, 435–447.

CALDWELL, M.W. 1997a. Limb ossification patterns of the ichthyosaur *Stenopterygius*, and a discussion of the proximal tarsal row of ichthyosaurs and other neodiapsid reptiles. *Zoological Journal of the Linnean Society,* **120**, 1–25.

CALDWELL, M.W. 1997b. Modified perichondral ossification and the evolution of paddle-like limbs in ichthyosaurs and plesiosaurs. *Journal of Vertebrate Paleontology,* **17** (3), 534–547.

CASTANET, J., FRANCILLON-VIEILLOT, H., MEURNIER, F.J. and RICQLÈS, A. DE. 1993. Bone and individual aging. 245–283. *In* HALL, B.K. (ed). *Bone: vol 7, Bone growth.* CRC Press.

CHINSAMY, A. and HILLENIUS, W.J. 2004. Physiology of nonavian dinosaurs. 643–659. *In* DODSON, P., OSMOLSKA, H. and WEISHAMPEL, D.B. (eds.) *The Dinosauria*. University of California Press.

D'EMIC, M.D., SMITH, K.M. and ANSLEY, Z.T. 2015. Unusual histology and morphology of the ribs of mosasaurs (Squamata). *Palaeontology,* **58**, 511–520.

DEAN, M.C. 1998. Comparative observations on the spacing of short period (von Ebner's) lines in dentine. *Archives of Oral Biology,* 43, 1009–1021.

DEAN, M.C. 2000. Incremental markings in enamel and dentine: what they can tell us about the way teeth grow. 119-130. *In* TEAFORD, M.F., SMITH, M.M. and FERGUSON, M.W.J. (eds). *Development, function and evolution of teeth*. Cambridge University Press.

EDMUND, A.G. 1960. Tooth replacement phenomena in the lower vertebrates. *Life Sciences Contributions, Royal Ontario Museum,* **52**, 1–190.

ENLOW, D.H. and BROWN, S.O. 1957. A comparative study of fossil and recent bone tissue. Part II: Reptiles and birds. *Texas Journal of Science,* **9**, 186–214.

ERICKSON, G.M. 1996. Incremental lines of von Ebner in dinosaurs and the assessment of tooth replacement rates using growth line counts. *Proceedings of the National Academy of Sciences*, **93**, 14623–14627.

ERICKSON, G.M. 2005. Assessing dinosaur growth patterns: a microscopic revolution. *Trends in Ecology & Evolution,* **20**, 677–684.

ERICKSON, G.M. 2014. On dinosaur growth. *Annual Review of Earth & Planetary Sciences,* **42**, 675–697.

ERICKSON, G.M. and TUMANOVA, T.A. 2000. Growth curve of *Psittacosaurus mongoliensis* Osborn (Ceratopsia: Psittacosauridae) inferred from long bone histology. *Zoological Journal of the Linnean Society,* **130**, 551–566.

ERICKSON, G.M., CURRY ROGERS, K. and YERBY, S.A. 2001. Dinosaurian growth patterns and rapid avian growth rates. *Nature,* **412**, 429–433.

ERICKSON, G.M., MAKOVICKY, P.J., CURRIE, P.J., NORELL, M.A., YERBY, S.A. and BROCHU, C.A. 2004. Gigantism and comparative life-history parameters of tyrannosaurid dinosaurs. *Nature,* **430**, 772–775.

ERICKSON, G.M., ZELENITSKY, D.K., KAY, D.I. and NORELL, M.A. 2017. Dinosaur incubation periods directly determined from growth-line counts in embryonic teeth show reptilian-grade development. *Proceedings of the National Academy of Sciences,* **114**, 540–545.

FERNÁNDEZ, M.S. and TALEVI, M. 2014. Opthalmosaurian (Ichthyosauria) record from the Aalenian-Bajocian of Patagonia (Argentina): an overview. *Geological Magazine,* **151** (1), 49–59.

FRAAS, E. 1891. *Ichthyosaurier der süddeutschen Trias- und Jura- Ablagerungen*. H. Laupp, Tübingen, 81 pp.

FRANCILLON-VIEILLOT, H., BUFFRÉNIL, V. DE, CASTANET, J., GERAUDIE, J., MEUNIER, F.J., SIRE, J.Y., ZYLERBERG, L. and RICQLÈS, A. DE. 1990. Microstructure and mineralization of vertebrate skeletal tissues. 471–530. *In* CARTER, J.G. (ed). *Biomineralization: patterns and evolutionary trends*. Van Nostrand Reinhold.

GRAHAM, J.B. and DICKSON, K.A. 2004. Tuna comparative physiology. *The Journal of Experimental Biology,* **207**, 4015–4024.

GROSS, W. 1934. Die Typen des mikroskopischen Knochenbaues bei fossilen Stegocephalen und Reptilien. *Zeitschrifl fur Anatomic,* ***103***, 731–764.

HAUFF, B. 1921. Untersuchung der Fossilfundstätten von Holzmaden in Posidonienschiefer des oberen Lias Württembergs. *Palaeontographica,* **64**, 1–42.

HORNER, J.R. and PADIAN, K. 2004. Age and growth dynamics of *Tyrannosaurus rex*. Proceedings of the Royal Society B, **271**, 1875–1880.

HORNER, J.R., RICQLÈS, A. DE and PADIAN, K. 2000. Long bone histology of the hadrosaurid dinosaur *Maiasaura peeblesorum*: growth dynamics and physiology based on an ontogenetic series of skeletal elements. *Journal of Vertebrate Paleontology,* **20**, 115–129.

HOUSSAYE, A. 2013. Bone histology of aquatic reptiles: what does it tell us about secondary adaption to an aquatic life? *Biological Journal of the Linnaean Society,* **108** (1), 3–21.

HOUSSAYE, A. and BARDET, N. 2012. Rib and vertebral micro-anatomical characteristics of hydropelvic mosasauroids. *Lethaia,* **45**, 200–209.

HOUSSAYE, A., SCHEYER, T.M., KOLB, C., FISCHER, V. and SANDER, P.M. 2014. A new look at ichthyosaur long bone microanatomy and histology: implications for their adaptation to an aquatic life. *PLoS ONE,* **9** (4), e95637.

HOUSSAYE, A., TAFFOREAU, P., MUIZON, C. DE and GINGERICH, P.D. 2015. Transition of Eocene whales from land to sea: evidence from bone microstructure. *PLoS ONE,* **10** (2), e0118409.

HOUSSAYE, A., SANDER, P.M. and KLEIN, N. 2016. Adaptive patterns in aquatic amniote bone microanatomy—more complex than previously thought. *Integrative and Comparative Biology,* **56** (6), 1349–1369.

HOUSSAYE, A., NAKAJIMA, Y., and SANDER, P.M. 2018. Structural, functional, and physiological signals in ichthyosaur vertebral centrum microanatomy and histology. *Geodiversitas,* **40** (2), 161–170.

JOHNSON, R. 1977. Size independent criteria for estimating relative age and the relationship among growth parameters in a group of fossil reptiles (Reptilia: Ichthyosauria). *Canadian Journal of Earth Sciences,* **14**, 1916–1924.

KIPRIJANOFF, W. 1881. Studien über die fossilen Reptilien Russlands. Theil 1. Gattung *Ichthyosaurus* König aus dem Sewerischen Sandstein oder Osteolith der Kreide-Gruppe. *Mémoires de l'Académie Impériale des Sciences de Saint-Pétersbourg,* **28**, 1–103.

KOLB, C., SÁNCHEZ-VILLAGRA, M.R. and SCHEYER, T.M. 2011. The palaeohistology of the basal ichthyosaur *Mixosaurus* Baur, 1887 (Ichthyopterygia, Mixosauridae) from the Middle Triassic: palaeobiological implications. *Comptes Rendus Palevol,* **10**, 403–411.

KOLOKOTRONES, T., SAVAGE, V., DEEDS, E.J. and FONTANA, W. 2010. Curvature in metabolic scaling. *Nature Letters,* **464**, 753–756.

LIEBE, L. and HURUM, J.H. 2012. Gross internal structure and microstructure of plesiosaur limb bones from the Late Jurassic, central Spitsbergen. *Norwegian Journal of Geology,* **92**, 285–309.

LOPUCHOWYCZ, V.B. and MASSARE, J.A. 2002. Bone microstructure of a Cretaceous ichthyosaur. *Paludicola,* **3** (4), 139–147.

MAISCH, M.W. 2008. Revision of the genus *Stenopterygius* Jaekel, 1904 emend. Von Huene, 1922 (Reptilia: Ichthyosauria) from the Lower Jurassic of Western Europe. *Palaeodiversity,* **1**, 227–271.

MARSAC, F. and CAYRÉ, P. 1998. Telemetry applied to behaviour analysis of yellowfin tuna (*Thunnus albacares*, Bonnaterre 1788) movements in a network of fish aggregating devices. *In* LAGARDERE, J.-P., BEGOUT ANRAS, M.-L., CLAIREAUX, G. (eds). *Advances in invertebrates and fish telemetry*. Kluwer Academic Publishers.

MARTILL, D.M. 1987. A taphonomic and diagenetic case study of a partially articulated ichthyosaur. *Palaeontology,* 30(3), 543–555.

MARTILL, D.M. 1993. Soupy substrates: a medium for the exceptional preservation of ichthyosaurs of the Posidonia Shale (Lower Jurassic) of Germany. *Kaupia,* **2**, 77–97.

MASSARE, J.A. 1988. Swimming capabilities of Mesozoic marine reptiles: implications for method of predation. *Paleobiology,* **14**, 187–205.

MASSARE, J.A., WAHL, W. R., ROSS, M. and CONNELY, M. V. 2014. Palaeoecology of the marine reptiles of the Redwater Shale Member of the Sundance Formation (Jurassic) of central Wyoming, USA. *Geological Magazine,* **151**, 167–182.

MAXWELL, E.E. 2012a. New metrics to differentiate species of *Stenopterygius* (Reptilia: Ichthyosauria) from the Lower Jurassic of Southweastern Germany. *Journal of Paleontology,* **86** (1), 105–115.

MAXWELL, E.E. 2012b. Unraveling the influences of soft-tissue flipper development on skeletal variation using an extinct taxon. Journal of Experimental Zoology B, **318B**, 545–554.

MAXWELL, E.E., CALDWELL, M.W. and LAMOUREUX, D.O. 2011. Tooth histology in the Cretaceous ichthyosaur *Platypterygius australis* and its significance for the conservation and divergence of mineralized tooth tissues in amniotes. *Journal of Morphology,* **272**, 129–135.

MAXWELL, E.E., CALDWELL, M.W. and LAMOUREUX, D.O. 2012. Tooth histology, attachment, and replacement in the Ichthyopterygia reviewed in an evolutionary context. *Paläontologische Zeitschrift,* **86**, 1–14.

MAXWELL, E.E., SCHEYER, T.M. and FOWLER, D.A. 2014. An evolutionary and developmental perspective on the loss of regionalization in the limbs of derived ichthyosaurs. *Geological Magazine,* **151** (1), 29–40.

MCGOWAN, C. 1979. A revision of the Lower Jurassic ichthyosaurs of Germany with descriptions of two new species. *Palaeontographica Abteilung A,* **166**, 93–135.

MCGOWAN, C. and MOTANI, R. 2003. Ichthyopterygia. *In* SUES, H.-D. (ed.) *Handbook of Paleoherpetology*. Dr. Friedrich Pfeil, München, 175 pp.

MORRISON, P. 1962. Body temperatures in some Australian mammals. III. Cetacea Megaptera). *Biological Bulletin,* **123**, 154–169.

MOTANI, R., ROTHSCHILD, B.M. and WAHL, W. Jr 1999. Large eyeballs in diving ichthyosaurs. *Nature* **402**, 747.

MOTANI, R. 2002a. Swimming speed estimation of extinct marine reptiles: energetic approach revisited. *Paleobiology,* **28**, 251–262.

MOTANI, R. 2002b. Scaling effects in caudal fin propulsion and the speed of ichthyosaurs. *Nature,* **415**, 309.

MOTANI, R. 2005. Evolution of fish-shaped reptiles (Reptilia: Ichthyopterygia) in their physical environments and constraints. *Annual Review of Earth & Planetary Sciences,* **33**, 395–420.

MOTANI, R. 2010. Warm-blooded "sea dragons"? *Science,* **328**, 1361.

NAKAJIMA, Y., HOUSSAYE, A. and ENDO, H. 2014. Osteohistology of *Utatsusaurus hataii* (Reptilia: Ichthyopterygia): Implications for early ichthyosaur biology. *Acta Palaeontologica Polonica,* **59**, 343–352.

NOPCSA, F.B. 1933. On the histology of the ribs in immature and half-grown Trachodont dinosaurs. *Proceedings of the Zoological Society of London,* **103**(1), 221–226.

ORBAN, B.J. and SICHER, H. 1966. *Orban's oral histology and embryology*. Mosby.

PALLADINO, F.V., O'CONNOR, M.P. and SPOTILA, J.R. 1990. Metabolism of leatherback turtles, gigantothermy and thermoregulation of dinosaurs. *Nature,* **344**, 858–860.

PARDO-PÉREZ, J. M., KEAR, B. P., GÓMEZ, M., MORONI, M. and MAXWELL, E. E. 2018. Ichthyosaurian palaeopathology: evidence of injury and disease in fossil 'fish-lizards'. *Journal of Zoology,* **304**, 21–33.

QUEKETT, J. 1855. *Descriptive and illustrated catalogue of the histological series contained in the museum of the Royal College of Surgeons of England: structure of the skeleton of vertebrate animals.* Vol. 2. R. and J.E. TAYLOR.

RICQLÈS, A. DE, MEUNIER, F.J., CASTANET, J. and FRANCILLON-VIEILLOT, H. 1991 Comparative microstructure of bone. 1–78. *In* Hall, B.K. (ed). *Bone, Vol. 3. Bone Matrix and bone specific products*. CRC-press, Boca Raton, FL.

RHODIN, A.G.J. 1985. Comparative chrondro-osseous development and growth of marine turtles. *Copeia,* **1985** (3), 752–771.

RICQLÈS, A. DE, MEUNIER, F.J., CASTANET, J. and FRANCILLON-VIEILLOT, H. 1991. Comparative microstructure of bone. 1–78. *In* HALL, B.K. (ed.) *Bone. Vol. 3: Bone matrix and bone specific products*. CRC Press.

RICQLÈS, A. DE, TAQUET, P. and BUFFRÉNIL, V. DE. 2009. "Rediscovery" of Paul Gervais' paleohistological collection. *Geodiversitas,* **31**(4), 943–971.

RÖHL, H.-J. and SCHMID-RÖHL, A. 2005. Lower Toarcian (Upper Liassic) black shales of the central European epicontinental basin: a sequence stratigraphic case study from the SW German Posidonia Shale. 165–189. *In* HARRIS, N.B. (ed.) *The deposition of organic-carbon-rich sediments: models, mechanisms, and consequences.* Society for Sedimentary Geology Special Publication **82**.

RÖHL, H.-J., SCHMID-RÖHL, A., OSCHMANN, W., FRIMMEL, A. and SCHWARK, L. 2001. The Posidonia Shale (Lower Toarcian) of SW-Germany: an oxygen-depleted ecosystem controlled by sea level and palaeoclimate. *Palaeogeography, Palaeoclimatology, Palaeoecology,* **165**, 27–52.

SANCHEZ, S., AHLBERG, P.E., TRINAJSTIC, K.M., MIRONE, A. and TAFFOREAU, P. 2012. Three-dimensional synchrotron virtual paleohistology: a new insight into the world of fossil bone microstructures. *Microscopy and Microanalysis,* **18**, 1095–1105.

SANDER, P.M. 2000. Ichthyosauria: their diversity, distribution, and phylogeny. *Paläontologische Zeitschrift,* **74**, 1–35.

SCHEYER, T.M. and M. MOSER. 2011. Survival of the thinnest: rediscovery of Bauer's (1898) ichthyosaur tooth sections from Upper Jurassic lithographic limestone quarries, south Germany. *Swiss Journal of Geosciences,* **104** (Suppl 1), S147–S157.

SCHMID-RÖHL, A., RÖHL, H.-J., OSCHMANN, W., FRIMMEL, A. and SCHWARK, L. 2002. Palaeoenvironmental reconstruction of Lower Toarcian epicontinental black shales (Posidonia Shale, SW Germany): global versus regional control. *Geobios,* **35**, 13–20.

SCHMIDT-NIELSEN, K. 1997. *Animal Physiology: adaptation and environment.* 5th edn. Cambridge University Press.

SEITZ, A.L.L. 1907. *Vergleichende Studien über den mikroskopischen Knochenbau fossiler und rezenter Reptilien und dessen Bedeutung für das Wachstum und Umbildung des Knochengewebes im Allgemeinen.* Vol. 87 (2). E. Karras.

TALEVI, M. and FERNÁNDEZ, M.S. 2012. Unexpected skeletal histology of an ichthyosaur from the Middle Jurassic of Patagonia: implications for evolution of bone microstructure among secondary aquatic tetrapods. *Naturwissenschaften,* **99**, 241–244.

TALEVI, M., FERNÁNDEZ, M.S. and SALGADO, L. 2012. Variación ontogenética en la ósea de *Caypullisaurus bonapartei* Fernández, 1997 (Ichthyosauria: Ophthalmosauridae). *Ameghiniana,* **49** (1), 38–46.

WALLACE, B.P. and JONES, T.T. 2008. What makes marine turtles go: a review of their metabolic rates and their consequences. *Journal of Experimental Marine Biology & Ecology,* **356**, 8–24.

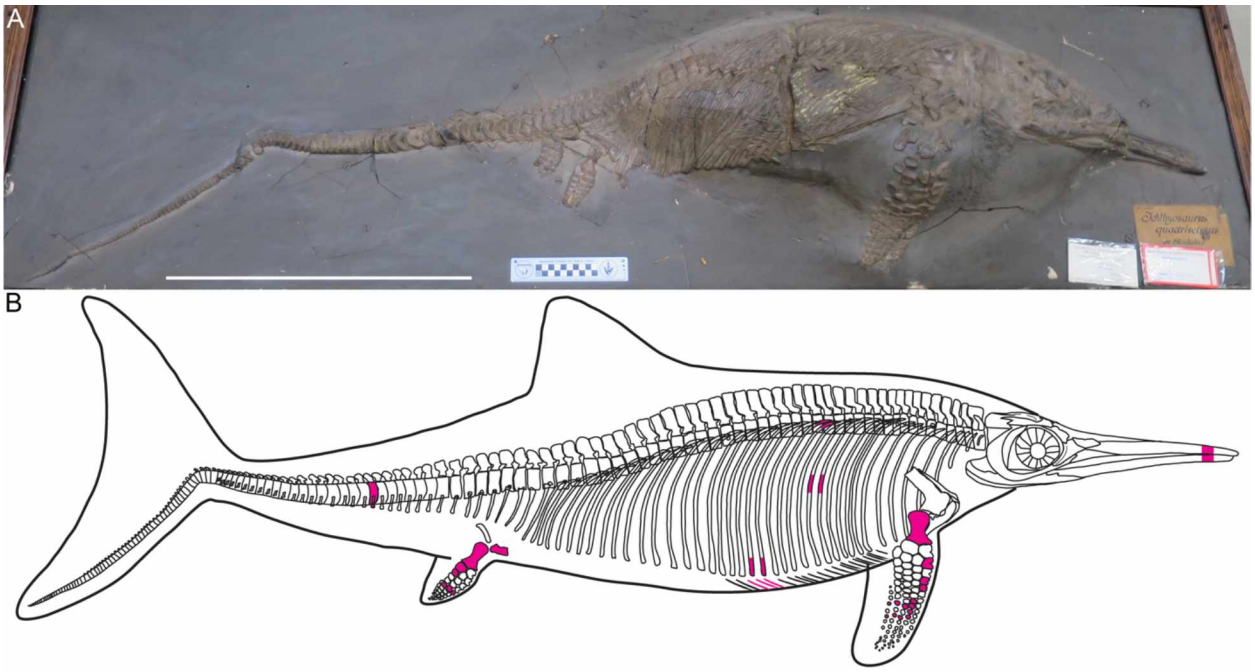

Figure 3-1. Overview of SMNS 4789, referred specimen of *Stenopterygius quadriscissus*. A, The specimen is articulated and almost complete. The mid-section of the specimen is wrapped around a large concretion, and there is pyritization of some elements, most noticeably in the ribs. B, Silhouette of *Stenopterygius* with the elements whose microstructure are described in this study highlighted. Scale bar presents 50 cm (A).

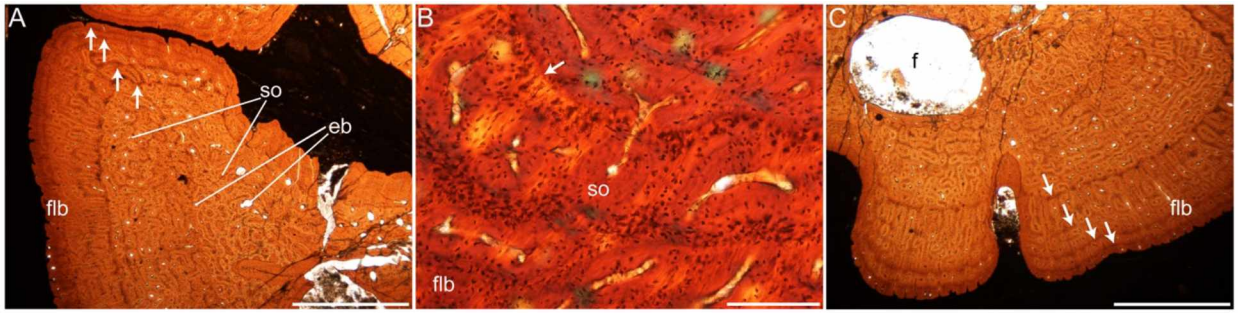

Figure 3-2. Dentary and premaxilla of SMNS 4789, referred specimen of *Stenopterygius quadriscissus*. A, Section of dentary in frontal plane showing secondary bone with secondary osteons and erosion bays at its center, and fibrolamellar bone at the periphery. Arrows denote four annuli. B, Detail of dentary in cross-polarized light with lambda filter showing lamellar bone surrounding a secondary osteon cutting into primary fibrolamellar bone. Note changes in osteocyte lacunae density. Arrow denotes annulus. C, Section of premaxilla in frontal plane showing similar microstructure to dentary. Arrows denote four annuli. Abbreviations: eb erosion bay, f foramen, flb fibrolamellar bone, so secondary osteon. Scale bars represent 2 mm (A, C), 0.25 mm (B).

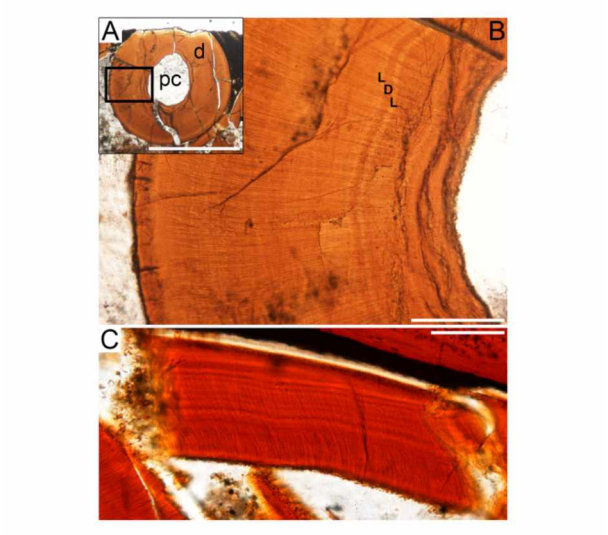

Figure 3-3. Teeth of SMNS 4789, referred specimen of *Stenopterygius quadriscissus*. A, Overview of transverse section of tooth crown showing dentine (d) and pulp cavity (pc). B, Detail of tooth (area outlined in A) with radial dentinal tubules and weak circumferential lines of von Ebner in the dentine. Light (L) and dark (D) banding attributed to weekly increments. C. Fragment of tooth showing evenly spaced light and dark banding in normal light. Scale bars represent 2 mm (A), 0.25 mm (B), 0.5 mm (C).

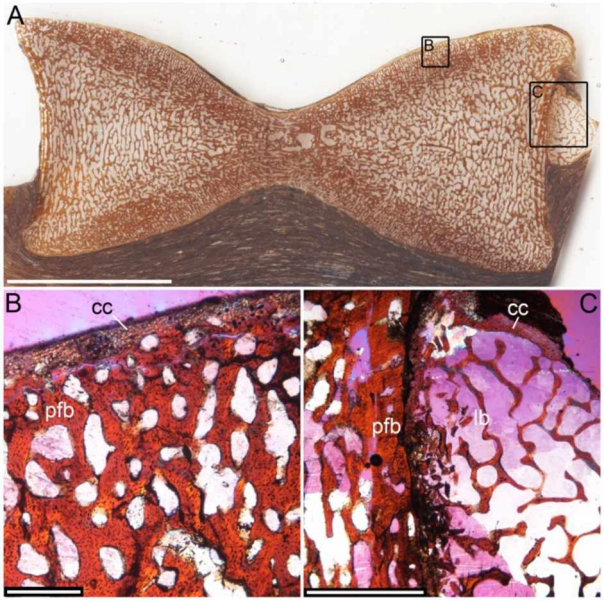

Figure 3-4. Sagittal section of caudal centrum of SMNS 4789, referred specimen of *Stenopterygius quadriscissus*. A, Overview of caudal centrum showing overall organization of trabecular bone. Vascularization is oriented perpendicular to surface at the anterior and posterior, versus parallel to surface at the dorsal and ventral. B, Detail of cortex of caudal centrum with a thin layer of calcified cartilage at the periphery, and highly vascularized primary parallel fibered and spongious secondary lamellar bone C, Detail of dorsal periosteal cortex of the caudal centrum and element that is likely a caudal rib. Abbreviations: cc calcified cartilage, lb lamellar bone, pfb parallel fibered bone. C and D shown in cross-polarized light with lambda filter. Scale bars represent 10 mm (A), 0.5 mm (B), 2 mm (C).

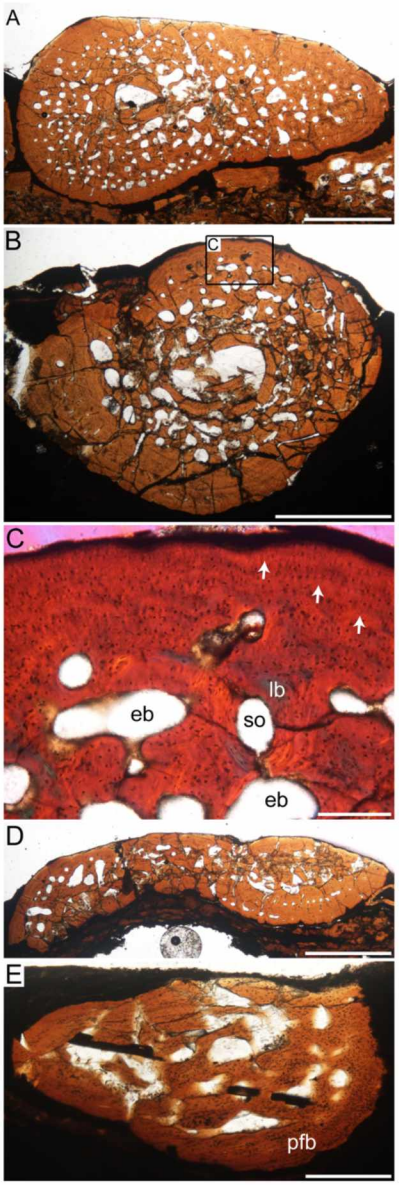

Figure 3-5. Transverse sections of dorsal ribs and gastralia of SMNS 4789, referred specimen of *Stenopterygius quadriscissus*. A, Proximal transverse section with material missing at exposed surface due to historical preparation. B, Mid-shaft transverse section. C, Detail in cross-polarized light with lambda filter of cortex of mid-rib showing cycles of annuli (denoted by arrows) consisting of parallel fibered bone with low numbers of osteocyte lacunae and zones consisting of fibrolamellar bone with higher numbers of osteocyte lacunae in the primary bone, and formation of erosion bays surrounded by secondary lamellar bone through remodeling. D, Distal rib transverse section. E, Transverse section of gastralia. Abbreviations: eb erosion bay, lb lamellar bone, pfb parallel fibered bone, so secondary osteon. Scale bars represent 2 mm (A, B, D), 0.5 mm (C), 0.8 mm (E).

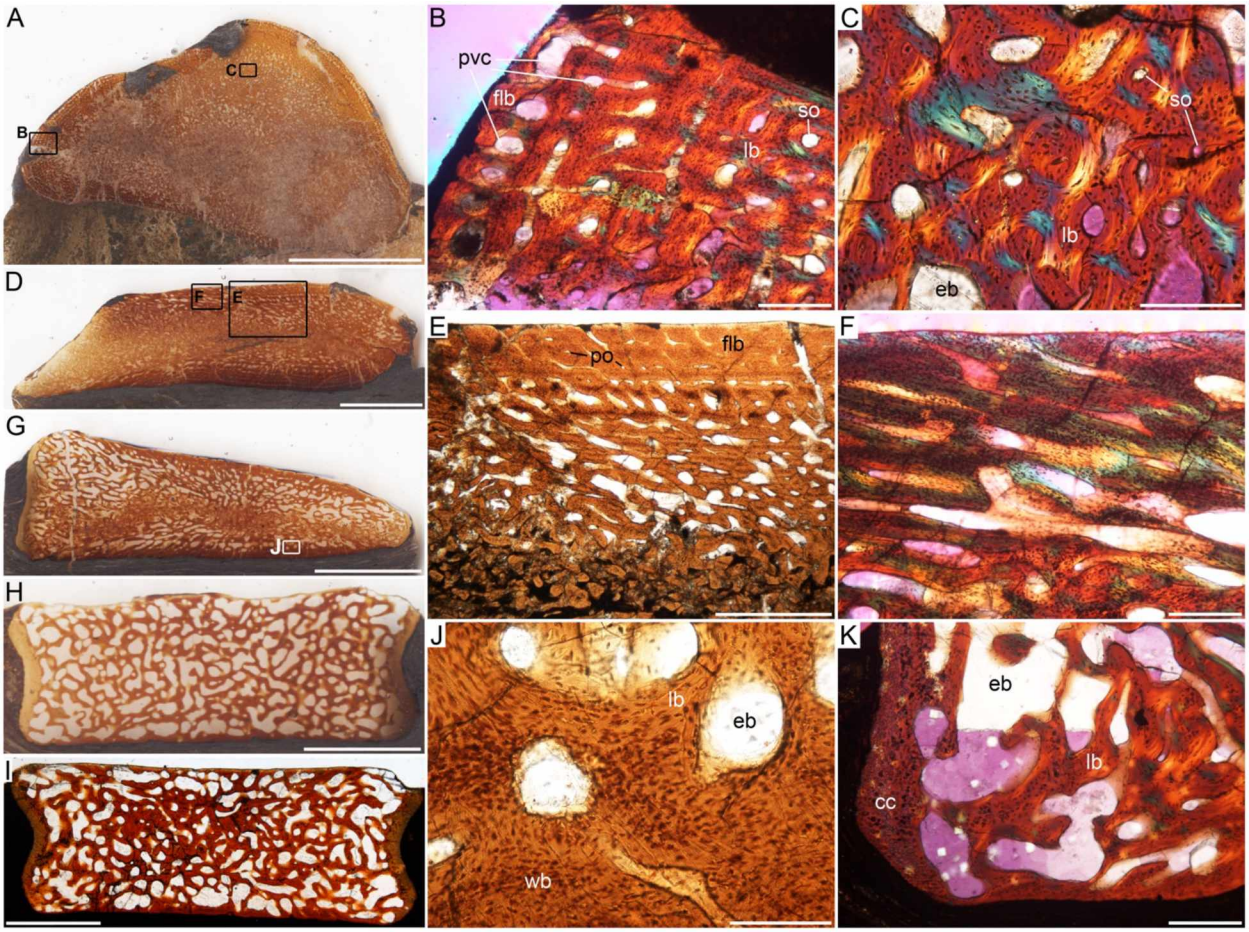

Figure 3-6. Transverse sections of elements of the forelimb of SMNS 4789, referred specimen of *Stenopterygius quadriscissus*. A, Overview of mid-diaphysis section of the humerus. There is no distinct medullary cavity. Anterior is located at the right side of figure. B, Cortical bone of the humerus in cross-polarized light with lambda filter showing primary osteons in fibrolamellar bone and longitudinal primary vascular canals oriented in circumferential rows. C, The secondary lamellar bone and erosion bays of the humerus in cross-polarized light with lambda filter. D, Mid-diaphysis section of the radiale. There is periosteal bone at the anterior; whereas, the posterior shows a cap of calcified cartilage. E, Cortex of the radiale in normal light showing fibrolamellar bone with circumferentially oriented longitudinal primary osteons and vascular canals transitioning into secondary bone and a zone of crushed bone in place of the medullary region. F, Detail of the posteriorly-angled vascularization of the cortex of the radiale in cross-polarized light with lambda filter. G, Transverse section of metacarpal II showing tapering of element at the anterior (leading edge of the paddle). Both the anterior and posterior have a cartilage cap. H, Transverse section of phalanx (5th phalanx of digit IV) showing spongious organization, and anterior and posterior concave cartilage caps. I, Transverse section of phalanx (7th phalanx of digit IV) showing more compact centers compared to proximal phalanges. J, Cortex of metacarpal II in normal light. K, Calcified cartilage cap and spongious secondary lamellar bone of the phalanx from the posterior accessory digit in cross-polarized light with lambda filter. Abbreviations: cc calcified cartilage, eb erosion bay, flb fibrolamellar bone, lb

lamellar bone, po primary osteon, pvc primary vascular canal, so secondary osteon, wb woven bone. B, C, F and K are shown in cross-polarized light with lambda filter. Scale bars represent 10 mm (A), 0.5 mm (B, F, K), 0.25 mm (C, J), 5 mm (D, G), 2 mm (E), 2.5 mm (H), 1 mm (I).

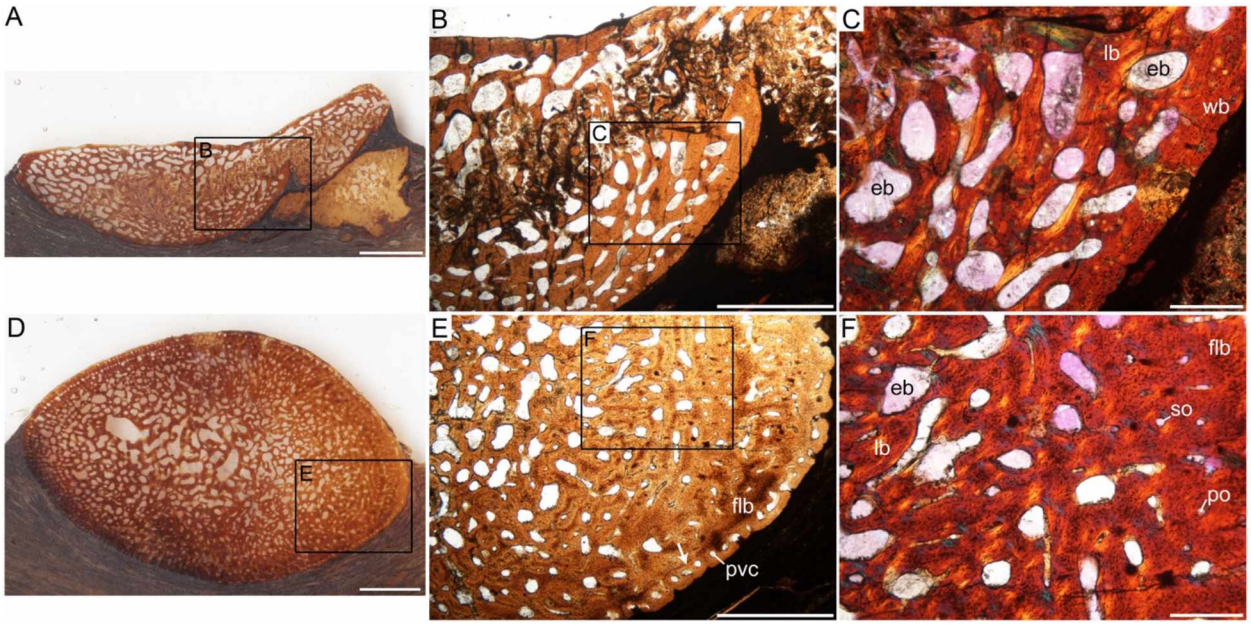

Figure 3-7. Transverse sections of ischiopubis and femur of SMNS 4789, referred specimen of *Stenopterygius quadriscissus*. A, Overview of transverse section near acetabular end of ischiopubis. B, Detail of ischiopubis. Note zone of crushed trabecular bone. C, Detail of ischiopubis in cross-polarized light with lambda filter highlighting woven bone at the periphery, and secondary lamellar bone toward the center of the element. D, Overview of mid-diaphysis section of femur. There is no distinct medullary cavity. Anterior is located at the right side of the figure. E, Detail of femur showing primary longitudinal vascular canals oriented circumferentially in primary bone, and the transition into spongious secondary bone. F, Detail of femur in cross-polarized light with lambda filter showing transition from fibrolamellar primary bone to secondary lamellar bone with erosion bays. Arrow denotes annulus near bone surface. Abbreviations: eb erosion bay, flb fibrolamellar bone, lb lamellar bone, po primary osteon, pvc primary vascular canal, so secondary osteon, wb woven bone. Scale bars represent 2.5 mm (A, D), 2 mm (B, E), 0.5 mm (C, F).

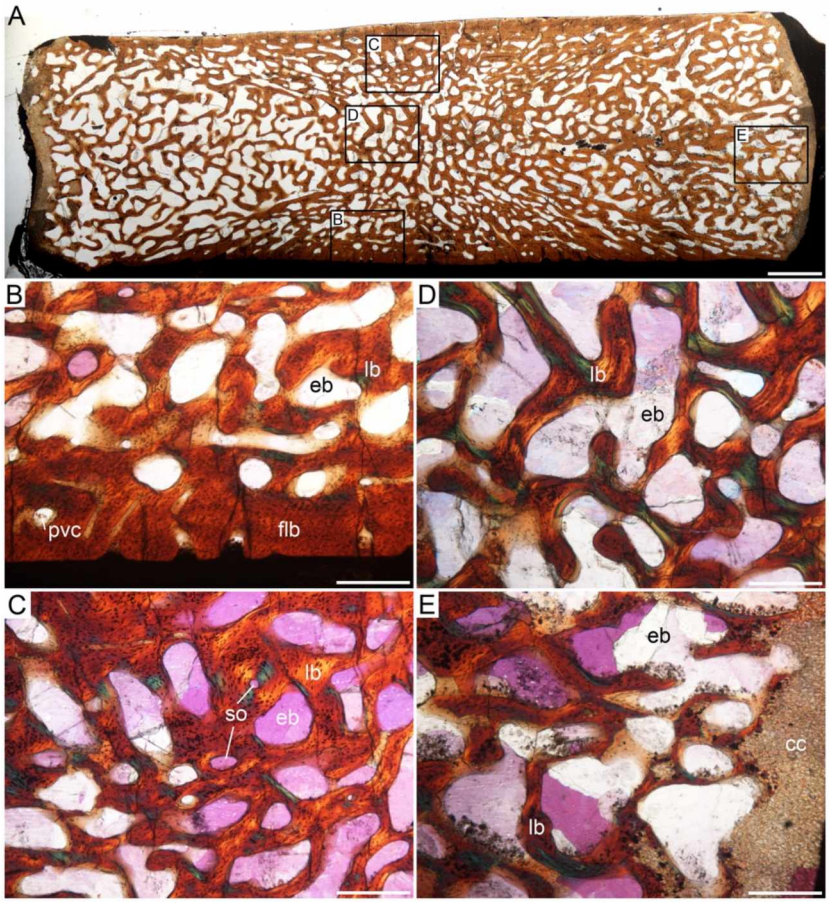

Figure 3-8. Transverse section of fibula of SMNS 4789, referred specimen of *Stenopterygius quadriscissus*. A, Overview of fibula in normal light. B, Detail of cortex showing transition from primary fibrolamellar bone to spongious lamellar bone. C, Remodeled bone with secondary osteons. D, Large erosion bays surrounded by lamellar bone near the center of the fibula. E, Detail of transition from secondary lamellar bone to calcified cartilage cap at the anterior. B-D shown in cross-polarized light with lambda filter. Abbreviations: cc calcified cartilage, eb erosion bay, flb fibrolamellar bone, lb lamellar bone, pvc primary vascular canal, so secondary osteon. Scale bars represent 2 mm (A), 0.5 mm (B-D).

Table 3-1. A selection of existing histological study of bone microstructure of ichthyopterygians. Identifications appear as determined in cited literature. Note: studies focused on description of tooth microstructure are excluded here.

Taxon	Elements sampled	Literature
Undetermined	vertebrae (2), rib	Ricqlès et al. 2009
Caypullisaurus bonapartei	ribs (3)	Talevi et al. 2012; Talevi and Fernández 2012
Cymbospondylidae	vertebrae (2)	Houssaye et al. 2018
Cymbospondylus	vertebra	Houssaye et al. 2018
Eurhinosaurus	dorsal vertebra	Houssaye et al. 2016, 2018
Eurhinosaurus	scapula	Pardo Pérez et al. 2018
Grippoidea	vertebrae (5)	Houssaye et al. 2018
Ichthyosaurus communis	rib	Ricqlès et al. 2009
Ichthyosaurus	vertebra, "lower jaw", "paddle"	Quekett 1855
Ichthyosaurus	"lower jaw"	Gross 1934
Ichthyosaurus	humerus	de Buffrénil and Mazin 1990; Houssaye et al. 2014
Ichthyosaurus	undetermined bone	Ricqlès et al. 2009
Ichthyosaurus	humerus (3), femur (3)	Houssaye et al. 2014
Ichthyosaurus	humerus	Pardo Pérez et al. 2018
Ichthyosaurus	vertebra	Houssaye et al. 2018
Mixosaurus	humerus (5), femur, fibula, ischium, ulna, phalanges (2), scapula, ribs, gastral ribs	Kolb et al. 2011; Houssaye et al. 2014
Mixosaurus	vertebrae (2)	Houssaye et al. 2018
Mollesaurus periallus	ribs (4)	Talevi and Fernández 2012; Fernández and Talevi 2014
Opthalmosaurus icenicus	ribs	Gross 1934
Opthalmosaurus natans	rib	Massare et al. 2014
Opthalmosaurus	ribs (2)	identified as *Baptanodon* in Seitz 1907, Enlow and Brown 1957
Opthalmosaurus	rib(s?)	Nopcsa 1933
Opthalmosaurus	ribs, vertebrae	Martill 1987
Opthalmosaurus	humerus (2)	Houssaye et al. 2014
Opthalmosaurus	vertebra	Houssaye et al. 2018
Pessopteryx nisseri	humerus (2), femur, tibia, autopodial bones (2)	identified as *Omphalosaurus nisseri* by de Buffrénil and Mazin 1990 (Houssaye et al. 2014)
Platypterygius americanus	"paddle bone" (3), "femur?" (1), vertebrae (2)	Lopuchowycz and Massare 2002

Platypterygius	premaxilla, dentary, surangular, angular, splenial, hyoid, cervical vertebrae (2), dorsal vertebrae (5), caudal vertebrae (3), rib, humerus, radius	identified as *Ichthyosaurus* by Kiprijanoff 1881-1883 (Houssaye et al. 2014)
Utatsusaurus hataii	humerus, ribs (2), radius, phalanx	Nakajima et al. 2014
Stenopterygius cayi	rib	Fernández and Talevi 2014
Stenopterygius quadriscissus	humerus (2), femur	de Buffrénil and Mazin 1990; Houssaye et. al 2014
Stenopterygius cf. uniter	tibia	Maxwell et al. 2014
Stenopterygius	rib(s?)	Nopcsa 1933
Stenopterygius	humerus (3), femur	Houssaye et al. 2014
Temnodontosaurus trigonodon	ribs (3)	Seitz 1907; Enlow and Brown 1957
Temnodontosaurus cf. trigonodon	metacarpal II	Maxwell et al. 2014
Temnodontosaurus	rib(s?)	Nopcsa 1933
Temnodontosaurus	humerus, femur	Houssaye et al. 2014
Temnodontosaurus	vertebra	Houssaye et al. 2018
Thunnisauria	vertebrae (3)	identified as "probably *Stenopterygius*" by Houssaye et al. 2018

Chapter 4. Preliminary osteohistological analysis of a scleral ossicle of *Stenopterygius triscissus* (Reptilia: Ichthyosauria) for skeletochronology and implications for eye growth[3]

4.1 Abstract

Ichthyosaurians are a clade of secondarily aquatic reptiles that globally dominated marine environments during the Mesozoic. Despite their prominence in the fossil record and well-supported hypotheses of rapid growth based on osteohistological analysis, their growth rates and age structure remain unquantified. Here we explore a formerly unutilized element in ichthyosaurians, the scleral ossicle, to examine its potential use for skeletochronology, or determination of an individual's age at death. We build on methods first developed in the study of marine turtles and more recently tested on extinct groups of dinosaurians. The results indicate paired light and dark growth marks present in the short axis section; however, the same banding is obscure or not preserved in other planes of sectioning. Due to the relative absence of remodeling of the primary bone, the entire growth record is preserved. The scleral ossicle has great potential to be used for skeletochronology of ichthyosaurians although the plane of sectioning is crucial to the visibility of growth banding. Further testing will compare the number of growth marks preserved in the scleral ossicle versus age inferred from growth marks preserved in other

[3] Anderson, K.L., Erickson, G.M., Druckenmiller, P.S. and Maxwell, E.E. Preliminary osteohistological analysis of a scleral ossicle of *Stenopterygius triscissus* (Reptilia: Ichthyosauria) for skeletochronology and implications for eye growth. Planned submission to *Historical Biology*.

skeletal elements. We corroborate the existing hypothesis of rapid growth of the eye in *Stenopterygius*.

4.2 Introduction

Ichthyosaurians are a clade of secondarily aquatic reptiles that globally dominated marine environments during the Mesozoic. Despite their prominence in the fossil record and well-supported hypotheses of rapid growth based on bone mineral organization (de Buffrénil and Mazin 1990; Kolb et al. 2011; Houssaye et al. 2014; Anderson et al. 2018), their growth rates and age structure remain unquantified. While definitive skeletal growth markers have been identified in *Mixosaurus* sp. (Kolb et al. 2011) and *Stenopterygius quadriscissus* (Anderson et al. 2018), they have yet to be used to determine the age of an individual at death. This method, known as skeletochronology, coupled with measurements of body size, allows modeling and quantification of growth and development of extinct taxa, including maximum growth rate and age at which it was experienced, as well as age at skeletal maturity (Chinsamy and Hillenius 2004; Erickson 2005, 2014).

With two exceptions (see Kolb et al. 2011 and Anderson et al. 2018), osteohistological studies of ichthyosaurians have primarily focused on the description of the humerus, vertebrae, and ribs (Anderson et al. 2018). Spongious primary bone and extensive remodeling preclude the use of limb bones for skeletochronological study of many ichthyosaurians, particularly post-Triassic taxa (Houssaye et al. 2014). Instead, small skeletal elements that grow slowly, such as ribs and gastralia (Seitz 1907; Gross 1934; Enlow and Brown 1957; Kolb et al. 2011; Anderson et al. 2018) and relatively dense

elements, such as the dentary and premaxilla (Anderson et al. 2018), preserve a more complete record of individual growth and numerous growth marks. Among extant reptiles, some marine turtles, including leatherback turtles (*Dermochelys coriacea*), exhibit similar spongious bone in their postcrania, resulting in exploration of other skeletal elements for study of age and growth, specifically scleral ossicles (Zug and Parham 1996; Avens and Goshe 2007; Avens et al. 2009).

Scleral ossicles comprise the scleral ring, a dermally-derived skeletal tissue embedded in the sclera of the eye of reptiles and birds (Franz-Odendaal 2005). Ichthyosaurs have the largest eyes of any extinct or extant vertebrate, and their correspondingly large scleral rings were likely used to stabilize the eye (Motani et al. 1999). Existing studies utilize measurements of the scleral ring to infer metrics of the eyeball, visual acuity and ability to dive, as well as relative growth and age of some ichthyosaurian taxa (McGowan 1972; Motani et al. 1999; Fernández et al. 2005). Scleral ossicles of ichthyosaurians have yet to be osteohistologically described, though their microstructure could corroborate the hypothesis that ichthyosaur eyes reached near-maximum size early in ontogeny, similar to humans (Fernández et al. 2005).

Following methods developed in the study of sea turtles, Erickson et al. (unpublished data) demonstrates the use of scleral ossicles for skeletochronology in an extinct taxon. The number of growth marks preserved in a scleral ossicle of the non-avian dinosaur *Citipati osmolskae* (Late Cretaceous, Mongolia) matches the number of lines of arrested growth (LAGs) preserved in the tibia of the same individual. The preservation of growth marks in the scleral ossicles of additional dinosaurian taxa (Erickson et al., unpublished data) suggests scleral ossicles may consistently preserve growth marks and

therefore be useful for skeletochronology across Reptilia as a whole (with the exception of taxa that have lost scleral rings during the course of their evolutionary history).

Although skeletochronology and the quantification of growth rates through growth curve models have revolutionized the study of dinosaur paleobiology (Chinsamy and Hillenius 2004; Erickson 2005, 2014), growth has yet to be quantified for any ichthyosaurian taxa, in part due to the lack of elements with identified growth marks in post-Triassic ichthyosaurs. This deficiency in the basic understanding of growth and development prevents deeper paleobiological study of this successful clade of Mesozoic marine reptiles, including the evolution of growth strategy and physiology across time and space. Here, we explore a new element, a scleral ossicle, from the ichthyosaurian *Stenopterygius triscissus* from the Posidonienschiefer Formation (Posidonia Shale, Lower Jurassic) of Germany, and assess the use of scleral ossicles for skeletochronology in ichthyosaurians. This is the first osteohistological description of a scleral ossicle of any ichthyosaurian taxa, and we use the microstructure to test hypotheses of eyeball growth based on morphometrics. This is also the first application of this novel approach to ichthyosaurians, with important implications for future growth studies of this clade.

4.3 Materials and Methods

Stenopterygius triscissus (Quenstedt, 1856) is a moderately large-sized ichthyosaur (up to 3.5 m length), well known from the Lower Jurassic (lower Toarcian) deposits of the Posidonienschiefer Formation (Posidonia Shale; also known as the Late Liassic or Lias ε) of the Southwest German Basin (Hauff 1921; Sander 2000; McGowan and Motani 2003; Maisch 2008; Maxwell 2012). The formation is comprised of shale interbedded with

limestone deposited in an epicontinental basin that experienced periodic fluctuations in benthic oxygen levels (Röhl et al. 2001, 2002; Röhl and Schmid-Röhl 2005). It is one of the best examples of Konservat-Lagerstätten with exceptional faunal preservation, including complete, articulated ichthyosaur specimens, the majority of which are referable to the genus *Stenopterygius* (Martill 1993).

One scleral ossicle was mechanically removed from SMNS 50815 (Fig. 4-1A). SMNS 50815 (Staatliches Museum für Naturkunde Stuttgart, Germany), referred to *S. triscissus* (Maxwell 2012) is an articulated ichthyosaur recovered from the Posidonienschiefer Formation, Lias ε III Wildschiefer (*Hildoceras bifrons* ammonite zone) (Fig. 4-1B). The specimen is incomplete, consisting of a complete skull, dorsal vertebrae, and some ribs and paddle elements, with only 211.5 cm of its total body length preserved. With a jaw length of 68.5 cm, this specimen is classed as skeletally mature (Johnson 1977; Maxwell 2012). All scleral ossicles are preserved flattened, and several are disarticulated from the scleral ring and displaced from the orbit. The ossicle sampled here was disarticulated and overlaid the rostrum. A complete ossicle from the same specimen has a measured distance from inner to outer edge (long axis) of 44.4 mm; the sampled ossicle, once removed, measured 43.0 mm, thus some material is missing from the long axis.

The removed ossicle was consolidated and embedded in epoxy (Allied High Tech, Inc.) and sectioned in several planes (Fig. 4-1A) using a diamond tipped blade on a slow speed saw (Isomet 1000, Buehler). Thin sections were glued with epoxy to petrographic slides and ground and polished to thicknesses where the microstructure could be studied using petrographic microscopy. Microstructure is described using terminology outlined by Francillon-Vieillot et al. (1990). We refer to the area of the ossicle that contributes to the

internal diameter (aperture) of the scleral ring as the apertural surface or region; we refer to the area of the ossicle that contributes to the external diameter of the scleral ring as the external surface or region.

4.4 Results

The scleral ossicle was sectioned in 3 planes: the long axis, the short axis, and at an angle from the midpoint to the external edge (Fig. 4-1A, C-E).

4.4.1 Short axis section

In the short axis section, the ossicle has a dense spongious core, with no evidence of remodeling, surrounded by lamellar-zonal bone (Fig. 4-1C). At the core, the trabeculae and intertrabecular spaces run parallel to the medial and lateral surfaces, and all trabeculae consist of primary bone with round, globular osteocytes (Fig. 4-2). The medial side shows a distinct boundary between this spongious core and surrounding denser periosteal bone; on the lateral side, this boundary is less distinct, but can be inferred based on the change in tissue organization. From the spongious core toward the medial and lateral surfaces, the vascular canals become predominantly round or oblong, with more vascular canals present on the lateral than the medial side.

Further toward the medial and lateral surfaces, there is a decrease in the degree of vascularity in the periosteal bone, with distinct boundaries between the area of higher vascularization near the core and the area of lower vascularization at the periphery. Near the surface, the bone is relatively compact with few round vascular canals. At the lateral surface, there is anisotropic lamellar zonal primary bone with at least 7 cycles of paired

light and dark layers with different mineral orientations (Fig. 4-2). This surface is characterized by dimples that the lamellae and zones wrap around. The medial surface shows the same lamellar zonal bone with less conspicuous pairs of light and dark banding. Although classed as lamellar zonal bone based on the organization of the tissue, the osteocyte lacunae are abundant and appear rounder and more globular than expected for this tissue type.

At the edge of the short axis of the ossicle (i.e., where the ossicle would have abutted another ossicle in the scleral ring), the spongy core pinches out, and there are only layers of light and dark banded, anisotropic periosteal bone (Fig. 4-1C). Sharpey's fibers are also prominent and organized at oblique angles to the surface of the bone.

4.4.2 Long axis section

The surface that would have comprised part of the internal diameter of the scleral ring is almost complete, suggesting very little loss of material. In contrast, the opposite end of the long axis section is broken, thus supporting that there is material missing along this axis from the surface that would have comprised part of the external diameter of the scleral ring. The overall shape of this section demonstrates that the ossicle is thicker medial-laterally at the apertural and external regions relative to the thin middle region (Fig. 4-1D). In this middle region, the core spongious bone is thin medial-laterally, and has round to oblong vascular spaces and primary osteons. There is some secondary lamellar bone surrounding oblong secondary osteons suggesting limited remodeling in this area. The boundary between the core spongious bone and denser surrounding periosteal bone is distinct in this region of the section.

Moving away from this middle section to both the apertural and external regions of the ossicle, there is a shift in the spongious organization of the internal core area to relatively larger, oblong intertrabecular spaces. At the furthest point toward the apertural edge, the bone shows no sign of remodeling and consists of a dense spongiosa dominated by intertrabecular spaces that are round to oblong in shape, similar to what is seen at the core of the short axis section. The oblong spaces are oriented at an oblique angle from the medial, middle surface of the ossicle toward the lateral, apertural surface. The external area of the ossicle has a looser sponge in its core surrounded by lamellar secondary bone, pointing to limited remodeling of the primary bone.

In all areas, the periosteal bone is comprised of anisotropic lamellar zonal bone similar to that seen in the short axis section, with light and dark layers. The osteocytes are oblong and oriented in the same direction as the layers. These layers are distinct and clearly visible in the thinner, middle region of the ossicle. Visibility of the layers at both the apertural and external areas of the ossicle is obscured by the presence of dense Sharpey's fibers. The layers are thin and pinch out toward the almost complete apertural surface.

4.4.3 Oblique angle section

The core of oblique angle section shows a dense spongious primary bone with oblong intertrabecular spaces oriented at an oblique angle, similar to what is seen in the core of the short axis section, and the core of the long axis section near the apertural surface (Fig. 4-1E). There is no evidence of remodeling as seen by a lack of secondary bone. Moving toward the external region of the ossicle, the spongiosa becomes looser, and there is some evidence of remodeling in the form of secondary lamellar bone. This spongiosa

pinches out further toward the external edge of the ossicle, becoming one single line of round to oval vascular spaces with no remodeling.

The spongious core and surrounding denser periosteal regions are distinct throughout. The periosteal bone surrounding the spongiosa is anisotropic, lamellar-zonal bone organized in light and dark layers, as seen in the other sections described above. Sharpey's fibers run at oblique angles to the medial and lateral surfaces throughout the section, but are more prominent on the lateral surface. Where the spongiosa pinches out toward the furthest external point of the ossicle preserved, the section is predominantly periosteal bone.

4.5 Discussion

The scleral ossicle consists of primary spongious bone with very little evidence of remodeling at its core, surrounded by lamellar-zonal periosteal bone in light and dark cycles with very little remodeling. We interpret the dense spongious primary bone at the core of the ossicle to be the skeletal tissue present at birth (age 0), and the boundary between this primary spongious bone and the primary periosteal bone to be the core mark as described by Avens and Goshe (2007). The paired light and dark cycles in the primary periosteal bone outside the core mark are likely annual, as has been demonstrated in extant sea turtles and the dinosaur *Citipati* through comparison of these growth marks with LAGs in elements of the postcrania (Zug and Parham 1996; Avens and Goshe 2007; Avens et al. 2009; Erickson et al. unpublished data).

The plane of section is crucial to the visibility of the growth bands of the ossicle. In chelonoideans the wider tip of the long axis of the ossicle best preserves growth marks

(Avens et al. 2009); however, we did not see this in the ossicle of *Stenopterygius triscissus*. The long axis shows some light and dark banding at its minimum medial-lateral thickness, but it does not clearly or consistently preserve growth banding in this plane, and is dominated by the presence of Sharpey's fibres. In *S. triscissus*, we found that the growth marks are clearly preserved in the short axis section, thus the banding conserves the growth record in terms of the thickening of the ossicle in the medial-lateral plane. While the long axis and oblique sections informed our overall understanding of the microstructure and growth of the ossicle, the short axis is the only plane of sectioning we were able to use for preliminary skeletochronological analysis.

Based on these paired growth marks and assuming that they are annual, this individual was a minimum of 7 years old at the time of death. Because there is very little remodeling, back calculation of missing growth bands is not necessary; however, it is possible that growth bands may not have been formed early in ontogeny if the growth rate was high. This is a minimum inferred age due to this potential lack of growth bands early in ontogeny. Because ichthyosaurian development and physiology is hypothesized to consist of raised growth rates and metabolic rates and very little is understood about where ichthyosaurians fit in a broader evolutionary context, it is difficult to compare their inferred age structure and development with modern ectothermic reptiles of similar body size.

Where growth banding is clearly visible in the short axis section, both the medial and lateral edges show a slowing in growth, with zones of primary periosteal bone that dramatically decrease in size after 1 cycle on the medial edge and 2 cycles on the lateral edge. Following this, the zones are equal in size and tightly stacked, reflecting that the

ossicle is not significantly thickening in the medial-lateral plane after 1-2 years of age. Morphometric study of scleral rings show that ichthyosaur eyeballs reached near full size early in ontogeny similar to growth seen in human eyeballs (Fernández et al. 2005). The microstructure seen in *S. triscissus* also shows that the scleral ossicle, and in turn the scleral ring as a whole, slowed in growth early in ontogeny.

Although the ossicle sampled here is incomplete at its external surface, the thinning and pinching out of the core dense spongious primary bone toward its external most point in the long axis section suggests that primary periosteal bone deposition is mainly occurring on the external surface of the ossicle to increase its length along the long axis. This shows that the external diameter of the scleral ring increases relative to the internal diameter through deposition of primary periosteal bone at the external surface of the ossicles throughout ontogeny. Again, this agrees with a morphometric study of scleral ossicles that suggests the growth of the cornea, as indicated by measurement of the internal diameter of the sclerotic ring, slows relative to the overall size of the eyeball, as indicated by measurement of the external diameter which continues to grow throughout ontogeny (Fernández et al. 2005).

Scleral ossicles are potentially very useful for skeletochronology of *Stenopterygius* due to the presence of growth banding and little remodeling, but this method requires further testing through comparison with growth marks (LAGs or annuli) found elsewhere in the skeleton. In *Stenopterygius*, annuli are clearly identifiable in the premaxilla and dentary (Anderson et al. 2018). If the light and dark cycles seen in the ossicle are annual, their number should match the age estimates from analysis of LAGs or annuli in other elements of the same specimen, as has been demonstrated in the dinosaurian *Citipati*

(Erickson et al. unpublished data). Future testing will explore the microstructure of the scleral ossicles of additional ichthyosaurian taxa. Due to the body size disparity across the clade, we expect some variation in the microstructure of scleral ossicles of ichthyosaurians. The presence of growth marks in the scleral ossicles of chelonoideans (Zug and Parham 1996; Avens and Goshe 2007; Avens et al. 2009), dinosaurians (Erickson et al. unpublished data), and one ichthyosaurian shows great potential for their use for skeletochronology across Reptilia. This method could be of particular importance for determining age of groups like ichthyosaurians that rarely preserve growth marks due to spongious primary bone and extensive remodeling in many of their bones (Houssaye et al. 2014; Anderson et al. 2018).

4.6 Acknowledgements

This research was funded by the National Science Foundation GK-12 Changing Alaska Science Education fellowship (NSF DGE-0948029; PIs R. Boone, L. Conner, and K. Winker) and the University of Alaska Museum.

4.7 References

Anderson KL, Druckenmiller PS, Erickson GM, Maxwell EE. 2018. Skeletal microstructure of *Stenopterygius quadriscissus* (Reptilia: Ichthyosauria) from the Posidonienschiefer (Posidonia Shale, Lower Jurassic) of Germany. Palaeontol. 62(3):433-449.

Avens L, Goshe LR. 2007. Comparative skeletochronological analysis of Kemp's ridley (*Lepidochelys kempii*) and loggerhead (*Caretta caretta*) humeri and scleral ossicles. Mar Biol. 152(6):1309-1317.

Avens L, Taylor JC, Goshe LR, Jones TT, Hastings M. 2009. Use of skeletochronological analysis to estimate the age of leatherback sea turtles *Dermochelys coriacea* in the western North Atlantic. Endanger Species Res. 8(3):165-177.

de Buffrénil V, Mazin J-M. 1990. Bone histology of the ichthyosaurs: comparative data and functional interpretation. Paleobiology 16:435–447.

Chinsamy A, Hillenius WJ. 2004. Physiology of nonavian dinosaurs. In Dodson P, Osmolska H, Weishampel DB, editors. The Dinosauria. University of California Press; p. 643–659.

Enlow DH, Brown SO. 1957. A comparative study of fossil and recent bone tissue. Part II: Reptiles and birds. Tex J Sci. 9:186–214.

Erickson, GM. 2005. Assessing dinosaur growth patterns: a microscopic revolution. Trends Ecol Evol. 20:677–684.

Erickson, GM. 2014. On Dinosaur Growth. Annu Rev Earth Planet Sci. 42:675–697.

Erickson GM, Anderson KL, Watabe M, Norrell MA. Unpublished data. Age and growth pattern for a specimen of non-avian dinosaur *Citipati osmolskae* determined from growth lines in scleral ossicles.

Fernández MS, Archuby F, Talevi M, Ebner R. 2005. Ichthyosaurian eyes: paleobiological information content in the sclerotic ring of *Caypullisaurus* (Ichthyosauria, Ophthalmosauria). J Vert Paleontol. 25(2):330-337.

Francillon-Vieillot H, de Buffrénil V, Castanet J, Geraudie J, Meunier FJ, Sire JY, Zylerbeg L, de Ricqlès A. 1990. Microstructure and mineralization of vertebrate skeletal tissues. 471–530. *In* Carter JG, editor. *Biomineralization: patterns and evolutionary trends*. Van Nostrand Reinhold, New York.

Franz-Odendaal TA. 2006. Intramembranous ossification of scleral ossicles in *Chelydra serpentina*. Zoology 109(1):75-81.

Gross W. 1934. Die Typen des mikroskopischen Knochenbaues bei fossilen Stegocephalen und Reptilien. Z Anat Entwicklungsgesch. 203:731–764.

Hauff B. 1921. Untersuchung der Fossilfundstätten von Holzmaden in Posidonienschiefer des oberen Lias Württembergs. Palaeontographica 64:1–42.

Houssaye A, Scheyer TM, Kolb C, Fischer V, Sander PM. 2014. A new look at ichthyosaur long bone microanatomy and histology: implications for their adaptation to an aquatic life. Plos One 9(4):e95637.

Johnson R. 1977. Size independent criteria for estimating relative age and the relationship among growth parameters in a group of fossil reptiles (Reptilia: Ichthyosauria). Can J Earth Sci. 14:1916–1924.

Kolb C, Sánchez-Villagra MR, Scheyer TM. 2011. The palaeohistology of the basal ichthyosaur *Mixosaurus* Baur, 1887 (Ichthyopterygia, Mixosauridae) from the Middle Triassic: palaeobiological implications. C R Palevol. 10:403–411.

Martill DM. 1993. Soupy substrates: a medium for the exceptional preservation of ichthyosaurs of the Posidonia Shale (Lower Jurassic) of Germany. Kaupia 2:77–97.

Maxwell EE. 2012. New metrics to differentiate species of *Stenopterygius* (Reptilia: Ichthyosauria) from the Lower Jurassic of Southweastern Germany. J Paleontol. 86(1):105–115.

McGowan C. 1972. Evolutionary trends in longipinnate ichthyosaurs with particular reference to the skull and fore fin. Toronto: Royal Ontario Museum.

McGowan C, Motani R. 2003. Ichthyopterygia. In Sues H-D, editor. Handbook of Paleoherpetology. München: Verlag Dr. Friedrich Pfeil.

Motani R, Rothschild BM, Wahl W Jr. 1999. Large eyeballs in diving ichthyosaurs. Nature 402:747.

Quenstedt FA. 1856. Der Jura. Tübingen: H. Laupp.

Röhl H-J, Schmid-Röhl A, Oschmann W, Frimmel A, Schwark L. 2001. The Posidonia Shale (Lower Toarcian) of SW-Germany: an oxygen-depleted ecosystem controlled by sea level and palaeoclimate. Palaeogeogr Palaeoclimatol Palaeoecolo. 165:27–52.

Röhl H-J, Schmid-Röhl A. 2005. Lower Toarcian (Upper Liassic) black shales of the central European epicontinental basin: a sequence stratigraphic case study from the SW German Posidonia Shale. In Harris NB, editor. The deposition of organic-carbon-rich sediments: models, mechanisms, and consequences. SEPM Spec P. 82:165–189.

Sander PM. 2000. Ichthyosauria: their diversity, distribution, and phylogeny. Paläont Z. 74:1–35.

Schmid-Röhl A, Röhl H-J, Oschmann W, Frimmel A, Schwark L. 2002. Palaeoenvironmental reconstruction of Lower Toarcian epicontinental black shales (Posidonia Shale, SW Germany): global versus regional control. Geobios. 35:13–20.

Seitz ALL. 1907. Vergleichende Studien über den mikroskopischen Knochenbau fossiler und rezenter Reptilien und dessen Bedeutung für das Wachstum und Umbildung des Knochengewebes im allgemeinen. E. KARRAS. 87(2).

Zug GR, Parham JF. 1996. Age and growth in leatherback turtles, *Dermochelys coriacea* (Testudines: Dermochelyidae): a skeletochronological analysis. Chelonian Conserv Bi. 2:244-249.

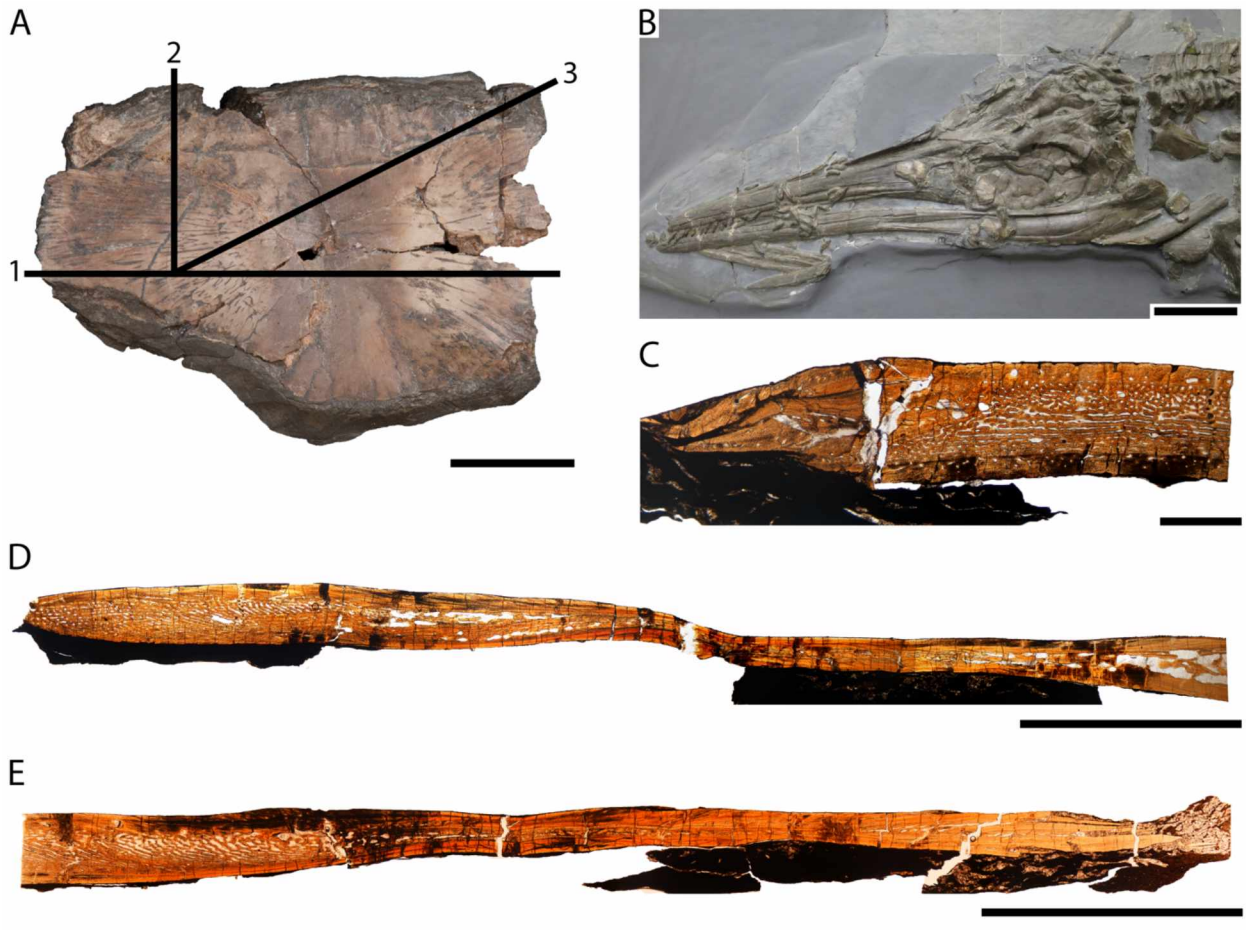

Figure 4-1. Overview of the scleral ossicle of SMNS 50815 referred specimen of *Stenopterygius triscissus*. A, Removed scleral ossicle with lines illustrating where sections were made along the long axis (1), the short axis (2), and an oblique angle toward the external point (3). Shown in lateral view with left side being part of the internal diameter, and right-side being part of the external diameter of the scleral ring. B, Skull of SMNS 50815. C, Short axis section (line 2 in A). D, Long axis section (line 1 in A). E, Oblique section (line 3 in A). This image has been mirrored for consistency of this figure. Scale bars represent 1 cm (A), 10 cm (B), 1 mm (C), 5 mm (D, E).

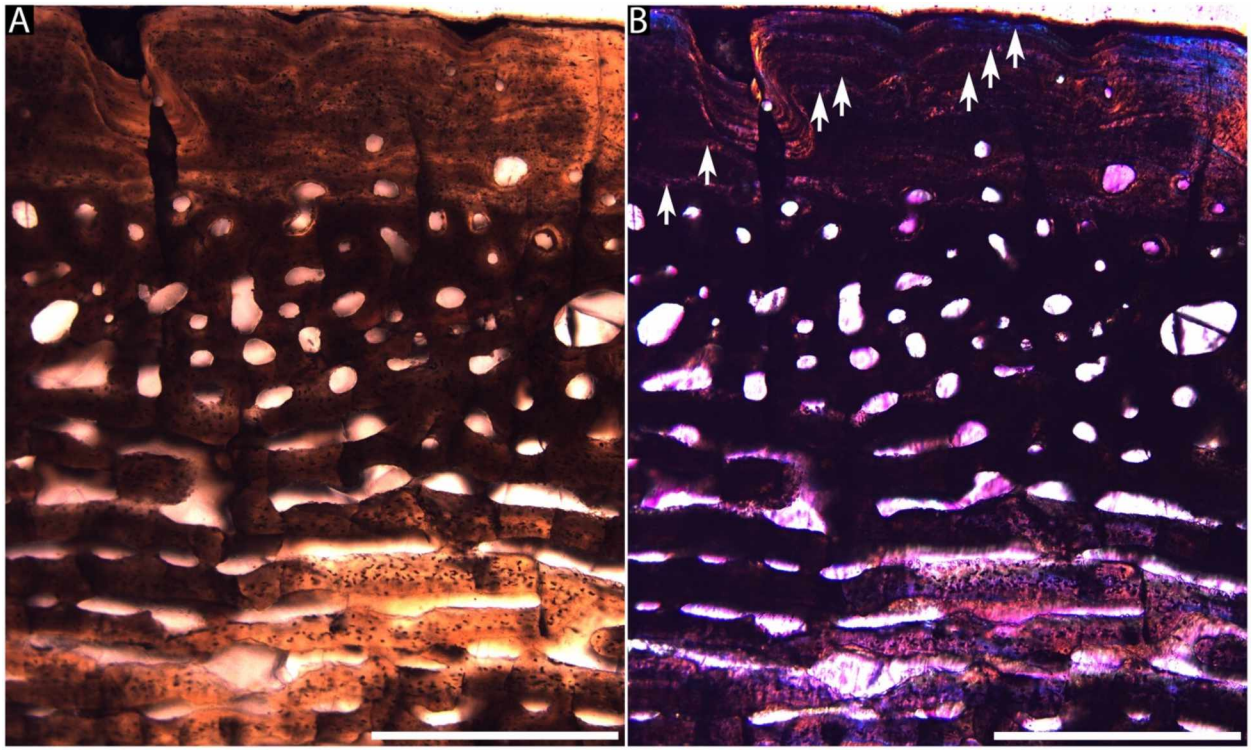

Figure 4-2. Detail of the short axis section of the scleral ossicle of SMNS 50815 referred specimen of *Stenopterygius triscissus*. A, Cross-polarized light with no filter. B, Cross-polarized light with filter showing spongious primary bone with globular osteocytes at the core of the ossicle, and lamellar-zonal bone with light and dark growth cycles (denoted by arrows) in the periosteal cortex. Scale bar represents 0.5 mm (A, B).

Chapter 5. Conclusion

Ichthyosaurians (Ichthyosauria) are considered one of the most successful clades of Mesozoic marine reptiles given their extensive fossil record (160 million years), cosmopolitan distribution, and taxonomic diversity (McGowan and Motani, 2003). Despite their prominence in the fossil record, there remains much to be learned about aspects of their biology, including quantification of age structure and growth rates. Multiple lines of evidence suggest that ichthyosaurians experienced elevated growth rates and likely maintained an elevated body temperature relative to ambient sea temperature (Massare, 1988; de Buffrénil and Mazin, 1990; Motani, 2002a, b, 2010; Bernard et al., 2010; Kolb et al., 2011; Houssaye et al., 2014; Anderson et al., 2018). In this dissertation, I sought to test these hypotheses using osteohistological methods.

In the first manuscript, we describe an articulated, partial skeleton of the small-bodied ichthyosaur *Toretocnemus* from Gravina Island (Nehenta Formation, Norian, Upper Triassic), as well as an isolated femur from temporally equivalent deposits on Hound Island (Hound Island Volcanics, Norian, Upper Triassic) in Southeast Alaska. The partial skeleton of *Toretocnemus* is comprised of two dorsal vertebrae, dorsal ribs, pelvic elements, an articulated hindlimb, a femur, and 18 articulated caudal vertebrae including apical vertebrae. We compared these specimens to other small-bodied, Upper Triassic ichthyosaurians. Both specimens are referred to *Toretocnemus* based on the unique morphology of the hindlimb, particularly the femur. Due to the fragmentary nature and poor preservation of the material, we refer them to the generic rather than specific level. Prior to this, *Toretocnemus* was known from Carnian-aged deposits of California and possibly Sonora, Mexico (Merriam, 1903; Lucas, 2002); thus, this occurrence expands both

the geographic and stratigraphic range of the genus. This is also the first documentation of a tail bend in this genus. There are few occurrences of ichthyosaurians in the Norian, the majority of which are referable to the large-bodied Shastasauridae (see table 2-1). These specimens are significant because they suggest that small-bodied ichthyosaurians typical of the Carnian persisted into the Norian ahead of the end-Triassic extinction.

The second manuscript lays important groundwork for future work that will quantify growth rates in the ichthyosaurian *Stenopterygius quadriscissus* from the Posidonia Shale (Lower Jurassic) of Germany. We sampled over 40 elements across the skeleton of one individual to describe the overall microstructure, to infer relative growth rates of various elements based on mineral tissue organization, and to identify skeletal elements that preserve growth marks (Anderson et al., 2018). Our findings indicate that this species grew rapidly relative to modern ectothermic reptiles of similar body mass based on the presence of fibrolamellar primary bone in nearly all elements sampled. The limb elements that are typically used for growth studies of terrestrial taxa have spongious primary and secondary bone. Primary vascular cycles in the humerus and femur were cyclical and associated with annuli in some areas. We support the hypothesis of mesopodialization, or modified perichondral ossification, based on the microstructure of the limb elements (Caldwell, 1997; Maxwell et al., 2014). The densest bones sampled are the dentary and premaxilla. Growth marks in the form of annuli are present in the dentary, premaxilla, ribs, humerus, and femur. Because of their density and preservation of the most growth marks, the dentary and premaxilla are ideal candidates for future skeletochronology and growth studies of this species of ichthyosaurian. These elements had not been histologically described for any ichthyosaurian taxa prior to this study and

are a departure from elements typically chosen for study of development in extinct taxa. Future work building upon the findings of this study is discussed below.

The last manuscript presents preliminary results on the use of scleral ossicles of ichthyosaurians for skeletochronology. This builds on the demonstrated use of scleral ossicles for skeletochronology of extant sea turtles (Zug and Parham, 1996; Avens and Goshe, 2007; Avens et al., 2009) and more recent work that demonstrates their use for skeletochronology in dinosaurians (Erickson et al., unpublished data). We sampled a scleral ossicle from *Stenopterygius triscissus* from the Posidonia Shale (Lower Jurassic) of Germany and sectioned the ossicle in three planes to examine and describe the microstructure. The ossicle preserves almost the entire growth record due to the occurrence of very little remodeling. A transition in structure from spongious to more compact bone near the core of the ossicle is likely the "core mark," as defined by Avens et al. (2009). Growth marks in the form of light and dark cycles of different mineral orientation are clearly preserved in the short axis section; however, these growth marks are not as well preserved, or not present, in other planes. Backcalculation of missing growth marks is not necessary because almost the entire primary growth record is preserved due to the low degree of remodeling. If these growth bands are annual, we infer that the individual was a minimum of 7 years of age at the time of death, and we discuss implications of the microstructural organization for the growth of the eyeball. Future work (discussed below) will test these preliminary results through comparison of inferred age from the scleral ossicle versus the dentary of the same individual.

This dissertation lays critical groundwork for continued studies of age structure and growth of ichthyosaurians. Future work that builds on this foundation will address broader

research questions through quantification of age and growth rates of an ichthyosaurian species. Currently, we are in the process of sampling the dentary from a growth series of specimens referred to *S. quadriscissus* from the Posidonia Shale of Germany (Appendix B). All specimens are from a single stratigraphic interval due to the increase in maximum body size of this species through geological time (Maxwell and Vincent, 2016). Sampling a growth series, inferred from jaw length, allows us to see a "snapshot" of growth as preserved in the mineralized tissues at different points in an animal's life history. This method assumes that each individual in the series represents a typical record of growth for that species in that stratigraphic interval.

Using the growth series, we will backcalculate the number of growth marks that may have been lost to remodeling in larger individuals, therefore allowing us to infer minimum age based on growth marks for each individual in the series (Woodward et al., 2013). This will be the first time that skeletochronology is used to determine individual ichthyosaurians ages at death, and it is a major step in understanding their development. After plotting age versus jaw length (a metric that correlates with total body length in this species; Maxwell and Vincent, 2016), growth is modeled and quantified by fitting the data with various growth models (Lee et al., 2013). This approach allows quantification of growth rate at different ages and determination of maximum growth rate, as well as inference of age when sexual maturity is reached and age at somatic maturity.

The second step of this ongoing project is to test if scleral ossicles can be used for skeletochronology of ichthyosaurians. This has already been tested in the dinosaur *Citipati osmolskae* through comparison of growth marks preserved in the scleral ossicle and the tibia of one individual (Erickson et al., unpublished data). Because the number of growth

marks in each skeletal element matched, it is highly likely that scleral ossicles are a reliable element for skeletochronology in this dinosaur species (Erickson et al., unpublished data). We will use the same approach to test the use of scleral ossicles for ichthyosaurians (Appendix B). From the *S. quadriscissus* growth series, we sampled three scleral ossicles from three of the individuals to investigate if the number of growth marks in the ossicles match the individuals' ages inferred from the backcalculation method using growth marks preserved in the dentary. This test will have far reaching implications. Because the scleral ossicles of this species show very little remodeling, the entire growth record is preserved, therefore potentially mitigating the need to sample a growth series to backcalculate missing growth marks in the future. In addition, because ossicles are small and often disarticulated or displaced from the orbit, this method could offer a less destructive mode of determining age of ichthyosaurians. Further exploration of the microstructure of the ossicles of other taxa will be necessary; due to the diversity of ichthyosaurians across time and space, there will likely be variation in their ossicles.

In the Posidonia Shale, the maximum body size of *S. quadriscissus* increases in later stratigraphic intervals (Maxwell and Vincent, 2016). If the test shows that scleral ossicles can be used for skeletochronology of this species, we can use this methodology to investigate how its development is evolving to reach these larger maximum body sizes. There are two primary ways in which a species can achieve a larger body size: 1) by increasing the growth rate, thereby reaching larger body sizes, but not increasing maximum age of the largest individuals, and 2) by keeping the growth rate constant and living longer, thereby increasing maximum age of the largest individuals. It is also possible that larger maximum body size can evolve through a combination of these two modes. We

can determine if individuals in the population were living longer to reach larger body sizes by sampling a scleral ossicle from an individual of maximum body size for skeletochronology and then comparing the inferred age of this individual with an individual of maximum body size from older strata. If ages are the same or comparable, it is likely that the population was not living longer to reach larger body sizes but instead increasing their growth rates through geological time. This is one potential question that can be addressed based on this body of work.

The use of bone microstructure to infer aspects of paleobiology has revolutionized the field of dinosaur paleobiology (Chinsamy and Hillenius, 2004; Erickson, 2005, 2014). Surprisingly, prior to this dissertation, these methods have only been applied to a limited number of taxa of ichthyosaurians, and very few skeletal elements have been studied (Anderson et al., 2018). *Stenopterygius* was chosen for this study, because it is well represented by a large number of individuals, including embryos and neonates (Hauff, 1921; Sander, 2000; McGowan and Motani, 2003; Maisch, 2008; Maxwell, 2012). From here, we can begin to apply what we have learned to other taxa to understand how ichthyosaurian development and physiology evolved over time and space. It has been suggested, based on the presence of fibrolamellar bone, that Lower Triassic ichthyopterygians (Ichthyopterygia) were capable of rapid growth rates, potentially as a precursor to evolving elevated body temperatures (Nakajima et al., 2014). With quantification of this clade's age and growth, we can begin to answer higher order questions about their metabolic rates and ability to maintain elevated body temperatures. Although ichthyosaurians have been studied by paleontologists for well over a century, the use of osteohistological methods building on the foundation of this dissertation has the

potential to revolutionize our understanding of this fascinating and successful clade of secondarily aquatic vertebrates.

5.1 References

Anderson, K.L., Druckenmiller, P.S., Erickson, G.M. and Maxwell, E.E. 2018. Skeletal microstructure of *Stenopterygius quadriscissus* (Reptilia: Ichthyosauria) from the Posidonienschiefer (Posidonia Shale, Lower Jurassic) of Germany. *Palaeontology*, 62(3):433-449. https://doi.org/10.1111/pala.12408

Avens, L. and Goshe, L.R. 2007. Comparative skeletochronological analysis of Kemp's ridley (*Lepidochelys kempii*) and loggerhead (*Caretta caretta*) humeri and scleral ossicles. *Marine Biology,* 152(6):1309-1317.

Avens, L., Taylor, J.C., Goshe, L.R., Jones, T.T. and Hastings, M., 2009. Use of skeletochronological analysis to estimate the age of leatherback sea turtles *Dermochelys coriacea* in the western North Atlantic. *Endangered Species Research,* 8(3):165-177.

Bernard, A., Lécuyer, C., Vincent, P., Amiot, R., Bardet, N., Buffetaut, E., Cuny, G., Fourel, F., Martineau, F., Mazin, J.M. and Prieur, A. 2010. Regulation of body temperature by some Mesozoic marine reptiles. *Science*, *328*(5984):1379-1382.

Buffrénil, V. de and Mazin, J.-M. 1990. Bone histology of the ichthyosaurs: comparative data and functional interpretation. *Paleobiology,* 16:435–447.

Caldwell, M.W. 1997. Modified perichondral ossification and the evolution of paddle-like limbs in ichthyosaurs and plesiosaurs. *Journal of Vertebrate Paleontology*, *17*(3):534-547.

Chinsamy, A. and Hillenius, W.J. 2004. Physiology of nonavian dinosaurs, p. 643–659. In Dodson, P., Osmolska, H. and Weishampel, D.B. (eds.), *The Dinosauria*. University of California Press.

Erickson, G.M. 2005. Assessing dinosaur growth patterns: a microscopic revolution. *Trends in Ecology & Evolution,* 20:677–684.

Erickson, G.M. 2014. On dinosaur growth. *Annual Review of Earth and Planetary Sciences,* 42:675–697.

Erickson, G.M., Anderson, K.L., Watabe, M. and Norrell, M.A. Unpublished data. Age and growth pattern for a specimen of non-avian dinosaur *Citipati osmolskae* determined from growth lines in scleral ossicles.

Hauff, B. 1921. Untersuchung der Fossilfundstätten von Holzmaden im Posidonienschiefer des Oberen Lias Württembergs. *Palaeontographica, (1846-1933)*:1-42.

Houssaye, A., Scheyer, T.M., Kolb, C., Fischer, V. and Sander, P.M. 2014. A new look at ichthyosaur long bone microanatomy and histology: implications for their adaptation to an aquatic life. *Plos One,* 9(4):e95637.

Kolb, C., Sánchez-Villagra, M.R. and Scheyer, T.M. 2011. The palaeohistology of the basal ichthyosaur *Mixosaurus* Baur, 1887 (Ichthyopterygia, Mixosauridae) from the Middle Triassic: palaeobiological implications. *Comptes Rendus Palevol,* 10:403–411.

Lee, A.H., Huttenlocker, A.K., Padian, K. and Woodward, H.N. 2013. Analysis of growth rates. In Padian, K. and Lamm, E.-T. (eds.) *Bone histology of fossil tetrapods: Advancing methods, analysis and interpretation*. University of California Press.

Lucas, S.G. 2002. *Toretocnemus*, a Late Triassic ichthyosaur from California, U.S.A and Sonora, Mexico. *New Mexico Museum Natural History and Science Bulletin,* 21:275-282.

Maisch, M.W. 2008. Revision der Gattung *Stenopterygius* Jaekel, 1904 emend. von Huene, 1922 (Reptilia: Ichthyosauria) aus dem unteren Jura Westeuropas. *Paleodiversity*, 1:227-271.

Massare, J.A. 1988. Swimming capabilities of Mesozoic marine reptiles: implications for method of predation. *Paleobiology*, *14*(2):187-205.

Maxwell, E.E. 2012. New metrics to differentiate species of *Stenopterygius* (Reptilia: Ichthyosauria) from the Lower Jurassic of southwestern Germany. *Journal of Paleontology*, *86*(1):105-115.

Maxwell, E.E. and Vincent, P. 2016. Effects of the early Toarcian Oceanic Anoxic Event on ichthyosaur body size and faunal composition in the Southwest German Basin. *Paleobiology*, *42*(1):117-126.

Maxwell, E.E., Scheyer, T.M. and Fowler, D.A. 2014. An evolutionary and developmental perspective on the loss of regionalization in the limbs of derived ichthyosaurs. *Geological Magazine*, *151*(1):29-40.

McGowan, C. and Motani, R. 2003. Ichthyopterygia. In Sues, H.-D. (ed). *Handbook of Paleoherpetology*. Verlag Dr. Friedrich Pfeil, München.

Merriam, J.C. 1903. *New Ichthyosauria from the Upper Triassic of California*. University of California Press.

Motani, R. 2002. Scaling effects in caudal fin propulsion and the speed of ichthyosaurs. *Nature*, *415*(6869):309.

Motani, R. 2002. Swimming speed estimation of extinct marine reptiles: energetic approach revisited. *Paleobiology*, *28*(2):251-262.

Motani, R. 2010. Warm-blooded "sea dragons"? *Science*, *328*(5984):1361-1362.

Nakajima, Y., Houssaye, A. and Endo, H. 2014. Osteohistology of the Early Triassic ichthyopterygian reptile *Utatsusaurus hataii*: Implications for early ichthyosaur biology. *Acta Palaeontologica Polonica*, *59*(2):343-353.

Sander, P.M. 2000. Ichthyosauria: their diversity, distribution, and phylogeny. *Paläontologische Zeitschrift*, *74*(1-2):1-35.

Woodward, H.N., Padian, K. and Lee, A.H. 2013. Skeletochronology. In Padian, K. and Lamm, E.-T. (eds.) *Bone histology of fossil tetrapods: Advancing methods, analysis and interpretation*. University of California Press.

Zug, G.R. and Parham, J.F. 1996. Age and growth in leatherback turtles, *Dermochelys coriacea* (Testudines: Dermochelyidae): a skeletochronological analysis. *Chelonian Conservation and Biology, 2*:244-249.

Chapter 6. Appendices

Appendix A. Supplemental figures for Chapter 3. Skeletal microstructure of *Stenopterygius quadriscissus* (Reptilia, Ichthyosauria) from the Posidonienschiefer (Posidonia Shale, Lower Jurassic) of Germany[4]

[4] Anderson, K. L., Druckenmiller, P. S., Erickson, G. M. and Maxwell, E. E. 2018. Data from: Skeletal microstructure of *Stenoptergius quadriscissus* (Reptilia, Ichthyosauria) from the Posidonienschiefer (Posidonia Shale, Lower Jurassic) of Germany. *Dryad Digital Repository*. https://doi.org/10.5061/dryad.032cq64

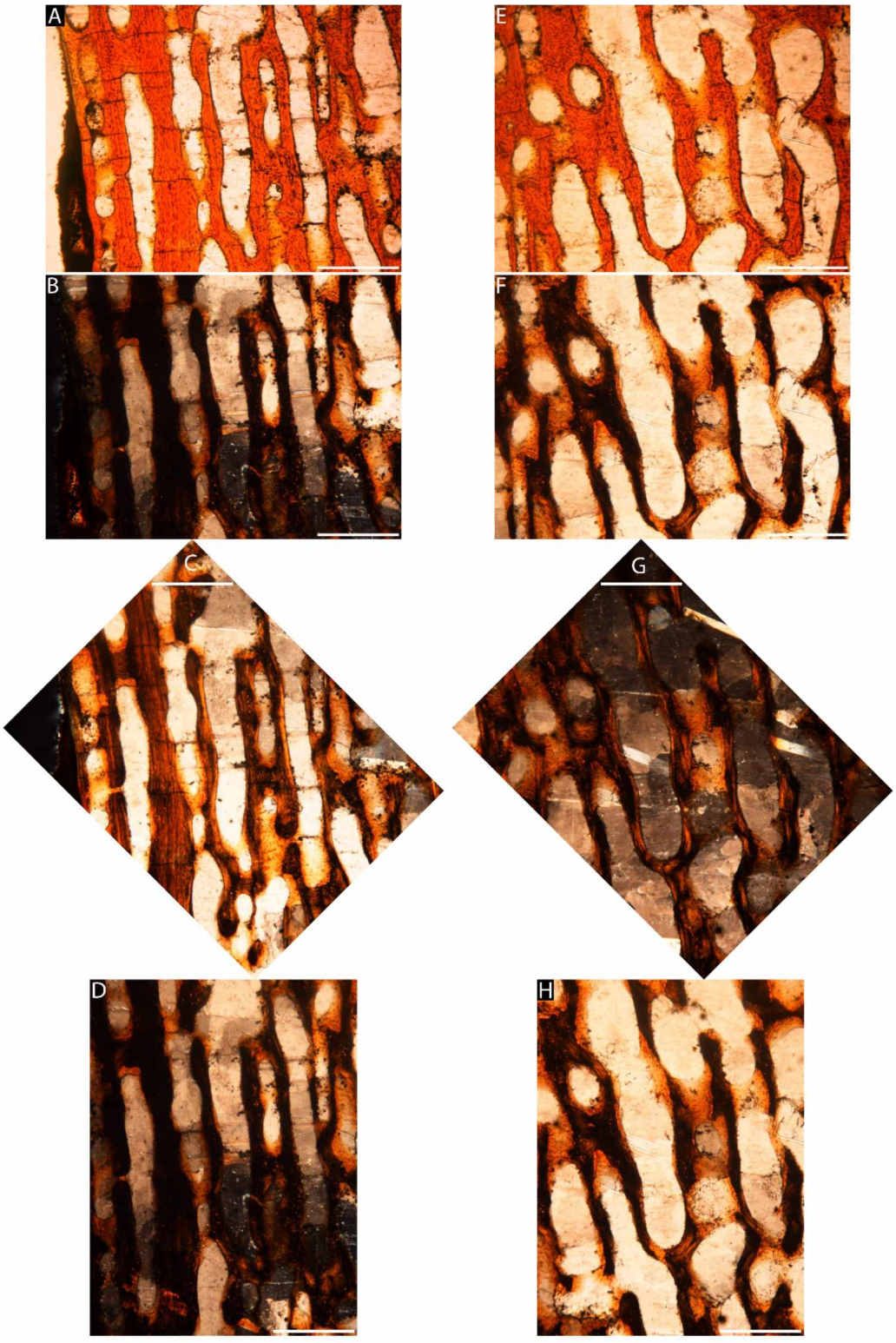

Figure 6A-1. Detail of caudal vertebra of SMNS 4789, referred specimen of *Stenopterygius quadriscissus*. A–D, detail of primary periosteal bone in normal (A) and cross-polarized (B–D) light at 0° (A, B), 45° (C), and 90° rotation (D). E–H, detail of remodeled secondary bone

in normal (E) and cross-polarized (F–H) light at 0° (E, F), 45° (G), and 90° rotation (H). All scale bars represent 0.25 mm.

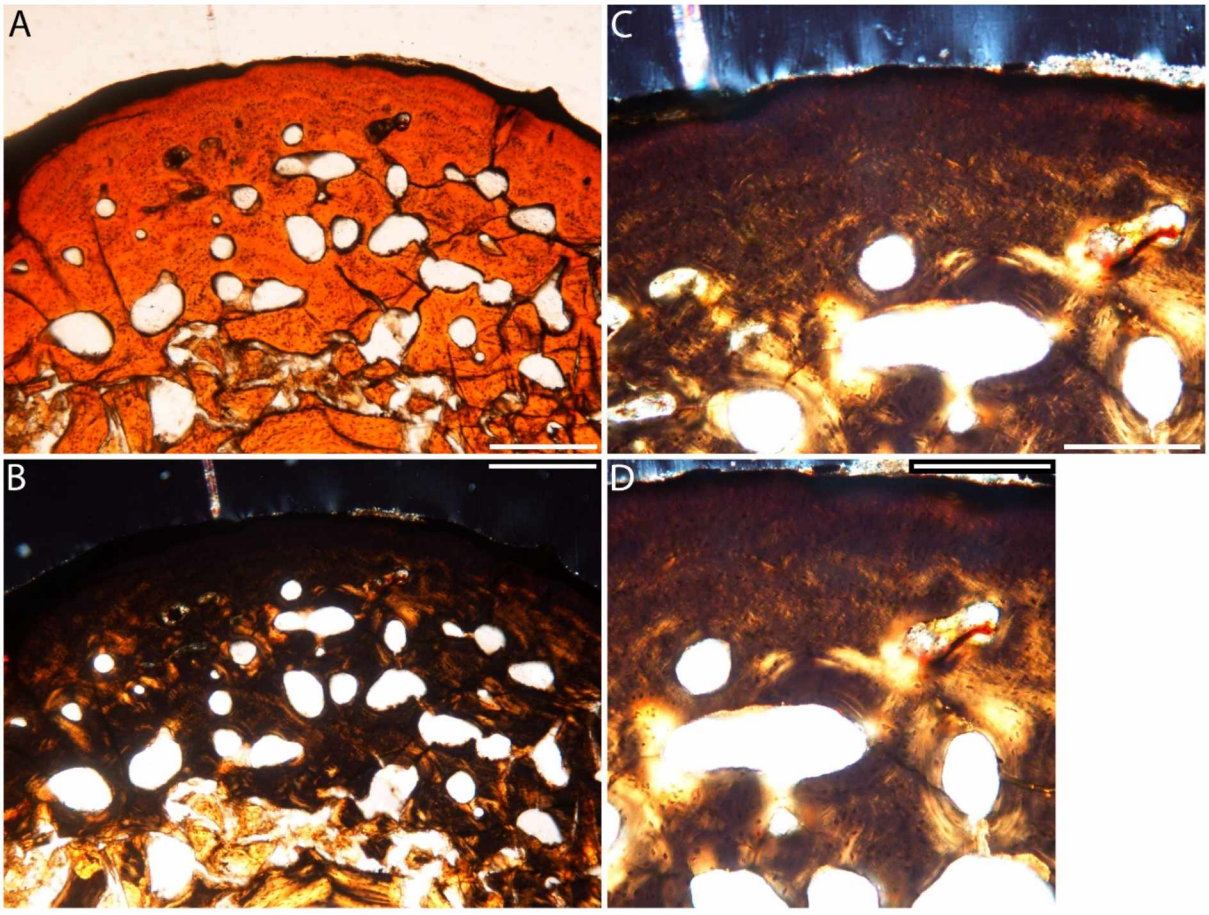

Figure 6A-2. Detail of mid-rib transverse section of SMNS 4789, referred specimen of *Stenopterygius quadriscissus* in normal (A) and cross-polarized (B–D) light. Scale bars represent 0.5 mm (A, B); 0.25 mm (C–D).

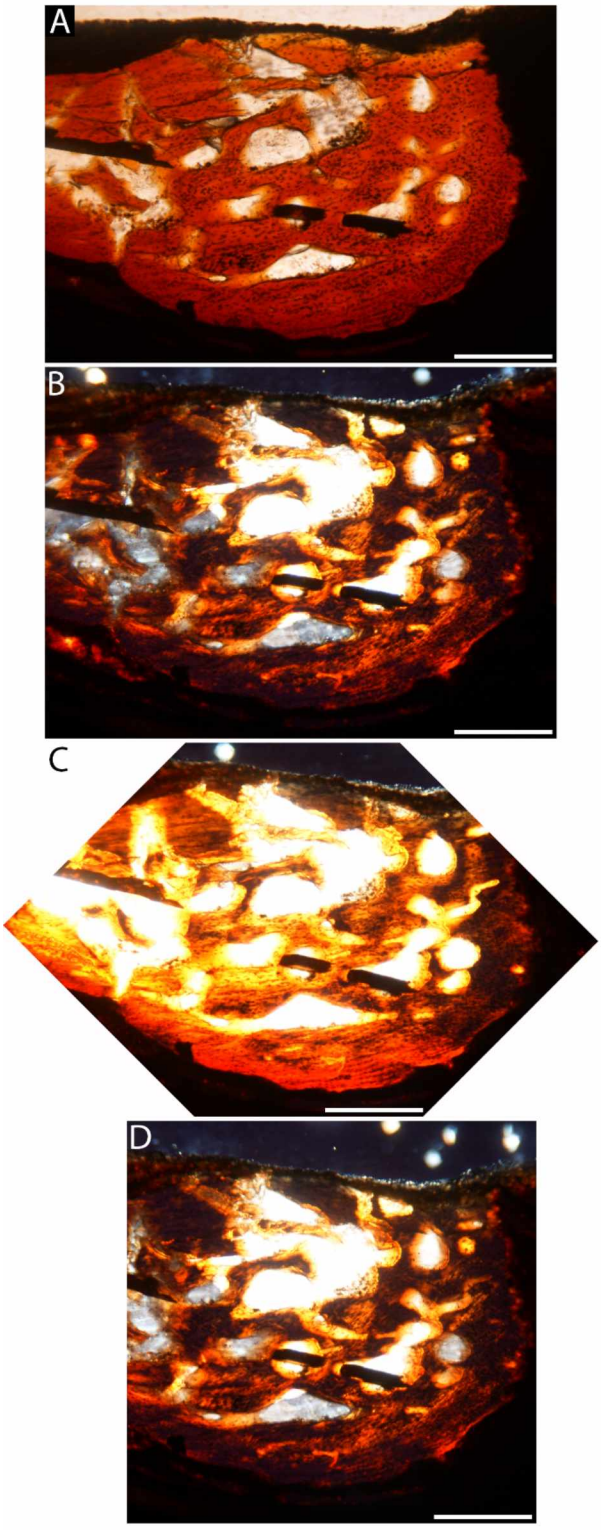

Figure 6A-3. Detail of gastralia transverse section of SMNS 4789, referred specimen of *Stenopterygius quadriscissus* in normal (A) and cross-polarized (B–D) light at 0° (A, B), 45° (C), and 90° (D) rotation. All scale bars represent 0.5 mm.

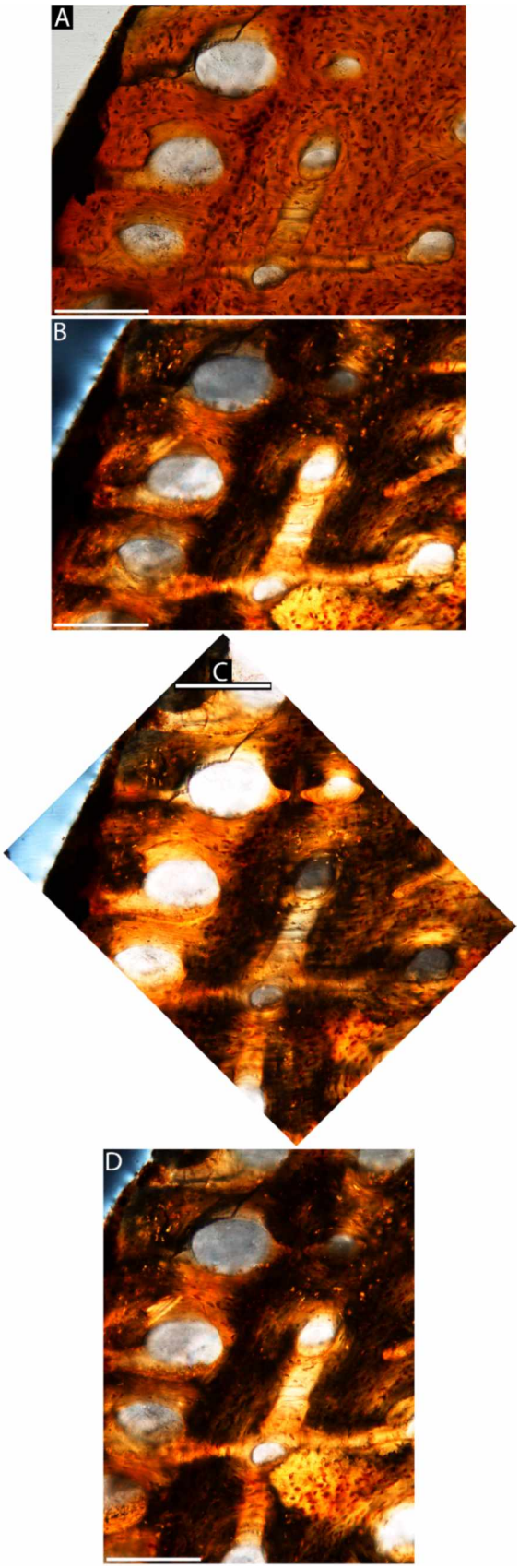

Figure 6A-4. Detail of the cortex of the humerus of SMNS 4789, referred specimen of *Stenopterygius quadriscissus* in normal (A) and cross-polarized (B-D) light at 0° (A, B), 45° (C), and 90° rotation (D). All scale bars represent 0.25 mm.

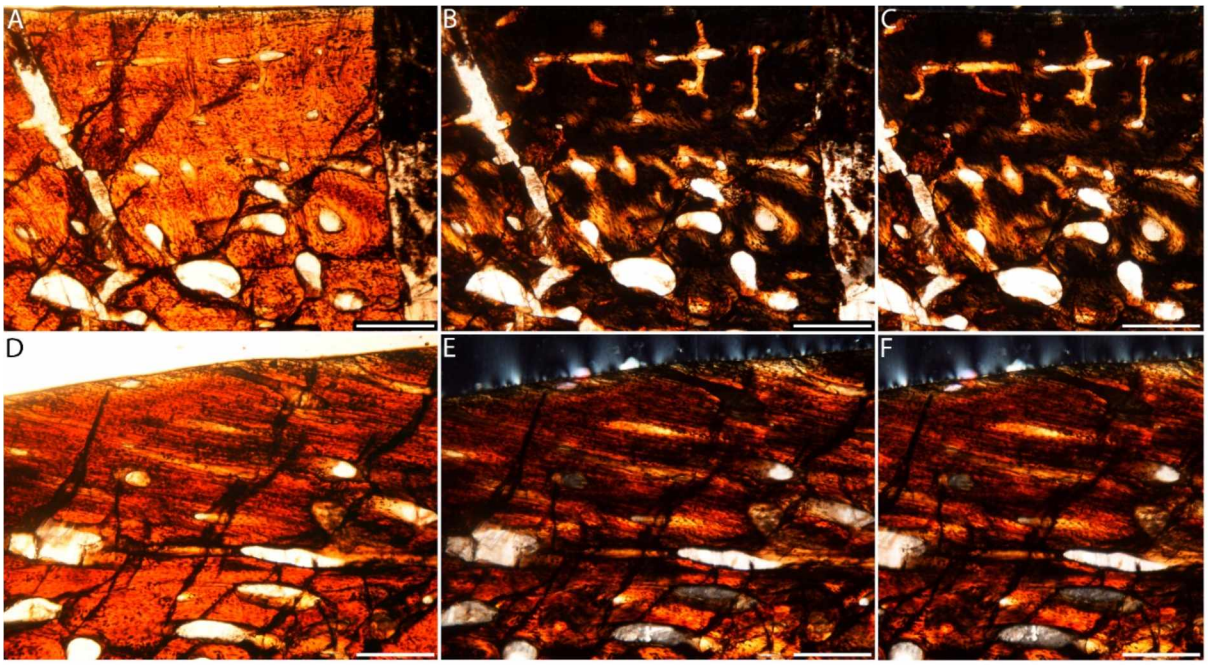

Figure 6A-5. Detail of the radiale of SMNS 4789, referred specimen of *Stenopterygius quadriscissus*. A–C, cortex of radiale in normal (A) and cross-polarized (B, C) light at 0° (A, B) and 90° (C) rotation. D–F, cortex of radiale with Sharpey's fibres in normal (D) and cross-polarized (E, F) light at 0° (D, E) and 90° (F) rotation. All scale bars represent 0.5 mm.

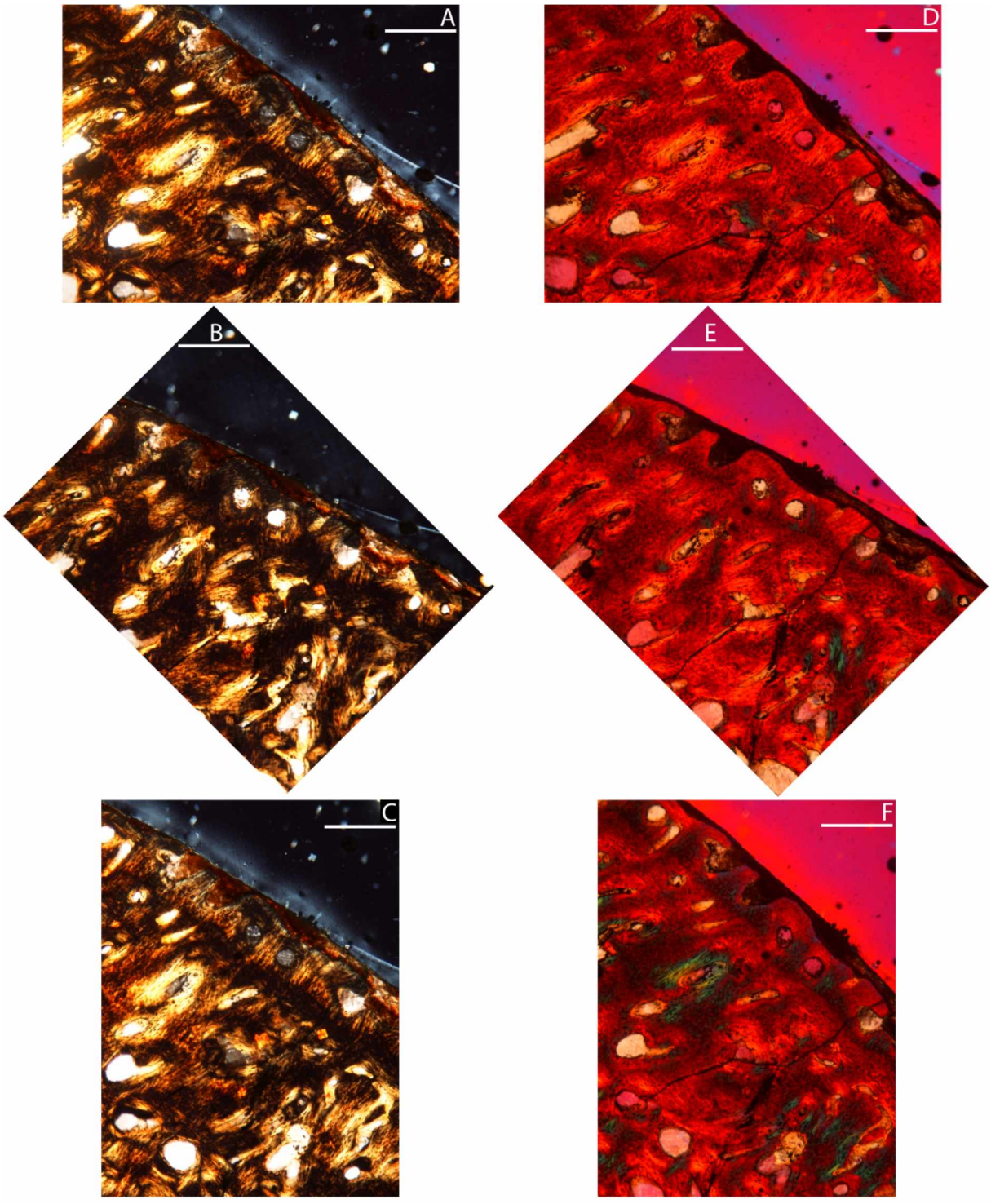

Figure 6A-6. Detail of the cortex of the femur of SMNS 4789, referred specimen of *Stenopterygius quadriscissus* in cross-polarized light with no filter (A–C) and with lambda filter (D–F) at 0° (A, C), 45° (B, E), and 90° rotation (C, F). All scale bars represent 0.5 mm.

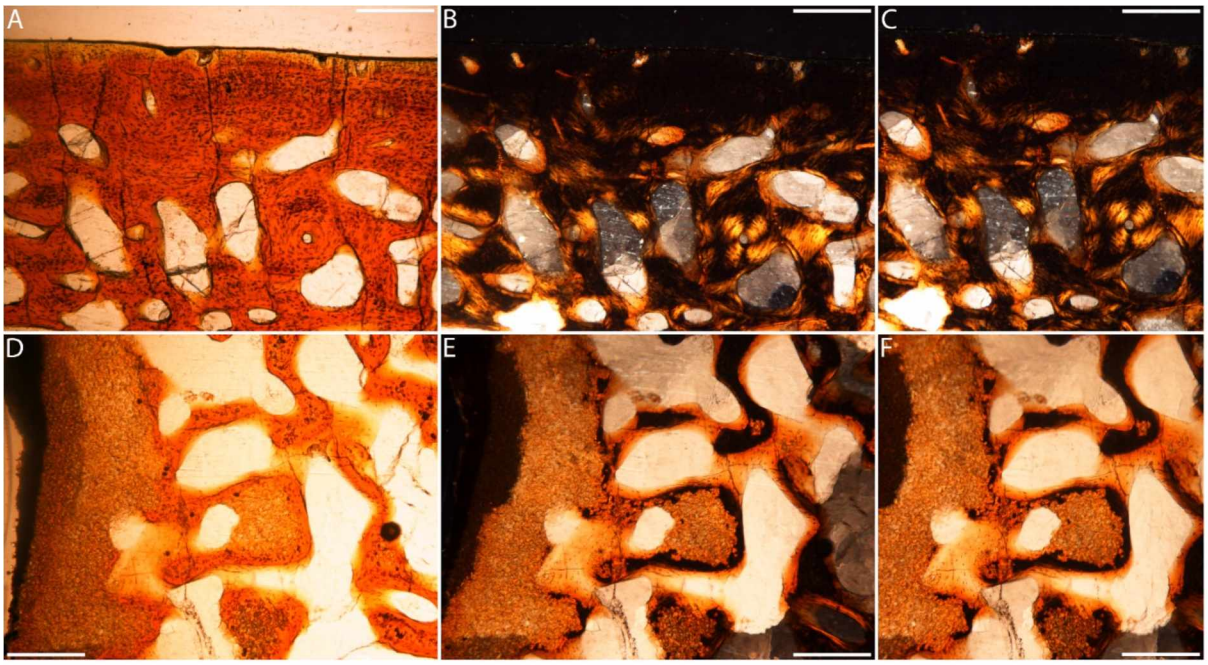

Figure 6A-7. Detail of the fibula of SMNS 4789, referred specimen of *Stenopterygius quadriscissus.* A–C, cortex of fibula in normal (A) and cross-polarized (B, C) light at 0° (A, B) and 90° (C) rotation. D–F, calcified cartilage of fibula in normal (D) and cross-polarized (E, F) light at 0° (D, E) and 90° (F) rotation. All scale bars represent 0.5 mm.

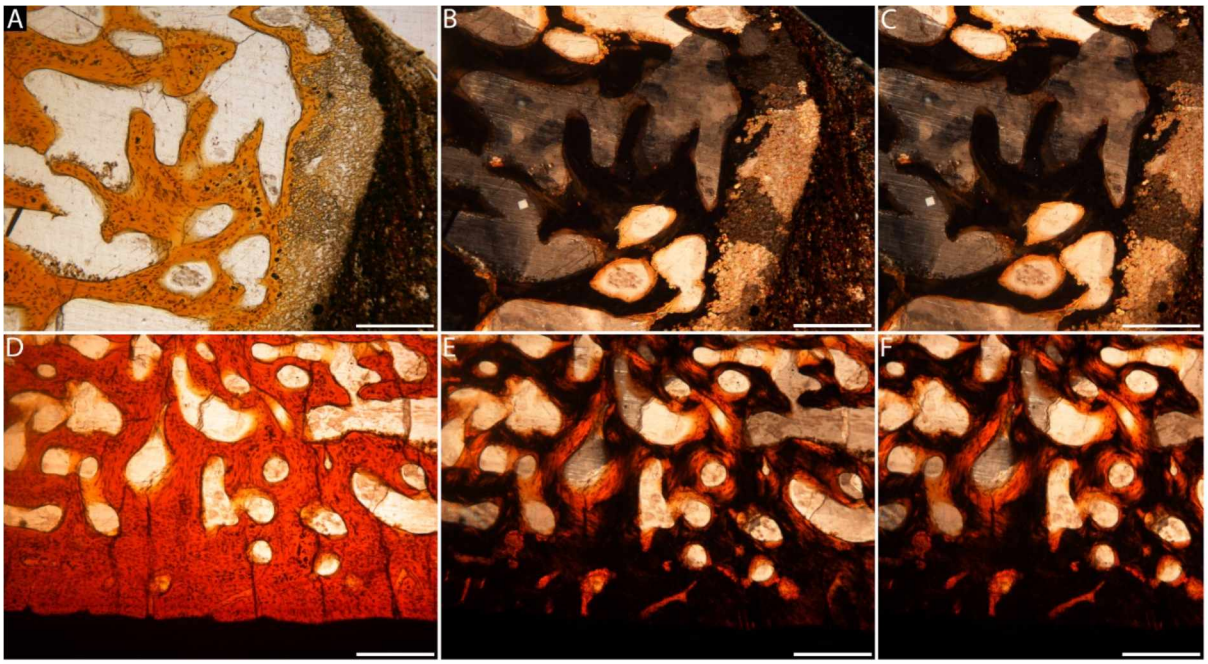

Figure 6A-8. Detail of the the 1st phalanx of digit III of the hindlimb of SMNS 4789, referred specimen of *Stenopterygius quadriscissus.* A–C, calcified cartilage in normal (A) and cross-polarized (B, C) light at 0° (A, B) and 90° (C) rotation. D-F, Cortex of fibula in normal (D) and cross-polarized (E, F) light at 0° (D, E) and 90° (F) rotation. All scale bars represent 0.5 mm.

Appendix B. Preliminary results of growth and age structure of *Stenopterygius qudriscissus* (Reptilia: Ichthyosauria) from the Posidonia Shale (Lower Jurassic) of Germany

6B.1 Introduction

Ichthyosaurians represent one of the most successful clades of Mesozoic marine reptiles in terms of their biological diversity and 160-million-year evolutionary history (McGowan and Motani, 2003). Despite their prominence in the fossil record, basic biological questions about ichthyosaurian development remain largely unanswered, including their age structure and growth rates across time and space. The Posidonienschiefer Formation (Lower Jurassic) is a Konservat-Lagerstätten known for its abundant complete, articulated ichthyosaurians, the majority of which are referable to *Stenopterygius* (Hauff, 1921; Martill, 1993; Sander 2000; McGowan and Motani, 2003; Maisch, 2008; Maxwell, 2012). The preservation of all size classes of this genus offers an unparalleled opportunity to quantify age and growth in an ichthyosaurian taxon.

Previous study has shown growth marks in the dentary and premaxilla of *Stenopterygius quadriscissus* and the scleral ossicle of *Stenopterygius triscissus* from the Posidonienschiefer Formation (see Chapters 3 and 4). Furthermore, following methods developed in the study of turtles (Zug and Parham, 1996; Avens and Goshe, 2007; Avens et al., 2009), unpublished work shows that the number of growth marks preserved in a scleral ossicle of the dinosaur *Citipati* match the number of lines of arrested growth preserved in the tibia of the same specimen, demonstrating the use of scleral ossicles for skeletochronoloy (determination of age at death) in dinosaurs (Erickson et al., unpublished work). The growth marks seen in the ossicle of *S. triscissus* are similar to those seen in

turtles, *Citipati* and other additional dinosaurian taxa suggesting that scleral ossicles may consistently preserve growth marks and therefore be useful for skeletochronology across Reptilia as a whole (see Chapter 4). In this study, we expand on these findings in order to test the use of scleral ossicles for skeletochronology in *S. quadriscissus* and to quantify age and growth rate of an ichthyosaurian taxon. Here I present preliminary results and discussion points of this study.

6B.2 Objectives

1. To test the use of scleral ossicles for skeletochronology in *Stenopterygius quadriscissus* through comparison with a skeletal element (dentary) that is known to demonstrate growth marks.
2. To construct a growth curve for *Stenopterygius quadriscissus* that would allow quantification of growth rate including maximum growth rate and growth milestones, such as age at maximum growth rate and age at somatic maturity which is known to be uncoupled from sexual maturity in this species (Johnson 1977).

6B.3 Material and Methods

We sampled the dentary of six specimens referred to *Stenopterygius quadriscissus* from the Posidonia Shale (Lower Jurassic) of Germany (Table 6B-1). Specimens were chosen from multiple size classes to examine growth at different stages in ontogeny. All specimens with exception of SMNS 4789 are from the same stratigraphic interval (Lias ε II_3) to control for the increase in maximum body size of this species through geological time (Maxwell and Vincent, 2016). SMNS 4789 is from stratigraphic unit Lias ε II_5 of the

Posidonia Shale and is included because it was previously sampled (see Chapter 3). We include this specimen with the caveat that its growth trajectory may vary from the rest of the individuals in the ontogenetic series. The dentaries were sampled in the middle 1/3 of their length. Because the specimens are slab-mounted, 2.5 cm diameter cores were removed using a drill bit, and in all cases the cores contained entire cross sections of the dentaries. If necessary, the area where the sample was taken was consolidated prior to sampling to minimize breakage and flaking.

We also sampled three scleral ossicles from three of the individuals in the ontogenetic series. These individuals represent different size classes: SMNS 50003 (juvenile), SMNS 4789 (subadult), and SMNS 54050 (adult). The samples were removed in the same manner as described above. Following the results of previous work (see Chapter 4), we required each sample to contain the inner-half (toward the apertural surface) of the ossicle. For SMNS 50003, the sample contained half of an ossicle. For SMNS 4789, the sample contained a fragmentary ossicle. For SMNS 54050, the sample contained the majority of one ossicle with the exception of the external surface.

The cores were embedded in epoxy (Allied High Tech Products, Inc.), sectioned using a diamond-tipped blade on a slow speed saw (Isomet 1000; Buehler) and mounted on petrographic slides. Sections were taken at the anterior-most and posterior-most points of the 2.5 cm cores of the dentaries. Scleral ossicles were sectioned along their short-axis near the apertural surface (as described in Chapter 4); serial sections were made in this area. The sections were ground and polished to thicknesses where the bone microstructure could be examined using petrographic microscopy. Sections were analyzed using a transmitted light microscope (Zeiss 47 30 28) in both normal and cross-polarized light

(Zeiss 47 30 59). Photographs were taken with a Nikon DS-Fi1 camera mounted on a Leitz Ortholux IIPOL-BK microscope.

All dentaries are processed, and the scleral ossicles of SMNS 50003 and SMNS 54050 are processed. The scleral ossicle of SMNS 4789 still requires sectioning and will not be described here. Microstructure is described using the terminology of Francillon-Vieillot et al., 1990.

6B.4 Preliminary Results

All dentaries show asymmetrical growth, with the majority of primary bone deposition occurring on the lateral surfaces and little deposition occurring on the medial surfaces. The core of the dentary is therefore shifted to the medial side and in most samples primary bone is visible only on the lateral surfaces.

6B.4.1 SMNS 55109 dentary

The dentary predominantly consists of round- to oblong-shaped secondary osteons surrounded by lamellar bone (Figure 6B-1). Near the medial surface, these secondary osteons formed relatively larger, branching erosion bays. Between the secondary osteons, there are still remnants of primary fibrolamellar bone with globular osteocyte lacunae. The lateral area has the most primary bone, but there are no growth marks present. The lateral surfaces have branching projections of bone tissue extending outward. Some of these branches show remodeling around the internal margins.

6B.4.2 SMNS 50003 dentary

The medial area is comprised of round to oblong and branching secondary osteons surrounded by secondary lamellar bone (Figure 6B-2A). There is an abrupt change from

this predominantly remodeled bone to a zone with smaller, round secondary osteons with primary fibrolamellar bone still present (Figure 6B-2B). This zone extends to the lateral surface of the element which is dimpled, but does not have the pronounced projections seen in SMNS 55109. This zonation in remodeling is visible both macro- and microscopically. There are no growth marks in the primary bone.

6B.4.3 SMNS 51551 dentary

The microstructure of this element is similar to that seen in SMNS 50003 (Figure 6B-3A). The zonation is clearly visible in the anterior-most section and still present but less pronounced in some areas of the posterior-most section (Figure 6B-3B, C).

6B.4.4 SMNS 54050 dentary

The medial area is highly remodeled and shows oval and branching secondary osteons surrounded by secondary lamellar bone with no remnants of primary bone. Moving laterally, there is a shift to smaller round secondary osteons surrounded by secondary lamellar bone, but with primary fibrolamellar bone still present between the secondary osteons. In most places, it grades from the highly remodeled to the less remodeled, but in one area it shows a distinct boundary between the two. From this area of distinct boundary to the lateral surface, the osteons as well as the primary vascular canals are arranged in rows. Near the lateral surface, there may be another zonation as the primary vascular canals change from round to radially oriented. In some areas, there is remodeling occurring near the lateral surface.

6B.4.5 SMNS 51843 dentary

The medial area is highly remodeled and shows only secondary lamellar bone surrounding secondary osteons (Figure 6B-4A). The innermost secondary osteons are

larger and oval to branching in shape and grade into smaller secondary osteons that are predominantly oval in shape. Again, there is zonation in the degree of remodeling (Figure 6B-4B). There is an abrupt change moving laterally to smaller, only oval-shaped secondary osteons with remnants of primary fibrolamellar bone between them. There is another abrupt change moving to the lateral-most area, this time associated with a line of arrested growth (LAG). This third zone is less remodeled, and consists of fibrolamellar primary bone with areas of oval primary vascular canals arranged in rows as well as radially oriented primary vascular canals (Figure 6B-4C). In some areas remodeling is occurring near the lateral surface.

6B.4.6 SMNS 50003 scleral ossicle

The core of the ossicle is spongious and there are few round secondary osteons surrounded by secondary lamellar bone (Figure 6B-5). Moving toward the medial and lateral surfaces, both show compact bone with Sharpey's fibers. Both surfaces have one clear pair of light and dark layers. The exposed surface shows at least two (potentially three) additional pairs of growth layers (Figure 6B-5B).

6B.4.7 SMNS 54050 scleral ossicle

The area sectioned is poorly preserved. The bone tissue that is visible consists of spongious primary fibrolamellar bone.

6B.5 Preliminary Discussion

- The scleral ossicle of SMNS 50003 preserves 3-4 pairs of growth bands, one of which is particularly clear. This does not match the number of zones preserved in the dentary, and no growth marks were preserved in the primary bone of the

dentary. Further work will compare growth bands in the ossicles and dentaries of SMNS 4789 and SMNS 54050.

- Additional sections will need to be made of the scleral ossicle from specimen SMNS 54050 to locate an area that may be better preserved.
- Growth marks in primary bone and remodeling zonations are in some cases clearer in the anterior sections of the dentary compared to the posterior sections. Areas with less deposition are more likely to show clear growth marks and zonations.
- Further work needs to be done to examine the remodeling zonations described here. They are not LAGs, but could represent an area where extensive remodeling occurred while primary growth had slowed or stopped. I will consult the literature to find an extant animal that may display similar zonations.
- The dentary of SMNS 4789, a subadult based on its body measurements, preserved four annuli (Chapter 3). The lower jaw of this specimen is incomplete so it is possible this size classification is underestimating its size class. In addition, the section potentially preserves more growth marks than those of the adults (SMNS 54050 and SMNS 51843) because the section was taken near the anterior-most point of the dentary.

6B.6 References

Avens, L. And L.R. Goshe. 2007. Comparative skeletochronological analysis of Kemp's ridley (*Lepidochelys kempii*) and loggerhead (*Caretta caretta*) humeri and scleral ossicles. *Marine Biology,* 152:1309—1317.

Avens, L., J. C. Taylor, L.R. Goshe, T.T. Jones, and M. Hastings. 2009. Use of skeletochronological analysis to estimate age of leatherback sea turtles *Dermochelys coriacea* in the western North Atlantic. *Endangered Species Research,* 8:165—177.

Erickson, G.M., Anderson, K.L., Watabe, M. and Norrell, M.A. Unpublished data. Age and growth pattern for a specimen of non-avian dinosaur *Citipati osmolskae* determined from growth lines in scleral ossicles.

Francillon-Vieillot, H., Buffrénil, V. de, Castanet, J., Geraudie, J., Meunier, F.J., Sire, J.Y., Zylerberg, L. and Ricqlès, A. de. 1990. Microstructure and mineralization of vertebrate skeletal tissues. 471–530. In Carter, J.G. (ed). *Biomineralization: patterns and evolutionary trends*. Van Nostrand Reinhold.

Hauff, B. 1921. Untersuchung der Fossilfundstätten von Holzmaden in Posidonienschiefer des oberen Lias Württembergs. *Palaeontographica,* 64:1–42.

Johnson, R. 1977. Size independent criteria for estimating relative age and relationships among growth parameters in a group of fossil reptiles (Reptilia: Ichthyosauria). *Canadian Journal of Earth Science,* 14:1916—1924.

Maisch, M.W. 2008. Revision of the genus *Stenopterygius* Jaekel, 1904 emend. Von Huene, 1922 (Reptilia: Ichthyosauria) from the Lower Jurassic of Western Europe. *Palaeodiversity,* 1:227–271.

Martill, D.M. 1987. A taphonomic and diagenetic case study of a partially articulated ichthyosaur. *Palaeontology,* 30(3):543–555.

Maxwell, E.E. 2012. New metrics to differentiate species of *Stenopterygius* (Reptilia: Ichthyosauria) from the Lower Jurassic of Southweastern Germany. *Journal of Paleontology,* 86(1):105–115.

Maxwell, E.E. and P. Vincent. 2016. Effects of the early Toarcian Oceanic Anoxic Event on ichthyosaur body size and faunal composition in the Southwest German Basin. *Paleobiology,* 42(1):117—126.

McGowan, C. and Motani, R. 2003. Ichthyopterygia. In Sues, H.-D. (ed). *Handbook of Paleoherpetology*. Verlag Dr. Friedrich Pfeil, München.

Sander, P.M. 2000. Ichthyosauria: their diversity, distribution, and phylogeny. *Paläontologische Zeitschrift,* 74:1–35.

Zug, G.R. and J.F. Parham. 1996. Age and growth in leatherback turtles, *Dermochelys coriacea* (Testudines: Dermochelyidae): A skeletochronological analysis. *Chelonian Conservation and Biology,* 2(2):244—249.

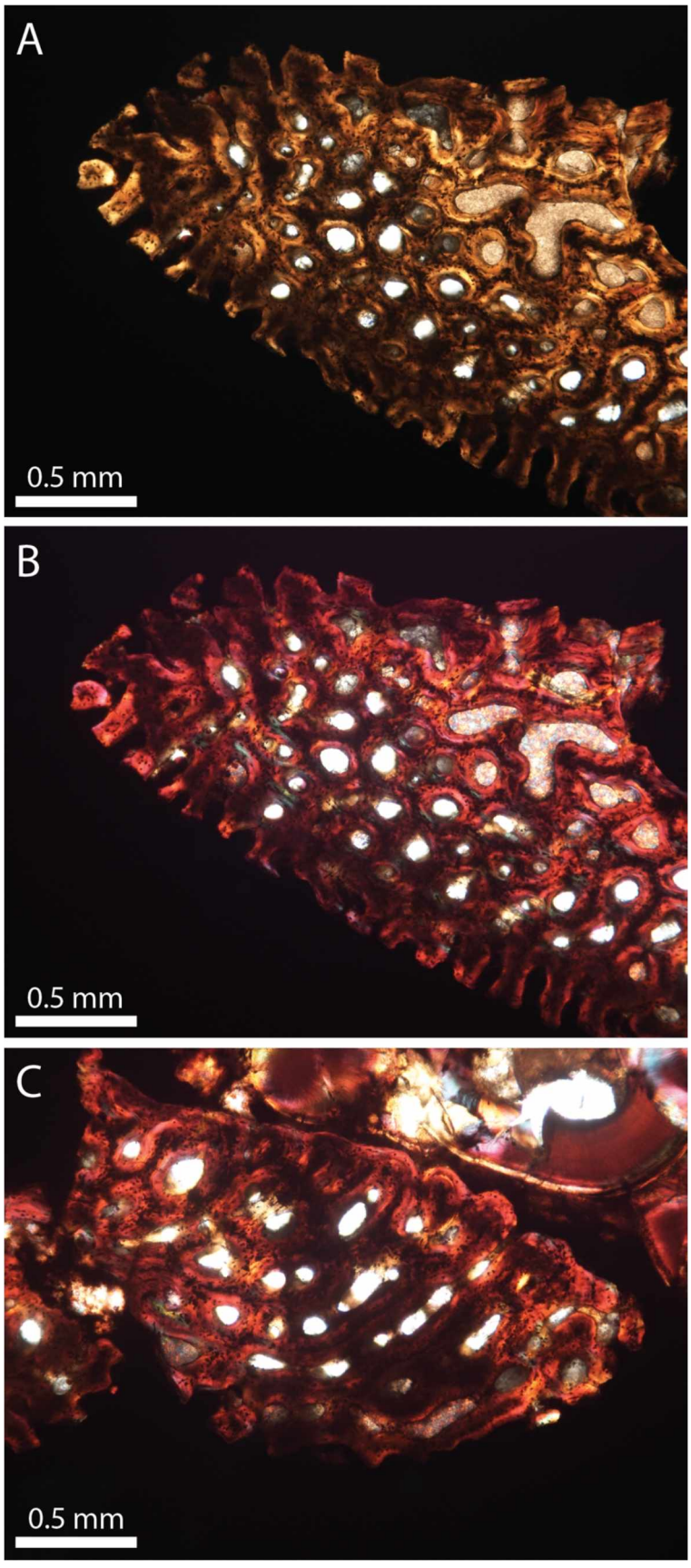

Figure 6B-1. Dentary of SMNS 55109 referred specimen of *Stenopterygius quadriscissus*. A. Medial surface at top of image showing predominantly secondary lamellar bone surrounding branching erosion bays and round secondary osteons. Lateral surface at bottom of image with branching projections consisting of primary fibrolamellar bone. Normal light. B. Same view as above. Cross-polarized light with lambda filter. C. Dentary with similar microstructure as described above, but with rows of secondary osteons. Cross-polarized light with lambda filter.

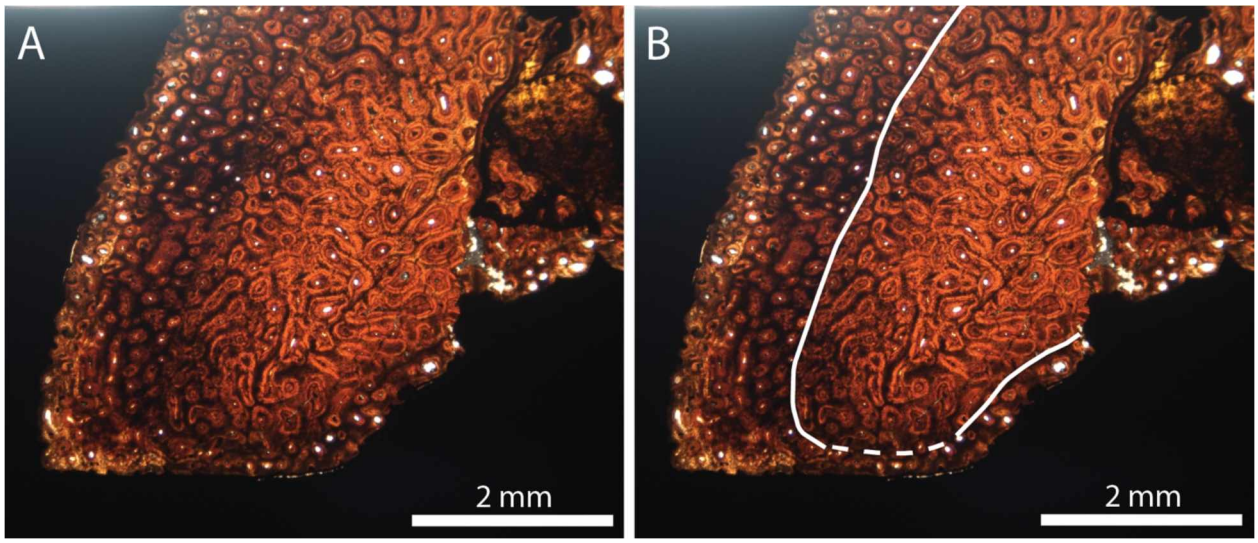

Figure 6B-2. Dentary of SMNS 50003 referred specimen of *Stenopterygius quadriscissus*. A. Overview of organization of microstructure showing zonation of remodeled bone. Large secondary osteons surrounded by secondary lamellar bone are present medially. There is a change to a lesser degree of remodeling, with smaller round secondary osteons separated by remnants of primary fibrolamellar bone. Normal light. B. Line illustrates boundary between zones of remodeling. Normal light.

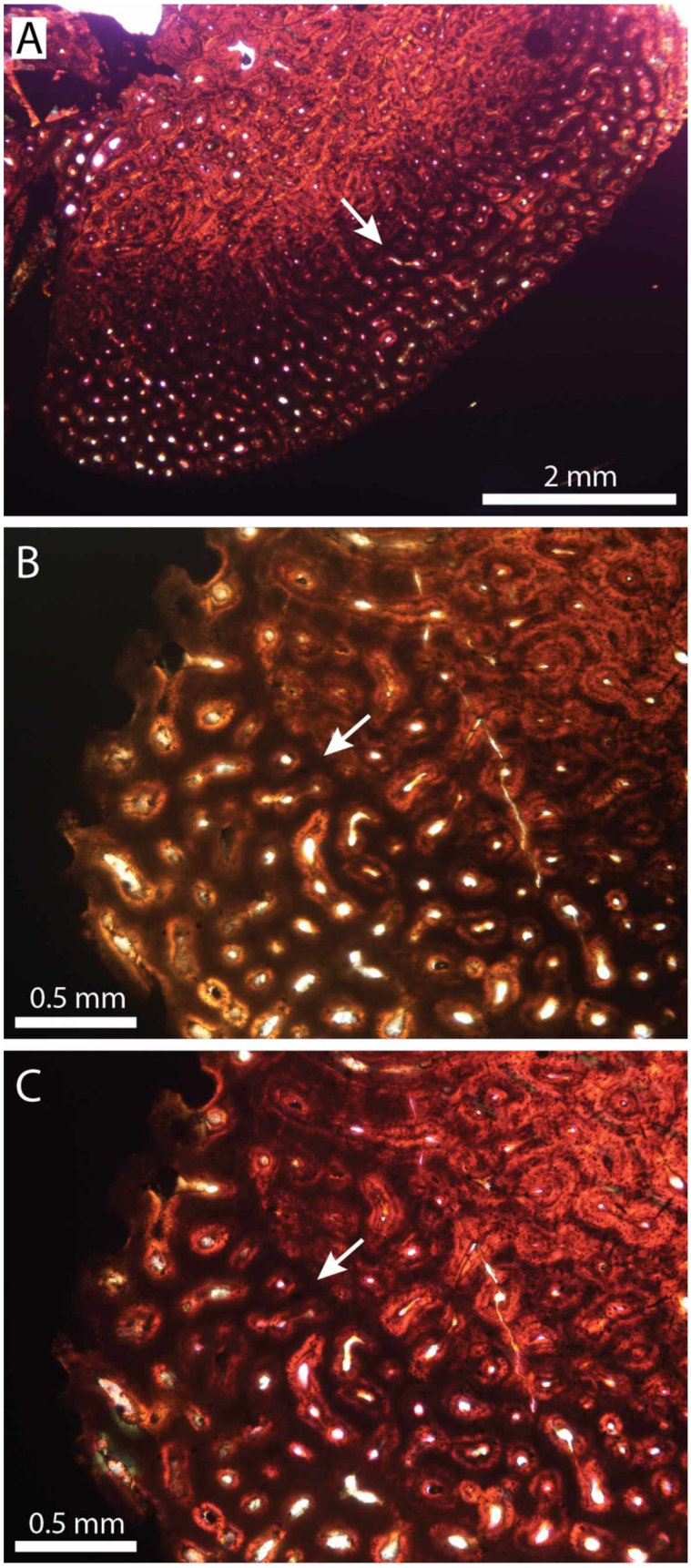

Figure 6B-3. Dentary of SMNS 51551 referred specimen of *Stenopterygius quadriscissus*. A. Overview of dentary showing overall organization and zonation of remodeling. Arrow indicates boundary between zones. Cross-polarized light with lambda filter. B. Detail of boundary between zones, indicated by arrow. Normal Light. C. Same as above. Cross-polarized light with lambda filter.

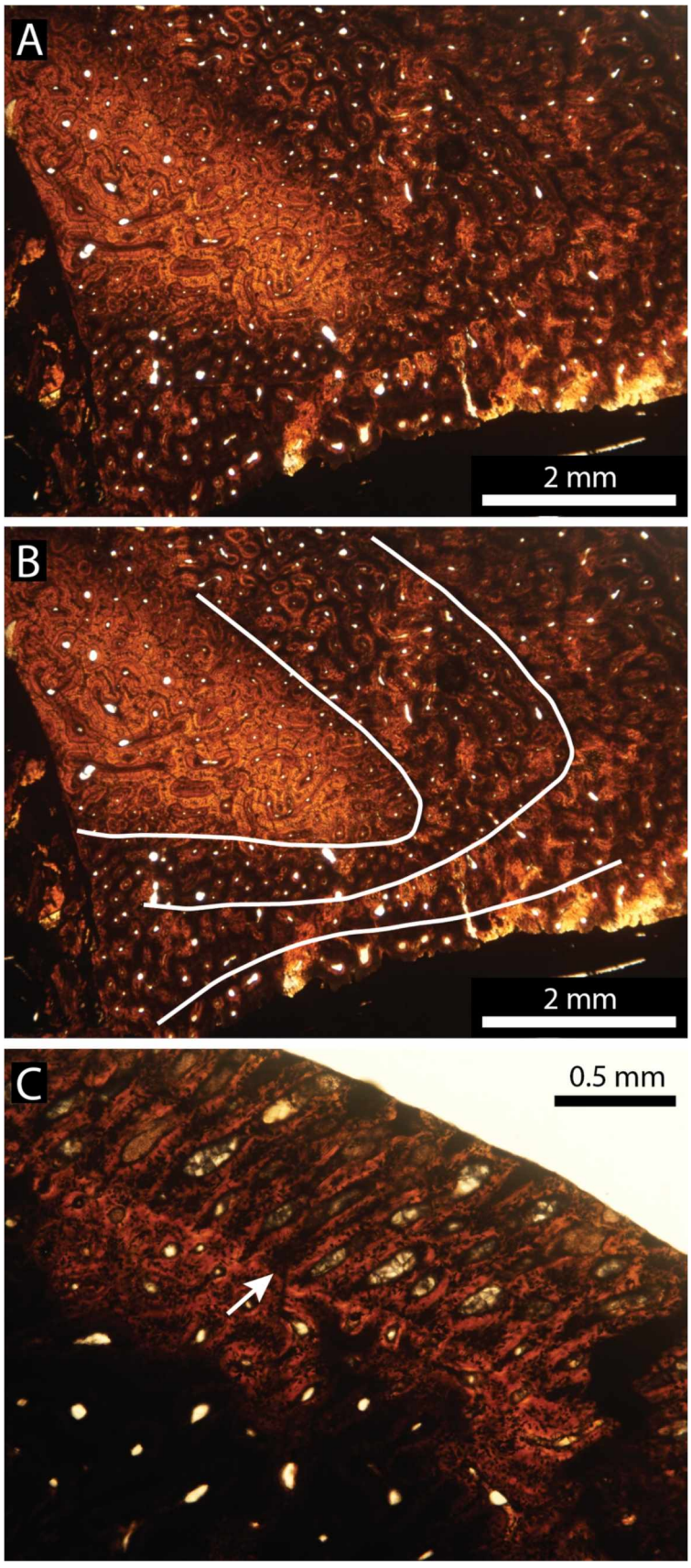

Figure 6B-4. Dentary of SMNS 51843 referred specimen of *Stenopterygius quadriscissus*. A. Overview of dentary showing organization of microstructure and boundaries between zones of varying degrees of remodeling. Normal light. B. Same as above with lines indicating boundaries. Normal light. C. Detail of outermost zone showing shift to predominantly radial vascularization. Arrow indicates boundary between zones. Normal light.

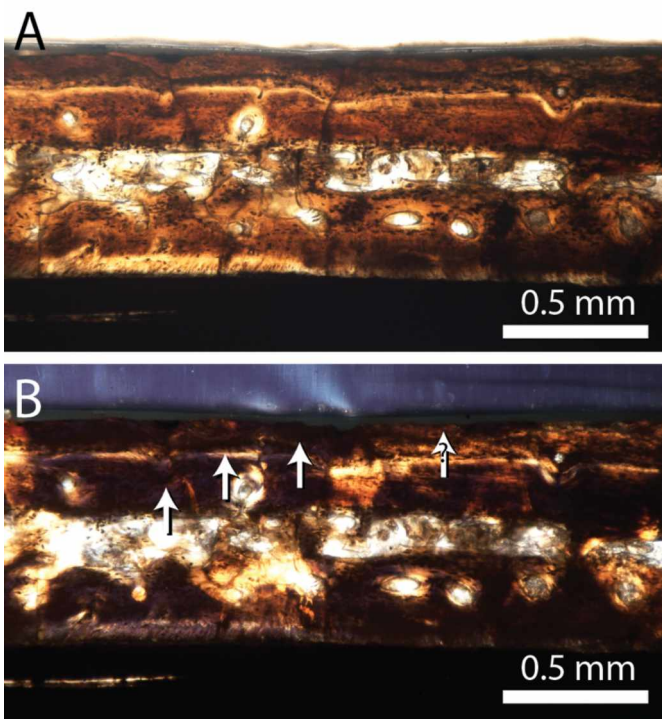

Figure 6B-5. Scleral ossicle of SMNS 50003 referred specimen of *Stenopterygius quadriscissus*. A. Short axis section with low degree of remodeling at the core surrounded by denser compact bone. Normal light. B. Same as above in cross-polarized light. Arrows indicate light cycles in light-dark paired cycles. Outermost arrow has a question mark indicating uncertainty if there is another light growth layer present.

Table 6B-1. Referred specimens of *Stenopterygius quadriscissus* sampled in the ontogenetic series. Dentaries were sampled from each individual. Scleral ossicles were also sampled for SMNS 50003, SMNS 4789 and SMNS 54050.

Specimen	Stratigraphic unit	Lower jaw length (mm)	Size class
SMNS 55109	II3	238	juvenile
SMNS 50003	II3	327	juvenile
SMNS 51551	II3	337	juvenile
SMNS 4789	II5	>425	subadult
SMNS 54050	II3	465	adult
SMNS 51843	II3	481	adult